OPTICAL RESPONSE PROPERTIES OF LARGE MOLECULES MODELLED BY AN INTERACTION MODEL

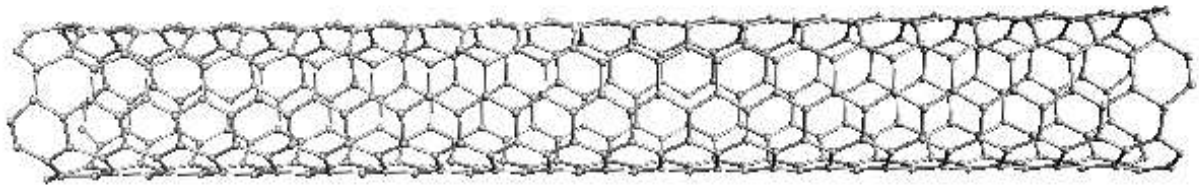

Master thesis, 2^{nd} edition

Lasse Jensen

Dept. of Chemistry, Chem. lab. 3
H.C. Ørsted Institute
University of Copenhagen
Universitetsparken 5
DK-2100 Copenhagen Ø
Denmark

There is a theory which states that if ever anyone discovers exactly what the Universe is for and why it is here, it will instantly disappear and be replaced by something even more bizarre and inexplicable.

There is another theory which states that this has already happened.

-Douglas Adams
The Restaurant at the End of the Universe, 1980

Acknowledgments

This thesis presents the major part of my work done as a master student at Chemistry Laboratory III, University of Copenhagen. The work has been supervised by Dr. Scient. Kurt V. Mikkelsen, Chemistry Laboratory III, and Dr. Per-Olof Åstrand, Risø National Laboratory. I would like to thank Kurt and Per-Olof for the opportunity to work together on this project which have been very fruitful. Especially the writing of the articles has been a very pleasant and instructive experience. I am also grateful for their continuing time and patience when answering my questions.

Acknowledgments also goes out to the following people for their help during the work presented here.

- Cand. Scient. Thomas Lorenzen, Chemistry Laboratory III: For always having time to fix my "small" computer problems.
- Dr. Kristian O. Sylvester-Hvid , EMI DTU: For the collaboration during my thesis work and especially for during all the SCF calculations on the aromatic molecules.
- Cand. Scient. Ole H. Schmidt, Chemistry Laboratory III : For making the structures and the SCF polarizability calculations of the carbon nanotubes.

Finally, I would like to thank Thomas and Kristian for kindly reading the manuscript.

Lasse Jensen, 29th August 2000

Contents

Chapter 1

Introduction

Computers are becoming a very important part of our every day life, and therefore a lot of jokes on computers are going around. One of the jokes reads " If the automobile had followed the same development as the computer, a Rolls-Royce would today cost $100, get a million miles per gallon, and explode once a year killing everyone inside ". This joke indicates that the computer development has followed the famous Moore's Law. Moore's Law in computer development is a statement that the switching speed of transistors has been doubled every 18 to 24 months by miniaturization thus leading to faster computers. But the joke is also an indications that every technology eventualy will reach its intrinsic limitations, in this case the development of cars.

As discussed recently the miniaturization of the traditional silicon-based transistors will reach its intrinsic limitation in the near future [1, 2]. Muller *et al.* found that the gate oxide which insulates the voltage electrodes from the current-carrying electrodes will reach its fundamental physical limitation in year 2012 [2]. They found that if the gate oxide, which consist of silicon dioxide, has a thickness of less than four layers of silicon atoms, current will penetrate through the gate oxide. There will with the increasing demand for faster computers and information distribution, therefore, be a need for new approaches. One approach emerges from Feynmans famous talk "There's Plenty of Room at the Bottom" [3]. The "bottom up" approach implies the construction of molecular-level components capable of performing the functions needed [4, 5]. It opens up a whole new area of electronics where we use molecules instead of macroscopic materials to construct devices. In order to construct molecular computers, component like molecular wires, transistors, memory elements and switches have to be constructed [6–9]. Nano-size molecules such as carbon nanotubes and DNA are very interesting candidates for the construction of these new molecular electronic devices [10, 11].

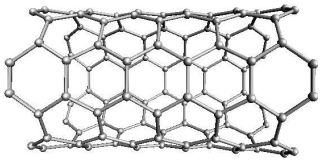

Figure 1.1: Structure of a (5,5) carbon nanotube with 110 atoms.

The way that information is distributed is also changing, going from electronic devices towards photonic devices. In the future a major goal will be the use of light as information carrier, in order to speed up the process of data transmission. The statement of P. Ball [12]; "*The next revolution in information technology will dispence with the transistor and use light,*

not electricity, to carry information. This change will rely on the development of photonic materials, which produce, guide, detect, and process light." clearly illustrates that photonic materials are the new materials of the 21^{st} century in the same way that silicon was for the 20^{th} century. New devices and materials such as optical memory storage [13, 14], photonic wires [15–18] and optical switches [19, 20] have to be constructed. Photonic devices rely on the interaction between matter and electromagnetic fields and the response of a material to the perturbation of a electromagnetic field can be linear and non-linear depending on the applied field. In the development of photonic materials it is, therefore, of fundamental importance to understand the optical response properties of the materials. In order to design new materials we need an understanding on how these properties depend on the molecular structure. Especially, the understanding of not only the static but also the frequency-dependent (hyper)polarizability at the molecular level is of fundamental importance [21–27].

Today new functional materials are being designed at the molecular level but it is not always clear how small changes in the molecular structure affects the response properties of the materials. *Ab initio* method used to calculate the molecular properties would therefore be an ideal tool for studying molecular based materials. However, these accurate methods are currently limited to small molecules. From a technological point of view the interest lies in predicting optical properties of large molecules which can be used in the contruction of new, molecular based, photonic devices. Therefore in order to treat large molecules such as polymers, carbon nanotubes, molecular crystals or the surrounding medium we have to look for less sophisticated models. Therefore, a combination of *ab initio* methods and less sophisticated models should be used to gain chemical insight into the structure-property relation and thereby guiding the experimentalist.

The purpose of this thesis has been to develop a model capable of calculating the frequency-dependent polarizability and hyper-polarizability of large molecules such as carbon nanotubes, polymers and molecular crystals. This is done by investigating a classical electrostatic model for interacting atoms, thereby parameterizing the frequency-dependent molecular properties. The idea is that from a single set of transferable atomic parameters we are able to calculate the frequency-dependent properties of all types of molecules including aromatic, aliphatic, olephinic and combinations of these. This implies that the parameters should only depend on the type of atom and not on the specific chemical surroundings associated with the atom. Using such model should easily predict properties of molecules containing several hundred atoms and the inclusion of new types of atoms should be straight forward. The model should also be of the "black-box" type meaning that in addition to the molecular structure as little information as possibly should be needed.

The outline of the thesis is as following

- Chapter 2 describes the quantum mechanical basis for calculating molecular properties. Appendices A, B and C should be consulted for some of the details.
- Chapter 3 gives a theoretical introduction to the different interaction models used in this work. A short historical review on the litterature of additivity and the interaction model is also presented.
- Chapter 4 presents the parameterization of the frequency-dependent molecular polarizability.
- Chapter 5 deals with the application of the interaction model parameterized in chapter 4 on carbon nanotubes.

- Chapter 6 describes the extension of the static model from chapter 4 to include intramolecular charge transfer.
- Chapter 7 illustrated shortly the application of the interaction model used on interaction induced polarizabilities in dimers.
- Chapter 8 summerizes and gives some concluding remarks and further directions for continuing investigations using the interaction model.

The results of the work presented in this thesis has been written into three articles where one has been accepted, one has been submitted and one is still in preperation. The abstracts for the articles are given in appendix G.

Unless otherwise stated atomic units have been used throughout the presents work. Also the Einstein summation convention, i.e. summing over repeated indices, will be used extensively.

Chapter 2

Molecular Properties and Non-linear Optics

As discussed in the introduction, photonics is going to be a major player in the development of technology in the future. Photonics rely on nonlinear optical processes such as frequency conversion and optical switching. In order to optimize the nonlinear processes, a knowledge on how the optical properties depend on the molecular structure is needed. In this chapter we will discuss the calculation of molecular properties in terms of semi-classical radiation theory. We will also comment on the relation between calculated properties and experimentally determined properties.

2.1 Physical Insight into Optical Processes

When a medium is placed in a electric field, either static or optical, a nonlinear polarization of the medium occurs. This macroscopic polarization of the medium due to an external field $\mathbf{E}$ is given by

$$\mathbf{P} = \chi^{(1)}\mathbf{E} + \frac{1}{2!}\chi^{(2)}\mathbf{E}^2 + \frac{1}{3!}\chi^{(3)}\mathbf{E}^3 + \cdots, \tag{2.1}$$

where $\chi^{(n)}$ is the n'th order electrical susceptibility tensor of rank $(n+1)$. A simple way of gaining insight into the physics of nonlinear optics is to consider the medium as an assembly of forced anharmonic oscillators. Using Newton´s second law and considering damping, the equation of motion for a particle with mass m and charge q can in one dimension be written as

$$\frac{d^2x(t)}{dt^2} + \Gamma_x\frac{dx(t)}{dt} + \omega_x^2 x(t) + ax^2 = -\frac{q}{m}E(\omega_1)E(\omega_2). \tag{2.2}$$

The electric field is polarized along the x-direction and is evaluated at the origin of the oscillator motion. The solution to the equation of motion gives terms like [28, 29]

$$x = x_1(\omega_1) + x_2(2\omega_1) + x_2(0) + x_2(\omega_1+\omega_2) + x_2(\omega_1-\omega_2) + \mathcal{O}(\omega_2), \tag{2.3}$$

where $\mathcal{O}(\omega_2)$ denotes similar terms in ω_2. x_1 is the solution to the harmonic (linear) problem and x_2 is the nonlinear solution. Using that the polarization of the medium can be written as

$$P = P^{(1)} + P^{(2)} = -Nex_1 - Ne\{x_2(2\omega_1) + x_2(0) + x_2(\omega_1+\omega_2) + x_2(\omega_1-\omega_2)\}, \tag{2.4}$$

we can identify different susceptibilities having the same frequency-dependence as the solutions x_1 and x_2. We can therefore identify the following susceptibilities

- $\chi^{(1)}(-\omega;\omega)$,
  determines the linear response and is the dominating term in the refractive index.
- $\chi^{(2)}(0;\omega-\omega)$,
  gives optical rectification of the dynamic field yielding a static field.
- $\chi^{(2)}(-2\omega;\omega,\omega)$,
  Second Harmonic Generation (SHG) yielding a field at the double frequence.
- $\chi^{(2)}(-\omega_1 \pm \omega_2;\omega_1,\omega_2)$,
  Sum and Difference Generation.

This illustrates some of the important 2nd order nonlinear optical properties. Especially the SHG susceptibility is very important and can be used e.g. to convert a laserpulse at one frequency to a pulse with the double frequency, which frequently is used in femto-second spectroscopy. Having made these preliminary comments we will now turn our attention to the molecular level.

2.2 The Semi-Classical Hamiltonian

When a molecule is subjected to an electromagnetic field, the motion of the electrons will be altered. This is also the case for the nuclear motion but to a lesser extent because of the greater nuclear mass. A complete quantum mechanical treatment would require very time consuming quantum electrodynamics and therefore we will make some initial approximations. We will use a semi-classical approach where the molecule is treated by quantum mechanics and the electromagnetic field is treated classically. Only the molecular electronic structure is treated by non-relativistic quantum mechanics, *i.e.* by solving the Schrödinger equation A.1 in the Born-Oppenheimer approximation. A derivation of the Born-Oppenheimer approximation is presented in Appendix A. Since the electromagnetic field is treated classically it will only occur as a pertubation to the zeroth-order desciption and thus enters as an additional term in the electronic Hamiltonian, Eq. A.3.

The normal approach for deriving the additional terms in the Hamiltonian, which arises from the electromagnetic field, is to find the classical Lagrangian [30]. From the Lagrangian we can contruct the classical Hamiltonian which can then be converted to operator form thereby yielding the desired Hamiltonian. Classically, a particle with charge q subjected to an electromagnetic field will experience a force given by [30, 31]

$$\vec{F} = q(\vec{E} + \vec{v} \times \vec{B}), \tag{2.5}$$

called the Lorentz force, where $\vec{E}$, $\vec{B}$ is the electric and magnetic field, respectively, and $\vec{v}$ the velocity of the particle. Construcing the Lagrangian using the Lorentz force and converting it to operator form yields a Hamiltonian as [30, 31]

$$H = \frac{1}{2m}(\hat{p} + e\vec{A})^2 - e\phi + V, \tag{2.6}$$

where $\hat{p}$ is the normal linear momentum operator, V is the electrostatic potential, ϕ is a scalar potential and $\vec{A}$ is a vector potential. Since the original electric field $\vec{E}$ and magnetic field $\vec{B}$

are unchanged by a gauge transformation of the potentials we can transform the Schödinger equation provided that the wavefunction and the Hamiltonian transform as

$$\Phi = e^{\mathrm{i}eF}\Psi, \tag{2.7}$$

$$H' = e^{\mathrm{i}eF}He^{-\mathrm{i}eF} - ie^{\mathrm{i}eF}\frac{\partial}{\partial t}e^{-\mathrm{i}eF}, \tag{2.8}$$

where F is an arbitrary classical function [32]. We will choose F to be $r \cdot \vec{A}$ and make a Taylor expansion of the vector potential keeping only the first term. This still leaves us with a choice of the gauge used in the transformation. This is done by choosing the Coulomb gauge where $\phi = 0$ and $\nabla \cdot \vec{A} = 0$. Using this gauge and ignoring terms quadratic in $\vec{A}$ we can transform the Hamiltonian in the following way

$$\begin{aligned} H &= H_0 + \frac{1}{m}e^{\mathrm{i}er\cdot A_0}(A_0 \cdot \hat{p})e^{-\mathrm{i}er\cdot A_0} - ie^{\mathrm{i}er\cdot A_0}\frac{\partial}{\partial t}e^{-\mathrm{i}er\cdot A_0} \\ &= H_0 + \frac{1}{m}e^{\mathrm{i}er\cdot A_0}(A_0 \cdot \hat{p})e^{-\mathrm{i}er\cdot A_0} - e^{\mathrm{i}er\cdot A_0}(e\frac{\partial}{\partial t}r \cdot A_0)e^{-\mathrm{i}r\cdot A_0} \\ &= H_0 - e^{\mathrm{i}er\cdot A_0}(er\frac{\partial A_0}{\partial t})e^{-\mathrm{i}r\cdot A_0} \\ &= H_0 - er\frac{\partial A_0}{\partial t} = H_0 - \hat{\mu}\vec{E}_0, \end{aligned} \tag{2.9}$$

where we have used that $m\frac{\partial\langle r\rangle}{\partial t} = \langle\hat{p}\rangle$ and introduced the dipole operator $\hat{\mu}$. This approximation is called the electric dipole approximation and can be extended by keeping more terms in the Taylor expansion of the vector potential. It is this Hamiltonian that will be our starting point in the following discussion of molecular properties.

2.3 Molecular Properties

When a molecule is subjected to a static electric field the energy of the molecule will be altered. This can be expressed as a Taylor expansion of the energy in terms of powers of the electric field

$$W = W_0 + \left(\frac{dW}{d\vec{E}}\right)_0\vec{E} - \frac{1}{2}\left(\frac{d^2W}{d\vec{E}^2}\right)_0\vec{E}^2 + \frac{1}{3!}\left(\frac{d^3W}{d\vec{E}^3}\right)_0\vec{E}^3 + \cdots. \tag{2.10}$$

In order to make the conection to molecular properties we will use the Hellmann-Feynmann theorem

$$\frac{dW(P)}{dP} = \left\langle\frac{\partial H}{\partial P}\right\rangle, \tag{2.11}$$

where P is some parameter on which the energy depend. The Hellmann-Feynmann theorem is valid for exact and variational optimized wave functions. Using this on the Hamiltonian in Eq. 2.9 with respect to the electric field strength we get

$$\frac{dW(\vec{E})}{d\vec{E}} = \left\langle\frac{\partial(H_0 - \mu\vec{E})}{\partial\vec{E}}\right\rangle = -\langle\mu\rangle. \tag{2.12}$$

The expectation value of a component of the dipole operator in the presence of a static electric field is normally expanded in the following way [33]

$$\langle\mu_\alpha\rangle = \mu^0_\alpha + \alpha_{\alpha\beta}(0;0)E_\beta + \frac{1}{2}\beta_{\alpha\beta\gamma}(0;0,0)E_\beta E_\gamma + \frac{1}{3!}\gamma_{\alpha\beta\gamma\delta}(0;0,0,0)E_\beta E_\gamma E_\delta + \cdots, \tag{2.13}$$

where the expansion coefficients $\alpha_{\alpha\beta}(0;0)$, $\beta_{\alpha\beta\gamma}(0;0,0)$ and $\gamma_{\alpha\beta\gamma\delta}(0;0,0,0)$ are the static molecular dipole polarizability, first and second hyperpolarizability tensors, respectively. We now have a connection between derivatives of the energy and the expectation value of the dipole operator. We can therefore define the molecular polarizability and hyperpolarizability as

$$\alpha_{\alpha\beta}(0;0) = \left.\frac{\partial \langle \mu_\alpha \rangle}{\partial E_\beta}\right|_{\vec{E}=0} = -\left.\frac{d^2W}{dE_\alpha dE_\beta}\right|_{\vec{E}=0}, \tag{2.14}$$

and

$$\beta_{\alpha\beta\gamma}(0;0,0) = \left.\frac{\partial^2 \langle \mu_\alpha \rangle}{\partial E_\beta \partial E_\gamma}\right|_{\vec{E}=0} = -\left.\frac{d^3W}{dE_\alpha dE_\beta dE_\gamma}\right|_{\vec{E}=0}. \tag{2.15}$$

However, since the electric field is time-dependent

$$\vec{E}(t) = \int_{-\infty}^{\infty} d\omega \vec{E}^\omega \cos(\omega t) = \frac{1}{2}\int_{-\infty}^{\infty} d\omega \vec{E}^\omega \left(e^{-i\omega t} + e^{i\omega t}\right), \tag{2.16}$$

the expansion coefficience will also be time-dependent and we can therefore write Eq. 2.13 in the Fourier representation as

$$\begin{aligned} \langle \mu_\alpha \rangle &= \mu_\alpha^0 + \int_{-\infty}^{\infty} d\omega_1 \alpha_{\alpha\beta}(-\omega_1;\omega_1) E_\beta^{\omega_1} \cos(\omega_1 t) \\ &+ \frac{1}{2}\int_{-\infty}^{\infty} d\omega_1 \int_{-\infty}^{\infty} d\omega_2 \beta_{\alpha\beta\gamma}(-\omega_1-\omega_2;\omega_1,\omega_2) E_\beta^{\omega_1} \cos(\omega_1 t) E_\gamma^{\omega_2} \cos(\omega_2 t) \\ &+ \cdots. \end{aligned} \tag{2.17}$$

Since the Hellmann-Feynmann theorem, Eq. 2.11, is only valid in the time-indenpedent case we can not make the link between derivatives of the energy and the molecular properties. We will therefore use Eq. 2.17 when indentifying the molecular properties.

2.3.1 Molecular Properties from Pertubation Theory

In the previous section we defined our static properties as derivatives of the energy with respect to the electric field. We can therefore use time-independent pertubation theory to express the properties in terms of the unpertubed wavefunction. In non-degenerate Rayleigh-Schrödinger pertubation theory we expand the energy and the wavefunction in a series as

$$W = W_0^{(0)} + W_0^{(1)} + W_0^{(2)} + \cdots, \tag{2.18}$$

$$\Psi = \Psi_0^{(0)} + \Psi_0^{(1)} + \Psi_0^{(2)} + \cdots, \tag{2.19}$$

where $W_n^{(0)}$ and $\Psi_n^{(0)}$ are the solutions to the unperturbed problem. The corrections to the energy are then given by [31, 32]

$$W = W^{(0)} + \left\langle \Psi_0^{(0)} \middle| \mu_\alpha \middle| \Psi_0^{(0)} \right\rangle E_\alpha + (1+P(\alpha,\beta)) \sum_{n\neq 0} \frac{\left\langle \Psi_0^{(0)} \middle| \mu_\alpha \middle| \Psi_n^{(0)} \right\rangle \left\langle \Psi_n^{(0)} \middle| \mu_\beta \middle| \Psi_0^{(0)} \right\rangle}{W_0^{(0)} - W_n^{(0)}} E_\alpha E_\beta + \cdots, \tag{2.20}$$

where $P(\alpha,\beta)$ permutes the indices α and β. From this expansion we can indentify the static polarizability as the sum-over-states (SOS) expression as

$$\alpha_{\alpha\beta}(0;0) = -\left.\frac{d^2W}{dE_\alpha dE_\beta}\right|_{\vec{E}=0} = -(1+P(\alpha,\beta)) \sum_{n\neq 0} \frac{\left\langle \Psi_0^{(0)} \middle| \mu_\alpha \middle| \Psi_n^{(0)} \right\rangle \left\langle \Psi_n^{(0)} \middle| \mu_\beta \middle| \Psi_0^{(0)} \right\rangle}{W_n^{(0)} - W_0^{(0)}}. \tag{2.21}$$

A similar expression can be derived using time-dependent pertubation theory to express the expectation value of the dipole operator yielding the following SOS expression for the time-dependent polarizability [31–33]

$$\alpha_{\alpha\beta}(-\omega;\omega) = \sum_{n\neq 0}\left\{\frac{\left\langle\Psi_0^{(0)}\right|\mu_\alpha\left|\Psi_n^{(0)}\right\rangle\left\langle\Psi_n^{(0)}\right|\mu_\beta\left|\Psi_0^{(0)}\right\rangle}{\omega_n-\omega}+\frac{\left\langle\Psi_0^{(0)}\right|\mu_\beta\left|\Psi_n^{(0)}\right\rangle\left\langle\Psi_n^{(0)}\right|\mu_\alpha\left|\Psi_0^{(0)}\right\rangle}{\omega_n+\omega}\right\}. \tag{2.22}$$

Therefore, in order to calculate the polarizability using the SOS expression we have to perform a sum over all excited states in the molecule. This is not possible and therefore the sum is often truncated to the lowest excited states. The SOS expression for calculating molecular properties is often used with semi-empirical methods to study hyperpolarizabilities of large molecules [22].

2.3.2 Molecular Properties from Response Theory

Another way of indentifying molecular properties is to use time-dependent response theory. A derivation of the time-dependent expectation value of an operator is presented in Appendix C. Using the Hamiltonian in Eq. 2.9 and Eq. C.14 we can write the expectation value of the dipole operator as

$$\begin{aligned}\langle\mu_\alpha\rangle &= \left\langle\Psi^{(0)}\right|\mu_\alpha\left|\Psi^{(0)}\right\rangle+\int_{-\infty}^{\infty}d\omega_1 e^{-i\omega_1 t}\left\langle\langle\mu_\alpha;-\mu_\beta\rangle\right\rangle_{\omega_1}\frac{E_\beta^{\omega_1}}{2}\\ &+ \int_{-\infty}^{\infty}d\omega_1 e^{i\omega_1 t}\left\langle\langle\mu_\alpha;-\mu_\beta\rangle\right\rangle_{-\omega_1}\frac{E_\beta^{\omega_1}}{2}+\cdots\\ &= \left\langle\Psi^{(0)}\right|\mu_\alpha\left|\Psi^{(0)}\right\rangle+\int_{-\infty}^{\infty}d\omega_1\left\langle\langle\mu_\alpha;-\mu_\beta\rangle\right\rangle_{\omega_1}E_\beta^{\omega_1}\cos(\omega_1 t)+\cdots,\end{aligned} \tag{2.23}$$

where we have used that a monochromatic pertubation operator in the Fourier representation can be written as

$$V^\omega = -\mu_\alpha\frac{E_\alpha^{\omega_0}}{2}(\delta(\omega-\omega_0)+\delta(\omega+\omega_0)), \tag{2.24}$$

and that the response functions $\langle\langle\mu_\alpha;\mu_\beta\rangle\rangle_{\omega_1}$ and $\langle\langle\mu_\alpha;\mu_\beta\rangle\rangle_{-\omega_1}$ are equal. This allows us to indentify the polarizability and hyperpolarizability as the linear and quadratic response function, respectively :

$$\alpha_{\alpha\beta}(-\omega;\omega) = -\left\langle\langle\mu_\alpha;\mu_\beta\rangle\right\rangle_{\omega_1}, \tag{2.25}$$

$$\beta_{\alpha\beta\gamma}(-\omega_1-\omega_2;\omega_1,\omega_2) = -\left\langle\langle\mu_\alpha;\mu_\beta,\mu_\gamma\rangle\right\rangle_{\omega_1,\omega_2}. \tag{2.26}$$

In Appendix C it is also shown that the response functions are indentical with the SOS expression. From the SOS-expression we see that responce functions have poles at the excitation energies of the unpertubed system and, that the residues at the poles correspond to the dipole transitions moments.

2.4 Calculating (hyper-)Polarizabilies

For some time, static molecular polarizabilities have been calculated using the Finite Field method, i.e. the molecular dipole moment is calculated for a set of explicit external electric fields and the polarizability is obtained from numerical differentiation [34–36]. A more attractive and computationally more efficient approach is to adopt quantum chemical response theory. For a general overview of calculating nonlinear properties see ref. [22, 24]. We will restrict the calculation to the SCF-level because of the computational time and the fact that we are more

interested in fundamental aspects rather than obtaining highly accurate values. In appendix B the optimization of the SCF wave function is described and appendix C describes how the SCF wave function can be used to calculate the response functions by solving linear sets of equations. The SCF (or Hartree-Fock) approach is a mean field approach meaning that the interaction between the electrons are only accounted for in an average way. The instantaneous electrostatic interaction (electron correlation) between electrons in the molecule are therefore not accounted for. Electron correlation can be accounted for using e.g. Coupled Cluster (CC) or Configuration Interaction(CI) methods, but with an increase in computational time. Response theory using a SCF wave function as reference state is often refered to as the Random Phase Approximation (RPA).

2.5 Macroscopic vs. Microscopic Properties

Until now we have only discussed the properties in terms of a single molecule, but experiments are in general done on a assembly of molecules. We therefore have to make some connection between our microscopic (molecular) properties and the macroscopic properties measured in experiments. The macroscopic polarization of the medium due to an external field $\mathbf{E}$ is given by Eq.2.1. We can write a similar expansion of the polarization of a single molecule as

$$\mathbf{p} = \alpha^{\text{eff}}\mathbf{E} + \frac{1}{2}\beta^{\text{eff}}\mathbf{E}^2 + \cdots. \tag{2.27}$$

The macroscopic susceptibilities are assumed related to the molecular susceptibilties by [28, 37]

$$\begin{aligned} \chi^{(1)}(-\omega;\omega) &= N f^{(1)}(-\omega;\omega)\overline{\alpha}^{\text{eff}}(-\omega;\omega), \\ \chi^{(2)}(-\omega_m-\omega_n;\omega_m,\omega_n) &= N f^{(2)}(-\omega_m-\omega_n;\omega_m,\omega_n)\overline{\beta}^{\text{eff}}(-\omega_m-\omega_n;\omega_m,\omega_n). \end{aligned} \tag{2.28}$$

The $\overline{\alpha}^{\text{eff}}$ and $\overline{\beta}^{\text{eff}}$ are orientationally averaged microscopic molecular properties and N is the number density. The $f^{(n)}$-factors are known as local field factors and correct for the difference between the applied macroscopic field and the local microscopic field felt by the molecules. The averaged microscopic molecular properties have to be calculated under the influence of the media into which the molecule is embedded. In a diluted gas there is no difference between the applied field and the local field. Therefore the local field factors are equal to unity and a direct comparison between experiments and calculations is possible. In the case of the liquid phase a determination of the local field factor often involves the Lorentz correction factor given by [37, 38]

$$f^{\omega} = \frac{1}{3}(\epsilon_{\omega}+2) = \frac{1}{3}(n_{\omega}^2+2), \tag{2.29}$$

where ϵ is the dielectric constant and n is the index of refraction. ω refers to the frequency of the external applied field. When this is used the local field factors in Eq. 2.28 are given by

$$\begin{aligned} f^{(1)}(-\omega;\omega) &= f^{\omega} f^{\omega} \\ f^{(2)}(-\omega_m-\omega_n;\omega_m,\omega_n) &= f^{\omega_m+\omega_n} f^{\omega_m} f^{\omega_n} \end{aligned} \tag{2.30}$$

In the case of a static field the Onsager expression is often used to decribe the local field factors [37].

$$f^0 = \frac{\epsilon_0(\epsilon_\omega + 2)}{2\epsilon_0 + \epsilon_\omega} = \frac{\epsilon_0(n^2 + 2)}{2\epsilon_0 + n^2}. \tag{2.31}$$

The subject of local field factors have also been the discussion of some recent investigations [39–41]. The effective polarizabilities in Eq. 2.28 have a vibrational, rotational and an electronic contribution. It is only the electronic contribution that are calculated in the RPA approach and therefore care has to be taken when comparing directly with experiments. A review by Bishop on the calculation of the vibrational and rotational contribution to the polarizabilty can be found in ref. [42]. In this treatment we will however ignore vibrational contributions and consider the rotational contribution by classical averaging over rotational states as [42]

$$\overline{\alpha}_{ZZ} = \frac{\int_0^{2\pi}\int_0^{\pi} \alpha_{ij}k_ik_je^{-\Delta E/kT}\sin\theta d\theta d\phi}{\int_0^{2\pi}\int_0^{\pi} e^{-\Delta E/kT}\sin\theta d\theta d\phi}, \tag{2.32}$$

where the k_i is the cosine of the angle between the molecular axis i and the laboratory axis Z. Upper case indices refer to laboratory fixed axises where as lower case indices refer to molecular axises. The energy in Eq. 2.32 is given by $-\Delta E = \mu_i k_i E + \alpha_{ij}k_ik_jE^2 + \cdots$, and an expansion of $\exp(-\Delta E/kT)$ gives

$$\overline{\alpha}_{ZZ} = \langle\alpha\rangle_{ZZ} + O(T), \tag{2.33}$$

where $O(T)$ designate the terms which are temperature dependent and $\langle\alpha\rangle_{ZZ}$ is the isotropic average given by

$$\begin{aligned}
\langle\alpha\rangle_{ZZ} &= \frac{1}{4\pi}\int_0^{2\pi}\int_0^{\pi} \alpha_{ij}k_ik_j\sin\theta d\theta d\phi \\
&= \frac{1}{2}\left[-\frac{1}{3}\cos^3\theta\right]_0^{2\pi}\alpha_{ii} \\
&= \frac{1}{3}(\alpha_{xx} + \alpha_{yy} + \alpha_{zz}).
\end{aligned} \tag{2.34}$$

In a similary manner isotropic averaged expressions for the hyperpolarizabilities may be obtained as

$$\langle\beta\rangle_{ZZZ} = \frac{1}{5}(\beta_{zii} + \beta_{izi} + \beta_{iiz}), \tag{2.35}$$

$$\langle\beta\rangle_{XXZ} = \frac{1}{5}(2\beta_{zii} - 3\beta_{izi} + 2\beta_{iiz}). \tag{2.36}$$

We have now made the connection between properties calculated using the RPA approach and the experimental properties. Since we only calculate the gas phase molecular properties ignoring vibrational contributions, we should compare with gas phase experiments or only use the experimental value as a guideline.

2.6 Experimental Polarizabiltities

We will restict the treatment of experimental methods to two traditional ways of determining the mean polarizability. For a more complete review on experimental determination of the polarizability see ref. [43] and for a description of experimental ways to determine the nonlinear response see e.g. ref. [28]. The polarizability can be related to the dielectric constant, ϵ, by the Debye equation [38]

$$\overline{\alpha}(0;0) = \frac{3}{4\pi\mathcal{N}}\frac{\epsilon - 1}{\epsilon + 2} - \frac{\mu_0^2}{3kT}, \tag{2.37}$$

where $\overline{\alpha}(0;0)$ is the average polarizability defined in Eq. 2.34, $\mathcal{N}$ is the number density and μ_0 is the permanent dipole moment. When the permanent dipole moment is zero, Eq. 2.37 reduces to the Clausius-Mossotti equation [38]. The experiment is done by measuring the capacitance, C, and then relating it to the dielectric contant by $\epsilon = \frac{lC}{A\epsilon_0}$, where ϵ_0 is the vacuum permitivity, l is the thickness and A is the area of the capacitor [43].
The frequency-dependent polarizability can be related to the index of refraction, n, i.e. the ratio of the speed of light in vacuum to the speed of light in the material. When the frequency is sufficiently high, so that the permanent dipole moment cannot instantaneously follow the electric field, the Lorentz-Lorenz equation can be used to make the following relation [38]

$$\overline{\alpha}(-\omega;\omega) = \frac{3}{4\pi\mathcal{N}}\frac{n^2 - 1}{n^2 + 2}. \tag{2.38}$$

The Lorentz-Lorenz equation and the Clausius-Mossotti equation are related by the Maxwell relation $\epsilon = n^2$.

Chapter 3

Modelling Molecular Properties

The molecular properties, that we are interested in, are the frequency-dependent molecular polarizability and first and second hyperpolarizability. As shown in section 2.3 and 2.4, these properties can be calculated using quantum chemical methods, but they are currently limited to small molecules due to large requirements in computational time. Therefore, if we are interested in molecular properties of large molecules such as polymers, proteins, molecular crystals or nanotubes, we have to use less sophisticated methods in order to calculate these properties. The idea that a simple model predicts molecular properties of both small and large molecules is very appealing. Thus several studies of this kind has previosly been undertaken. We will restrict our treatment to two models, i.e. the additivity model and the interaction model because of the simplicity of both models. Other models, that should be mentioned, are the work on the first hyperpolarizability by Oudar and Chemla [44,45]. They found that the first hyperpolarizability of donor/acceptor π-systems could be described by a sum of two contributions, $\beta = \beta_{\text{add}} + \beta_{\text{ct}}$, where β_{add} is an additive contribution arising from the substituents and β_{ct} is the contribution arising from the charge transfer between donor/acceptor. The charge transfer term was described by a two-level interaction between the ground state and the first excited state. This two-level approach has proven valuable for analysing calculations within the SOS-formalism [22,46]. Also, the coupled anharmonic oscillator model by Prasad *et. al.* [47] used to predict the polarizability and second hyperpolarizability as a function of repeated units of oligomers of thiophene and benzene is very illustative.

3.1 The Additivity Model

The molecular polarizability is to a good extent an additive property, indicating that the polarizability can be calculated simply from a sum of transferable atomic or bond contributions. Perfect additivity can only occur if the sub-units are non-interacting, which obviously is not the case for atoms in molecules. Therefore, a very simple model assigning one polarizability parameter to each type of atom and adding the contributions fails, see fig. 3.1. One of the earliest attemps to overcome this problem was the bond polarizability model [48] where each type of bond in the molecule was assigned a polarizability, which then were summed. This model was quite accurate in predicting the static mean polarizability of alkanes [49]. Several other methods using the additivity concept to calculate the static mean polarizability have been proposed using either atomic hybridization [50, 51] or atomic hybrid polarizabilities [52], where each atom is assigned a parameter accordingly to its state of hybridization. Also, recently has the additivity model been adopted for the static polarizability tensors of organic molecules [53, 54] and futhermore also for both the static and frequency-dependent polarizability tensors of halogen-derivatives of benzene [55] using atomic polarizability tensor elements. However, since the molecular polarizabilities are tensors, also the atomic contributions have to be tensors.

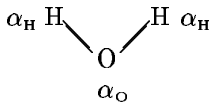

$$, \alpha^{mol} \approx \sum_p \alpha_p$$

Figure 3.1: Molecular polarizability is only approximatively a sum of atomic polarizability parameters.

The additivity model has been quite successfully in describing the static molecular polarizability. However, the use of the additivity model on the hyperpolarizabilites has shown to be less successful [44, 45, 56, 58]. Levine and Bethea [56] used scalar bond additivity for the second hyperpolarizability and vector bond additivity [57] for the first hyperpolarizability. They found for a very small set of experimental data, that the additivity model could to some extent describe the hyperpolarizabilities. By using additivity of atomic (hyper-)polarizability tensors on a set of organic molecules Zhou and Dykstra [58] found good agreement for the polarizability and reasonable agreement for the second hyperpolarizability.

3.2 The Interaction Model

Atoms are spherical particles and therefore atomic polarizabilities are isotropic, implying only one physical atomic polarizability parameter. Using isotropic atomic polarizabilities one needs an interaction model in order to describe the molecular polarizability tensors. An atom dipole interaction model was introduced by Silberstein [59–61] and was then to a large extent developed by Applequist *et. al.* [62–64]. The principle of the interaction model is that atoms in a molecule are regarded as isotropic particles, which interact by means of their atomic dipole moments induced by an external field. Since the dipole fields are anisotropic the molecule as a whole also becomes anisotropic. Both in the additivity and interaction models, the atomic (or bond) polarizabilities are fitted to the molecular polarizabilities of a trail set of molecules. Applequist *et. al.* [62] fitted there parameters to experimental mean polarizabilities and found that their model predicted mean polarizabiliy well but overshot the anisotropy. Birge [65] showed that the large anisotropy could be remove by using an extra atomic anisotropy parameter and including the effect of electron repulsion. Both parameterizations showed that the transferability of the parameters between different classes of molecules was rather bad. Therfore, they needed different parameters depending on the chemical environment. Thole [66] corrected this by replacing the point dipole interaction with a smeared out (damped) dipole interaction and thereby reducing the parameter set to atomic-type polarizabilities plus one overall damping parameter. Applequist *et. al.* [64] showed that the large anisotropy in their original work could be corrected by including anisotropy data in the parameterization.

All of the above investigations were on aliphatic systems and calculations on molecules having π-systems indicated that the model failed for such systems [63]. Olson and Sundberg [67] extended the dipole interaction model to include charge transfer effects between atoms. This was done by treating the atoms as capacitive points connected by conducting but noncapacitive wires. Applequist [68] adopted this model and found for a series af planer aromatic molecules that some modifications of the model was needed in order to obtain a physical parametrization. This modification, refered to as the partial neglet of ring interactions, consisted of introducing two parameters for each carbon atom, one perpendicular to and one in the plane of the molecule. Using this he found an improvement for the aromatic molecules, but for a serie of alkanes no

improvement was found.
Sundberg [69] has generalized the atomic dipole interaction model to include the molecular polarizability and the first and second hyperpolarizabilities. He used this model to treat the mean molecular second hyperpolarizability of a set of haloalkanes [70] and found reasonable agreement with experimental values. The interaction model has also been adopted with bond parameters and used to treat the molecular dipole moment, polarizability and hyperpolarizabilities [71, 72], showing the same accuracy.

3.3 Choice of Model

Since the interaction model originates from classical electrostatic it is more attractive from a physical point of view than the more simple additivity model. Also, the fact that there is an explicit dependence on the molecular geometry in the interaction model speaks in favour of this model. The explicit geometry dependence lacking in the additivity model is reflected in the fact that the model predicts the same polarizability of e.g. cis-trans isomers [56, 58]. The additivity model is a bit simpler than the interaction model and therefore also a bit faster computionally speaking. The small increase in the computational time is well spend, due to the explicit geometry dependence and the systematic ways of extending the model. The usefulness of the explicit geometry dependence of the interaction model is illustrated in the application of the model to e.g. optical rotation [73, 74], raman optical activity [75] and in polarizable force fields [76, 77]. We will, therefore, use the interaction model and the theory used in this thesis is presented in the following sections.

3.4 The Applequist Model

The molecular dipole moment induced by an external electric field is give by the sum of the induced atomic dipole moments

$$\mu_{\mathrm{mol}} = \sum_p \mu_p = \sum_p \sum_\alpha \mu_{p,\alpha}, \tag{3.1}$$

where indices $p, q, \cdots$, refer to atoms and indices $\alpha, \beta, \cdots$, denote cartesian components. A component of the atomic dipole moment in the present of a uniform electric field is given by a Taylor expansion in terms of the local field

$$\mu_{p,\alpha} = \alpha_{p,\alpha\beta} E^{\mathrm{tot}}_{p,\beta} + \frac{1}{6}\gamma_{p,\alpha\beta\gamma\delta} E^{\mathrm{tot}}_{p,\beta} E^{\mathrm{tot}}_{p,\gamma} E^{\mathrm{tot}}_{p,\delta} + \cdots, \tag{3.2}$$

where E^{tot}_p is the local electric field at atom p. Due to symmetry reasons the permanent dipole moment and the first hyperpolarizability vanish for a spherically symmetric element, i.e. an atom [33]. In the following we will truncate Eq. 3.2 after the polarizability term and the atomic induced dipole moment is thus given by

$$\mu_{p,\alpha} = \alpha_{p,\alpha\beta} E^{\mathrm{tot}}_{p,\beta}. \tag{3.3}$$

The electric field at atom p consists of a sum of the applied external field and the field from the induced dipole moments of the other atoms. The field can be written in the following way, where E^{ext}_β is a component of the applied field

$$E^{\mathrm{tot}}_{p,\beta} = E^{\mathrm{ext}}_\beta + \sum_{q \neq p} T^{(2)}_{pq,\alpha\beta} \mu_{q,\beta}, \tag{3.4}$$

and $T_{pq}^{(2)}$ is the dipol interaction tensor. An element in the dipole interaction tensor is defined as [38]

$$T_{pq,\alpha\beta}^{(2)} = \frac{3r_{pq,\alpha}r_{pq,\beta}}{R_{pq}^5} - \frac{\delta_{\alpha\beta}}{R_{pq}^3}, \tag{3.5}$$

where $r_{pq,\alpha}$ is a component of the vector from atom p to q and R_{pq} is the distance between atom p and q. If we consider a set of N atoms, each with an isotropic atomic polarizability $\alpha_{\alpha\beta} = \alpha\delta_{\alpha\beta}$ then the induced dipole moment of atom p can be written as

$$\mu_{p,\alpha} = \alpha_p \left(E_\alpha^{\text{ext}} + \sum_{q \neq p} T_{pq,\alpha\beta}^{(2)} \mu_{q,\beta} \right). \tag{3.6}$$

Rearranging Eq. 3.6 as

$$\alpha_p^{-1}\mu_{p,\alpha} - \sum_{q \neq p} T_{pq,\alpha\beta}^{(2)} \mu_{q,\beta} = E_\alpha^{\text{ext}}, \tag{3.7}$$

we obtain a system of N matrix equations which can be written as one matrix equation

$$\begin{bmatrix} \alpha_1^{-1} & -T_{12}^{(2)} & \cdots & -T_{1N}^{(2)} \\ -T_{21}^{(2)} & \alpha_2^{-1} & \cdots & -T_{2N}^{(2)} \\ \vdots & \vdots & \ddots & \vdots \\ -T_{N1}^{(2)} & -T_{N2}^{(2)} & \cdots & \alpha_N^{-1} \end{bmatrix} \begin{bmatrix} \mu_1 \\ \mu_2 \\ \vdots \\ \mu_N \end{bmatrix} = \begin{bmatrix} E^{\text{ext}} \\ E^{\text{ext}} \\ \vdots \\ E^{\text{ext}} \end{bmatrix}. \tag{3.8}$$

We now introduce a supermatrix notation as

$$\mu = \left(\alpha^{-1} - T^{(2)} \right)^{-1} E^{\text{ext}}, \tag{3.9}$$

where μ and E^{ext} are $3N$-dimensional vectors and α^{-1} and $T^{(2)}$ are $3N \times 3N$ matrices. We can define a two-atom relay tensor B as

$$B = \left(\alpha^{-1} - T^{(2)} \right)^{-1}, \tag{3.10}$$

where the name relay tensor indicates that the polarizability at atom p is relayed to the induced dipole moment at atom q. The molecular dipole moment, μ^{mol}, is then

$$\mu^{\text{mol}} = \left[\sum_p^N \sum_q^N B_{pq} \right] E^{\text{ext}} = \alpha^{\text{mol}} E^{\text{ext}}, \tag{3.11}$$

from which it is seen that the molecular polarizability, α^{mol}, is given by [62]

$$\alpha^{\text{mol}} = \sum_p^N \sum_q^N B_{pq}. \tag{3.12}$$

This is the approach taken by Applequist *et. al.* [62–64] in their original work and will from here on be refered to as the Applequist model.

3.5 The Thole Model

If we consider a case of a diatomic molecule $X - Y$ whose atoms have isotropic polarizabilities α_X and α_Y, respectively, we can rewrite the relay tensor explicitly as

$$B = \frac{1}{\alpha_X^{-1}\alpha_Y^{-1} - T_{XY}^{(2)}T_{XY}^{(2)}} \begin{bmatrix} \alpha_Y^{-1} & T_{XY}^{(2)} \\ T_{XY}^{(2)} & \alpha_X^{-1} \end{bmatrix}. \tag{3.13}$$

If we expand the relay matrix according to Eq. 3.12 we can write the molecular polarizability as

$$\alpha^{\text{mol}} = \frac{\alpha_X + \alpha_Y + 2T_{XY}^{(2)}\alpha_X\alpha_Y}{1 - \alpha_X\alpha_Y T_{XY}^{(2)}T_{XY}^{(2)}}. \tag{3.14}$$

The molecular polarizability of a diatomic molecule has two distinct components, namely $\alpha_\parallel$ and $\alpha_\perp$, parallel and perpendicular to the bond axis, respectively. If we place the atom along one of the cartesian axises we can write the interaction tensor as

$$T_{XY}^{(2)}(\parallel) = 2/r^3, \tag{3.15}$$

$$T_{XY}^{(2)}(\perp) = -1/r^3. \tag{3.16}$$

Inserting this explicit interaction tensor in Eq.3.14 gives Silberstein's equations [61]

$$\alpha_\parallel = \frac{\alpha_X + \alpha_Y + 4\alpha_X\alpha_Y/r^3}{1 - 4\alpha_X\alpha_Y/r^6}, \tag{3.17}$$

$$\alpha_\perp = \frac{\alpha_X + \alpha_Y - 2\alpha_X\alpha_Y/r^3}{1 - \alpha_X\alpha_Y/r^6}. \tag{3.18}$$

Inspection of Eqs. 3.17 and 3.18 shows that when r approaches $(4\alpha_X\alpha_Y)^{1/6}$ then $\alpha_\parallel$ goes to infinity, and in a similar manner does $\alpha_\perp$ when r approaches $(\alpha_X\alpha_Y)^{1/6}$. This means that the dipole interaction model predicts that the molecular polarizability goes to infinity when the distance between the atoms becomes to small. This effect is similar to what is observed in a system of undamped coupled harmonic oscillators. This is not observed in reality and therefore some sort of damping of the interaction at small distances must occur. Thole [66] included this damping by considering smeared out charge distributions and thereby modifying the interaction tensor in the following way

$$T_{pq,\alpha\beta}^{(2)} = \frac{3\upsilon_{pq}^4 r_{pq,\alpha}r_{pq,\beta}}{R_{pq}^5} - \frac{(4\upsilon_{pq}^3 - 3\upsilon_{pq}^4)\delta_{\alpha\beta}}{R_{pq}^3}, \tag{3.19}$$

where $\upsilon_{pq} = \frac{r_{pq}}{s_{pq}}$ if $r_{pq} < s_{pq}$ and if $r_{pq} > s_{pq}$ then $\upsilon_{pq} = 1$ and the normal interaction tensor is recovered. Thole defined the scaling factor s_{pq} as

$$s_{pq} = c_d(\alpha_p\alpha_q)^{1/6}, \tag{3.20}$$

where c_d is an extra fitting parameter originally obtained by Thole as $c_d = 1.662$ [66]. The scaling factor $(\alpha_p\alpha_q)^{1/6}$ has dimension of length and can thus be related to the average radius of atom p and q. This model is refered to as the Thole model. Since the scaling factor is propertional to the average radius of the atoms we can introduce an extra set of parameters, Φ_p, propertional to the second order moments of the atoms as

$$s_{pq} = (\Phi_p\Phi_q)^{\frac{1}{4}}. \tag{3.21}$$

This model with the extra set of parameters will be termed the modified Thole model. Accordingly we can also modify the zero and first order interaction tensors respectively as [66]

$$T_{pq}^{(0)} = \frac{(\upsilon_{pq}^4 - 2\upsilon_{pq}^3 + 2\upsilon_{pq})}{R_{pq}}, \tag{3.22}$$

$$T_{pq,\alpha}^{(1)} = -\frac{(4\upsilon_{pq}^3 - 3\upsilon_{pq}^4) r_{pq,\alpha}}{R_{pq}^3}. \tag{3.23}$$

These zero and first order interaction tensors will be used in the following section.

3.6 The Olson-Sundberg Model

Following the approach of Olson and Sundberg [67] we will introduce a set of atomic capacitances connected with conducting but noncapacitive wires in order to allow for charge transfer within the molecule. The idea is to minimize the total energy of the molecule in the presence of the external field. First, we recall that the energy of a capacitive point in an external potential, ϕ^{ext}, is

$$V = \frac{q^2}{2a} + q\phi^{\text{ext}}, \tag{3.24}$$

where q is the induced charge and a is the capacitance. The first term is the self-energy required for creating an induced charge and the second term is the interaction with the external potential. Now we construct the energy expression for a molecule with N atoms subjected to an external field, where each atom possess a capacitance, a_p, and a polarizability, $\alpha_{p,\alpha\beta}$. The energy of the N induced dipole moments is given by [38]

$$V_{\mu\mu} = \frac{1}{2}\sum_{p}^{N} \alpha_{p,\alpha\beta}^{-1} \mu_{p,\alpha}\mu_{p,\beta} - \frac{1}{2}\sum_{p}^{N}\sum_{q\neq p}^{N} T_{pq,\alpha\beta}^{(2)} \mu_{p,\alpha}\mu_{q,\beta} - \sum_{p}^{N} E_{\alpha}^{\text{ext}} \mu_{p,\alpha}, \tag{3.25}$$

where μ is the dipole moment, $T^{(2)}$ is the interaction tensor in Eq. 3.19 and E^{ext} is the uniform external field. The first term is the self-energy required for creating an induced dipole moment, the second term is the interaction between dipole moments on different atoms and the last term is the interaction with the external electric field. Analogously, the energy of N induced atomic charges is given as [67]

$$V_{qq} = \frac{1}{2}\sum_{p}^{N} \frac{q_p^2}{a_p} + \frac{1}{2}\sum_{p}^{N}\sum_{q\neq p}^{N} q_p q_q T_{pq}^{(0)} + \sum_{p}^{N} q_p \phi_p^{\text{ext}} - \lambda \sum_{p}^{N} q_p, \tag{3.26}$$

where $T_{pq}^{(0)}$ is the zero order interaction tensor defined in Eq. 3.22. The last term is a Lagrange multiplier which is included to ensure electrical neutrality during energy minimization. Finaly, the interaction between the charges and the dipoles is given as [38]

$$V_{q\mu} = \sum_{p}^{N}\sum_{q\neq p}^{N} q_p T_{pq,\alpha}^{(1)} \mu_{q,\alpha} = -\sum_{p}^{N}\sum_{q\neq p}^{N} \mu_{p,\alpha} T_{pq,\alpha}^{(1)} q_q. \tag{3.27}$$

The total energy is given as the sum of the above contributions

$$V = V_{qq} + V_{q\mu} + V_{\mu\mu}. \tag{3.28}$$

We continue by minimizing the total energy with respect to the induced charges, dipole moments and the Lagrange multiplier,

$$\frac{\partial V}{\partial \mu_{p,\alpha}} = 0 = \alpha^{-1}_{p,\alpha\beta}\mu_{p,\beta} - \sum_{q\neq p}^{N} T^{(2)}_{pq,\alpha\beta}\mu_{q,\beta} - E^{\text{ext}}_{\alpha} - \sum_{q\neq p}^{N} T^{(1)}_{pq,\alpha} q_q, \tag{3.29}$$

$$\frac{\partial V}{\partial q_p} = 0 = \frac{q_p}{a_p} + \sum_{q\neq p}^{N} q_q T^{(0)}_{pq} + \phi^{\text{ext}}_p + \sum_{q\neq p}^{N} T^{(1)}_{pq,\alpha}\mu_{q,\alpha} - \lambda, \tag{3.30}$$

$$\frac{\partial V}{\partial \lambda} = 0 = \sum_{p}^{N} q_p. \tag{3.31}$$

Eq. 3.29, 3.30 and 3.31 constitutes a set of linear equations which can be written in matrix form by defining the following submatrix elements

$$A_{pp,\alpha\beta} = \alpha^{-1}_{p,\alpha\beta} \;;\; A_{pq,\alpha\beta} = -T^{(2)}_{pq,\alpha\beta} \;(p \neq q), \tag{3.32}$$

$$M_{pp,\alpha} = 0 \;;\; M_{pq,\alpha} = T^{(1)}_{pq,\alpha} \;(p \neq q), \tag{3.33}$$

$$C_{pp} = a_p^{-1} \;;\; C_{pq} = T^{(0)}_{pq} \;(p \neq q). \tag{3.34}$$

Using these definitions we can write the set of equations as

$$E^{\text{ext}}_{\alpha} = \sum_{q} A_{pq,\alpha\beta}\mu_{q,\beta} - \sum_{q} M_{pq,\alpha} q_q, \tag{3.35}$$

$$\phi^{\text{ext}}_p = -\sum_{q} M_{pq,\alpha}\mu_{q,\alpha} - \sum_{q} C_{pq} q_q + \lambda, \tag{3.36}$$

$$0 = \sum_{q} q_q. \tag{3.37}$$

We now write this set of equations as a single matrix equation

$$\begin{pmatrix} E^{\text{ext}} \\ \phi^{\text{ext}} \\ 0 \end{pmatrix} = \begin{pmatrix} A & -M & 0 \\ -M^T & -C & 1 \\ 0 & 1 & 0 \end{pmatrix} \begin{pmatrix} \mu \\ q \\ \lambda \end{pmatrix}, \tag{3.38}$$

where we have introduced the submatrix notation. The dimension of the matrix is $(4N+1) \times (4N+1)$ arising from $3N$ dipoles, N charges and the Lagrange multiplier. Superscript T indicates tranposition . We solve for the dipole moments and charges in Eq. 3.38 by inverting the matrix

$$\begin{pmatrix} \mu \\ q \\ \lambda \end{pmatrix} = \begin{pmatrix} A & -M & 0 \\ -M^T & -C & 1 \\ 0 & 1 & 0 \end{pmatrix}^{-1} \begin{pmatrix} E^{\text{ext}} \\ \phi^{\text{ext}} \\ 0 \end{pmatrix} = \begin{pmatrix} B & g & h_1 \\ g^T & D & h_2 \\ h_1^T & h_2^T & h_3 \end{pmatrix} \begin{pmatrix} E^{\text{ext}} \\ \phi^{\text{ext}} \\ 0 \end{pmatrix}, \tag{3.39}$$

where we have written the inverted matrix as a blockmatrix. We can now indentify the terms contributing to the induced molecular dipole moment as

$$\begin{aligned} \mu^{mol}_{\alpha} &= \sum_{p} \mu_{p,\alpha} + \sum_{p} r_{p,\alpha} q_p \\ &= \sum_{p,q} B_{pq,\alpha\beta} E^{\text{ext}}_{\beta} + \sum_{p,q} g_{pq,\alpha}\phi^{\text{ext}}_q + \sum_{p} r_{p,\alpha} \sum_{q} \left(g_{qp,\beta} E^{\text{ext}}_{\beta} + D_{pq}\phi^{\text{ext}}_q \right). \end{aligned} \tag{3.40}$$

If ϕ_q^{ext} is the potential of a uniform field and we ignore the arbitrary constant contribution to the potential, we can write it as

$$\phi_p^{\text{ext}} = r_{p,\alpha} E_\alpha^{\text{ext}}, \tag{3.41}$$

and the total induced dipole moment is then given by

$$\mu_\alpha^{\text{mol}} = \sum_{p,q} \left(B_{pq,\alpha\beta} + g_{pq,\alpha} r_{q,\beta} + r_{p,\alpha} g_{qp,\beta} + r_{p,\alpha} D_{pq} r_{q,\beta} \right) E_\beta^{\text{ext}}. \tag{3.42}$$

Using that the matrix g has the useful property[1]

$$\sum_p g_{pq,\alpha} = \sum_q g_{pq,\alpha} = 0, \tag{3.43}$$

all contributions involving g in Eq. 3.42 vanish and the induced dipole moment becomes

$$\mu_\alpha^{\text{mol}} = \sum_{p,q} \left(B_{pq,\alpha\beta} + r_{p,\alpha} D_{pq} r_{q,\beta} \right) E_\beta^{\text{ext}}. \tag{3.44}$$

This leads to identifying the molecular polarizability as [67]

$$\alpha_{\alpha\beta}^{\text{mol}} = \sum_{p,q} \left(B_{pq,\alpha\beta} + r_{p,\alpha} D_{pq} r_{q,\beta} \right). \tag{3.45}$$

This model where we have introduced an atomic capacitance in order to describe intramolecular charge transfer will be termed the Olson-Sundberg model. As seen from in Eq. 3.44, the molecular dipole moment is zero if there is no external electric field and that is not true. The remedy is to consider the nuclear charges separately as described in the next section.

3.6.1 Inclusion of the Internal Field

The inclusion of the internal field of a molecule is accomplished by a minor modification of the Olson-Sundberg model and we will therefore use the same notation and follow their derivation as closely as possible. It should be noted that even if our method formally is very similar to the approach by Olson and Sundberg [67], it will be apparant that it is conceptually different. The atomic charge, q_p, may be divided into two parts: the nuclear charge, Z_p, and the electronic charge, N_p,

$$q_p = Z_p + N_p. \tag{3.46}$$

It is noted that it is only the electrons that can respond instantaneously to an external field and therefore contribute to the molecular polarizability. It should, therefore, be more correct to differentiate Eq. 3.30 with respect to N_p instead of q_p and treat the contributions from Z_p separately. Utilizing this separation Eq. 3.29 is rewritten as

$$\frac{\partial V}{\partial \mu_{p,\alpha}} = 0 = \alpha_{p,\alpha\beta}^{-1} \mu_{p,\beta} - \sum_{q \neq p}^{N} T_{pq,\alpha\beta}^{(2)} \mu_{q,\beta} - E_{p,\alpha}^{\text{perm}} - \sum_{q \neq p}^{N} T_{pq,\alpha}^{(1)} N_q, \tag{3.47}$$

where we have introduced the permanent electric field, $E_{p,\alpha}^{\text{perm}}$, which consists of the external field and an internal field arising from the nuclear charges

[1] Seen from the relations XX^{-1}=I and $X^{-1}X$=I of the matrices in Eq. 3.39

$$E^{\text{perm}}_{p,\alpha} = E^{\text{ext}}_{\alpha} + E^{\text{int}}_{p,\alpha} = E^{\text{ext}}_{\alpha} + \sum_{q\neq p}^{N} T^{(1)}_{pq,\alpha} Z_q. \tag{3.48}$$

Similar, Eq. 3.30 will, when differentiated with respect to the N_p then look like

$$\frac{\partial V}{\partial N_p} = 0 = \frac{N_p + Z_p}{a_p} + \sum_{q\neq p}^{N} N_q T^{(0)}_{pq} + \phi^{\text{perm}}_p + \sum_{q\neq p}^{N} T^{(1)}_{pq,\alpha}\mu_{q,\alpha} - \lambda, \tag{3.49}$$

where the permanent potential is given by the external and internal contributions as

$$\phi^{\text{perm}}_p = \phi^{\text{ext}}_p + \phi^{\text{int}}_p = \phi^{\text{ext}}_p + \sum_{q\neq p}^{N} Z_q T^{(0)}_{pq}. \tag{3.50}$$

In order to rearrange the equations in a manner similar to what was done in the previous section we introduce a new parameter, b_p, such that

$$\frac{N_p}{b_p} = \frac{N_p + Z_p}{a_p}. \tag{3.51}$$

The differentiation of the energy with respect to the Lagrange multiplier, Eq. 3.31, is trivially rewritten as

$$\frac{\partial V}{\partial \lambda} = 0 = \sum_{p}^{N} N_p + \sum_{p}^{N} Z_p. \tag{3.52}$$

Using the same notation as in Eq. 3.32 - 3.34 (apart from $C_{pp} = b_p^{-1}$) and writing it as the inverted matrix equation where we have solved for the dipole moment and charge we get

$$\begin{pmatrix} \mu \\ N \\ \lambda \end{pmatrix} = \begin{pmatrix} A & -M & 0 \\ -M^T & -C & 1 \\ 0 & 1 & 0 \end{pmatrix}^{-1} \begin{pmatrix} E^{\text{perm}} \\ \phi^{\text{perm}} \\ -Z \end{pmatrix} = \begin{pmatrix} B & g & h_1 \\ g^T & D & h_2 \\ h_1^T & h_2^T & h_3 \end{pmatrix} \begin{pmatrix} E^{\text{perm}} \\ \phi^{\text{perm}} \\ -Z \end{pmatrix}, \tag{3.53}$$

where $Z = \sum_p Z_p$ is the total nuclear charge. In comparison to the Olson-Sundberg model, the main difference is that the right-hand side contains the permanent potentials and electric fields, which also include contributions from nuclear charges. Again, we can indentify the terms contributing to the molecular dipole moment, now given in terms of the permanent field and potential

$$\begin{aligned} \mu^{\text{mol}}_{\alpha} &= \sum_{p} \mu_{p,\alpha} + r_{p,\alpha}\left(N_p + Z_p\right) \\ &= \sum_{p}\left[\sum_{q} B_{pq,\alpha\beta} E^{\text{perm}}_{q,\beta} + g_{pq,\alpha}\phi^{\text{perm}}_q\right] - h_{1,p,\alpha} Z \\ &+ r_{p,\alpha}\left[\left(\sum_{q} g_{qp,\beta} E^{\text{perm}}_{q,\beta} + D_{pq}\phi^{\text{perm}}_q\right) - h_{2,p} Z + Z_p\right], \end{aligned} \tag{3.54}$$

where we have used that $\sum_q h_{2,q} = 1$. We now divide Eq. 3.54 into external and internal contributions

$$\begin{aligned}
\mu_\alpha^{mol} &= \sum_{p,q}\left[B_{pq,\alpha\beta}\left(E_\beta^{\text{ext}}+E_{q,\beta}^{\text{int}}\right)+g_{pq,\alpha}\left(\phi_q^{\text{int}}+r_{q,\beta}E_\beta^{\text{ext}}\right)+r_{p,\alpha}g_{qp,\beta}\left(E_\beta^{\text{ext}}+E_{q,\beta}^{\text{int}}\right)\right.\\
&+ \left. r_{p,\alpha}D_{pq}\left(r_{q,\beta}E_\beta^{\text{ext}}+\phi_q^{\text{int}}\right)\right]+\sum_p r_{p,\alpha}\left(Z_p-h_{2,p}Z\right)-h_{1,p,\alpha}Z\\
&= \sum_{p,q}\left[B_{pq,\alpha\beta}E_{q,\beta}^{\text{int}}+g_{pq,\alpha}\phi_q^{\text{int}}+r_{p,\alpha}g_{qp,\beta}E_{q,\beta}^{\text{int}}+r_{p,\alpha}D_{pq}\phi_q^{\text{int}}\right]+\sum_p r_{p,\alpha}\left(Z_p-h_{2,p}Z\right)\\
&- h_{1,p,\alpha}Z+\sum_{p,q}\left[B_{pq,\alpha\beta}+g_{pq,\alpha}r_{q,\beta}+r_{p,\alpha}g_{qp,\beta}+r_{p,\alpha}D_{pq}r_{q,\beta}\right]E_\beta^{\text{ext}}, \qquad (3.55)
\end{aligned}$$

where we have used Eqs. 3.48 and 3.50 as well as Eqs. 3.43 and 3.41. The molecular dipole moment can be divided into a permanent part, μ_α^{perm}, and a part that is induced by the external electric field and thus defines the molecular polarizability. The permanent dipole moment is given by

$$\begin{aligned}
\mu_\alpha^{\text{perm}} &= \sum_{p,q}\left[B_{pq,\alpha\beta}E_{q,\beta}^{\text{int}}+r_{p,\alpha}g_{qp,\beta}E_{q,\beta}^{\text{int}}+r_{p,\alpha}D_{pq}\phi_q^{\text{int}}\right]\\
&+ \sum_p r_{p,\alpha}\left(Z_p-h_{2,p}Z\right)-h_{1,p,\alpha}Z, \qquad (3.56)
\end{aligned}$$

as seen by using the condition in Eq. 3.43. From the induced dipole moment we can indentify the molecular polarizability as

$$\alpha_{\alpha\beta}^{\text{mol}}=\sum_{p,q}\left[B_{pq,\alpha\beta}+r_{p,\alpha}D_{pq}r_{q,\beta}\right], \qquad (3.57)$$

again by using the condition in Eq. 3.43. The structure of the molecular polarizability is identical to the one given by the Olson-Sundberg model and in good agreement with the fact that the polarizability has contributions arising only from the external field. In the same manner, we identity the contributions to the atomic charges, q_p, as

$$\begin{aligned}
q_p &= Z_p+N_p=Z_p-h_{2,p}Z+\sum_q\left(g_{qp,\beta}E_{q,\beta}^{\text{perm}}+D_{pq}\phi_q^{\text{perm}}\right)\\
&= Z_p-h_{2,p}Z+\sum_q\left(g_{qp,\beta}E_{q,\beta}^{\text{int}}+D_{pq}\phi_q^{\text{int}}\right)+\sum_q\left(g_{qp,\beta}+D_{pq}r_{q,\beta}\right)E_\beta^{\text{ext}}, \qquad (3.58)
\end{aligned}$$

and in the limit of no external field we get the permanent atomic charges

$$q_p=Z_p-h_{2,p}Z+\sum_q\left(g_{qp,\beta}E_{q,\beta}^{\text{int}}+D_{pq}\phi_q^{\text{int}}\right). \qquad (3.59)$$

By separating the nuclear and electron charges we have modified the Olson-Sundberg model in a way that makes it possibly to treat the permanent dipole moment and charges in a similar way as the molecular polarizaility. This extention will be termed the modified Olson-Sundberg model. Finally, it is noted that an apparent atomic capacitance can be optained by rearranging Eq. 3.51 as

$$a_p=b_p\left(1+\frac{Z_p}{N_p}\right). \qquad (3.60)$$

Thus, different atomic capacitances are obtained for each atom and they can be used to analyze the conductivity of molecules.

3.7 The Nonlinear Interaction Model

If we include nonlinear terms in the expansion of the induced molecular dipole moment we can write it as

$$\mu_\alpha^{\text{mol}} = \alpha_{\alpha\beta}^{\text{mol}} E_\beta^{\text{ext}} + \frac{1}{2}\beta_{\alpha\beta\gamma}^{\text{mol}} E_\gamma^{\text{ext}} E_\beta^{\text{ext}} + \frac{1}{6}\gamma_{\alpha\beta\gamma\delta}^{\text{mol}} E_\delta^{\text{ext}} E_\gamma^{\text{ext}} E_\beta^{\text{ext}}. \tag{3.61}$$

The induced dipol moment of atom p is given by Eq. 3.2

$$\mu_{p,\alpha}^{\text{ind}} = \alpha_{p,\alpha\beta} E_{p,\beta}^{\text{tot}} + \frac{1}{6}\gamma_{p,\alpha\beta\gamma\delta} E_{p,\beta}^{\text{tot}} E_{p,\gamma}^{\text{tot}} E_{p,\delta}^{\text{tot}}, \tag{3.62}$$

where $E_{p,\beta}^{\text{tot}}$ is given by Eq. 3.4. Due to symmetry arguments, the polarizability of a spherically symmetric atom is given as

$$\alpha_{p,\alpha\beta} = \alpha_p \delta_{\alpha\beta}, \tag{3.63}$$

and the corresponding second hyperpolarizability as [33]

$$\gamma_{p,\alpha\beta\gamma\delta} = \frac{1}{3}\gamma_p(\delta_{\alpha\beta}\delta_{\gamma\delta} + \delta_{\alpha\gamma}\delta_{\beta\delta} + \delta_{\alpha\delta}\delta_{\beta\gamma}). \tag{3.64}$$

If we regard the electric field at each atom as an independent variable, we may expand the atomic induced dipole moment as [69]

$$\mu_{p,\alpha}^{\text{ind}} = \sum_q B_{pq,\alpha\beta} E_{q,\beta}^{\text{ext}} + \frac{1}{2}\sum_{q,r} C_{pqr,\alpha\beta\gamma} E_{r,\gamma}^{\text{ext}} E_{q,\beta}^{\text{ext}} + \frac{1}{6}\sum_{q,r,s} D_{pqrs,\alpha\beta\gamma\delta} E_{s,\delta}^{\text{ext}} E_{r,\gamma}^{\text{ext}} E_{q,\beta}^{\text{ext}}. \tag{3.65}$$

The coefficients in the Taylor expansion are termed relay tensors and by taking the appropriate gradients of Eq. 3.65 we get the definition of the two-atom relay tensor as

$$B_{pq,\alpha\beta} = \left[\frac{\partial \mu_{p,\alpha}^{\text{ind}}}{\partial E_{q,\beta}^{\text{ext}}}\right]_{E_{q,\beta}^{\text{ext}}=0}, \tag{3.66}$$

and the three-atom relay tensor as

$$C_{pqr,\alpha\beta\gamma} = \left[\frac{\partial^2 \mu_{p,\alpha}^{\text{ind}}}{\partial E_{q,\beta}^{\text{ext}} \partial E_{r,\gamma}^{\text{ext}}}\right]_{E_{q,\beta}^{\text{ext}}=0, E_{r,\gamma}^{\text{ext}}=0}, \tag{3.67}$$

and the four-atom relay tensor as

$$D_{pqrs,\alpha\beta\gamma\delta} = \left[\frac{\partial^3 \mu_{p,\alpha}^{\text{ind}}}{\partial E_{q,\beta}^{\text{ext}} \partial E_{r,\gamma}^{\text{ext}} \partial E_{s,\delta}^{\text{ext}}}\right]_{E_{q,\beta}^{\text{ext}}=0, E_{r,\gamma}^{\text{ext}}=0, E_{s,\delta}^{\text{ext}}=0}. \tag{3.68}$$

We know that the molecular induced dipole moment is the sum of all atomic induced dipole moments, i.e. Eq. 3.1, and for a homogeneous applied field we have $E_\beta^{\text{ext}} = E_{q,\beta}^{\text{ext}}$ for all q. Combining this with Eq. 3.65 allows us to write the molecular dipole moment as

$$\mu_{p,\alpha}^{\text{mol}} = \left(\sum_{p,q} B_{pq,\alpha\beta}\right) E_\beta^{\text{ext}} + \frac{1}{2}\left(\sum_{p,q,r} C_{pqr,\alpha\beta\gamma}\right) E_\gamma^{\text{ext}} E_\beta^{\text{ext}} + \frac{1}{6}\left(\sum_{p,q,r,s} D_{pqrs,\alpha\beta\gamma\delta}\right) E_\delta^{\text{ext}} E_\gamma^{\text{ext}} E_\beta^{\text{ext}}. \tag{3.69}$$

By comparing with Eq 3.61 we can define the molecular (hyper-)polarizabilities as [69]

$$\alpha_{\alpha\beta}^{\text{mol}} = \sum_{p,q} B_{pq,\alpha\beta}\ , \tag{3.70}$$

$$\beta^{\text{mol}}_{\alpha\beta\gamma} = \sum_{p,q,r} C_{pqr,\alpha\beta\gamma}, \tag{3.71}$$

and

$$\gamma^{\text{mol}}_{\alpha\beta\gamma\delta} = \sum_{p,q,r,s} D_{pqrs,\alpha\beta\gamma\delta}. \tag{3.72}$$

We have now related the molecular (hyper-)polarizabilities with the relay tensors. In the following we will derive explicit expression for the relay tensors.

3.7.1 The Polarizability

The two-atom relay tensor is obtained by combining Eqs. 3.62 and 3.66 (see appendix D.1 for details). For the relay tensor B, we obtain

$$B_{pr,\alpha\epsilon} = \frac{\partial \mu^{\text{ind}}_{p,\alpha}}{\partial E^{\text{tot}}_{p,\beta}} \frac{\partial E^{\text{tot}}_{p,\beta}}{\partial E^{\text{ext}}_{r,\epsilon}} = \left(\alpha_{p,\alpha\beta} + \frac{1}{2} \gamma_{p,\alpha\beta\gamma\delta} E^{\text{tot}}_{p,\delta} E^{\text{tot}}_{p,\gamma} \right) \left(\delta_{pr}\delta_{\beta\epsilon} + \sum_{q \neq p}^{N} T^{(2)}_{pq,\beta\gamma} B_{qr,\gamma\epsilon} \right), \tag{3.73}$$

c.f Eq. 11 in ref. [71], however we have no atomic first hyperpolarizability and we have carried out a Taylor expansion instead of a power expansion. As in section 3.4, this expression may be rewritten in a super-matrix notation

$$B = \alpha_{\text{eff}} \left(1 + TB\right), \tag{3.74}$$

where α_{eff} is given by

$$\alpha_{\text{eff},p,\alpha\beta} = \left(\alpha_{p,\alpha\beta} + \frac{1}{2} \gamma_{p,\alpha\beta\gamma\delta} E^{\text{tot}}_{p,\delta} E^{\text{tot}}_{p,\gamma} \right). \tag{3.75}$$

We can write B in a form similar to Eq. 3.10

$$B = \left(\alpha^{-1}_{\text{eff}} - T^{(2)} \right)^{-1}. \tag{3.76}$$

If γ_p vanishes for all atoms it follows from Eq. 3.75 that the two-atom relay tensor becomes identical with Eq. 3.10 and this model becomes identical with the one Applequist *et. al.* derived. Note that E^{tot} is calculated in the limit $E^{\text{ext}} = 0$, which means that for a system with only atomic polarizabilities and second hyperpolarizabilities, E^{tot} in Eq. 3.4 becomes zero and Eq. 3.76 is equivalent to Eq. 3.10. This is realized from Eq. 3.9 since there is no induced dipole moment in the limit of no external field. Therefore, in order to obtain a contribution from γ_p in Eq. 3.76, we need to include atomic charges which gives a permanent electric field. Thus, we need to modify Eq. 3.4 as

$$E^{\text{tot}}_{p,\beta} = E^{\text{ext}}_{p,\beta} + E^{\text{stat}}_{p,\beta} + \sum_{q \neq p}^{N} T^{(2)}_{pq,\beta\gamma} \mu^{\text{ind}}_{q,\gamma}, \tag{3.77}$$

where $E^{stat}_{p,\beta}$ is the permanent, static field from the atomic charges of the other atoms,

$$E^{\text{stat}}_{p,\beta} = \sum_{q \neq p}^{N} T^{(1)}_{pq,\beta} q_q, \tag{3.78}$$

where q_q is an atomic charge and $T^{(1)}$ is given in Eq. 3.23. The atomic charges could be calculated from Eq. 3.59 using the modified Olson-Sundberg model. However, since the induced dipole moment in Eq. 3.62 and E^{tot} depend on each other, we have to calculate μ^{ind} in an iterative and self-consistent procedure.

3.7.2 The First Hyperpolarizability

The three-atom relay tensor is obtained in a similar way (see appendix D.2 for details). We can therefore write the three-atom relay tensor in the following way

$$\begin{aligned} C_{pqr,\alpha\beta\gamma} &= \frac{\partial^2 \mu_{p,\alpha}}{\partial E^{\text{ext}}_{q,\beta} \partial E^{\text{ext}}_{r,\gamma}} \\ &= \gamma_{p,\alpha\epsilon\sigma\delta} E^{\text{tot}}_{p,\delta} \tilde{B}_{pr,\sigma\gamma} \tilde{B}_{pq,\epsilon\beta} + \left(\alpha_{p,\alpha\epsilon} + \frac{1}{2} \gamma_{p,\alpha\epsilon\gamma\delta} E^{\text{tot}}_{p,\delta} E^{\text{tot}}_{p,\gamma} \right) \tilde{C}_{pqr,\epsilon\beta\gamma}, \end{aligned} \tag{3.79}$$

where the matrices $\tilde{B}_{pr,\beta\epsilon}$ and $\tilde{C}_{prs,\beta\epsilon\sigma}$ respectively are given as

$$\tilde{B}_{pr,\beta\epsilon} = \delta_{pr}\delta_{\beta\epsilon} + \sum_{q \neq p}^{N} T^{(2)}_{pq,\beta\gamma} B_{qr,\gamma\epsilon}, \tag{3.80}$$

and

$$\tilde{C}_{prs,\beta\epsilon\sigma} = \sum_{q \neq p}^{N} T^{(2)}_{pq,\beta\gamma} C_{qrs,\gamma\epsilon\sigma}. \tag{3.81}$$

c.f Eq. 12 in ref. [71]. Since $\tilde{C}_{prs,\beta\epsilon\sigma}$ depends on $C_{qrs,\gamma\epsilon\sigma}$ it indicates that we have to solve the three-atom relay tensor in an iterative fasion. This can be avoided by rewriting the three-atom relay tensor as (see appendix D.2) [69]

$$C_{mqr,\sigma\tau\nu} = \sum_{p}^{N} \gamma_{p,\alpha\beta\gamma\delta} E^{\text{tot}}_{p,\delta} \tilde{B}_{pr,\gamma\nu} \tilde{B}_{pq,\beta\tau} \tilde{B}_{pm,\alpha\sigma}. \tag{3.82}$$

The three-atom relay tensor is thus writen in terms of the two-atom relay tensor which we already know. We are therefore able to calculate the molecular polarizability and first hyperpolarizability. Expressions for the second hyperpolarizability can also be derive in a similar manner, only with more complicated expressions.

3.8 Frequency-dependent Properties

Until now we have only discussed time-independent properties. However, as mentioned in the introduction it is really the time-dependent properties that we are interested in, and some extension has to be included in order to describe these properties. A time-dependent external field is given by Eq. 2.16 and can in the discrete form be writen as

$$E(t) = E(\omega = 0) + \frac{1}{2} \sum_{j} \left[E(\omega_j) e^{-i\omega_j t} + E(-\omega_j) e^{i\omega_j t} \right], \tag{3.83}$$

and the resultant electric dipole moment is then given by

$$\mu(t) = \mu(\omega = 0) + \frac{1}{2} \sum_{\sigma} \left[\mu(\omega_\sigma) e^{-i\omega_\sigma t} + \mu(-\omega_\sigma) e^{i\omega_\sigma t} \right]. \tag{3.84}$$

The frequency of which the dipole moment oscillates is defined in terms of the applied field frequencies as

$$\omega_\sigma = \omega_1 + \omega_2 + \ldots + \omega_n. \tag{3.85}$$

We can write the dipole moments at a specific frequency as [71]

$$\mu(\omega_\sigma) = \sum_{n=0}^{\infty} \left[\frac{1}{n!} K(-\omega_\sigma; \omega_1, \omega_2, \ldots, \omega_n)\, \xi^{(n)}(-\omega_\sigma; \omega_1, \omega_2, \ldots, \omega_n)\, E(\omega_1)\, E(\omega_2) \ldots E(\omega_n) \right], \tag{3.86}$$

where $\xi^{(n)}$ is the $(n-1)$'th hyperpolarizability. Therefore Eq. 3.86 is a generalization of Eq. 3.62 to the frequency-dependent regime. The numerical factor K is given by factors from the Fourier transform and the number of different field frequencies [78]. In order to get the correct behaviour in the limit of static fields the K factor has to be unity,

$$K(0; 0, 0, \ldots, 0) = 1 \text{ for all } n, \tag{3.87}$$

and the frequency-dependent (hyper)polarizabilities equal to there static counterparts

$$\lim_{all\ \omega \to 0} \xi^{(n)}(-\omega_\sigma; \omega_1, \omega_2, \ldots, \omega_n) = \xi^{(n)}(0; 0, 0, \ldots, 0). \tag{3.88}$$

We have now establish a formalism where we can treat frequency-dependent properties as well as static properties. We will now continue and describe the frequency-dependent polarizability and the hyperpolarizability corresponding to SHG in terms of the interaction model.

3.8.1 Frequency-dependent Polarizabilities

The frequency-dependent polarizability, $\alpha^{\text{mol}}_{\alpha\beta}(-\omega; \omega)$, may be obtained with the same approach as for the static polarizability in section 3.4. From Eq. 3.86, it is given as

$$\mu_\alpha(\omega) = \alpha^{\text{mol}}_{\alpha\beta}(-\omega; \omega)\, E^{\text{ext}}_\beta(\omega). \tag{3.89}$$

Considering a set of N point polarizabilities, the atomic induced dipole moment is

$$\mu_{p,\alpha}(\omega) = \alpha_p(-\omega; \omega)\, E^{\text{tot}}_\alpha(\omega) = \alpha_p(-\omega; \omega) \left[E^{\text{ext}}_\alpha(\omega) + \sum_{q \neq p}^{N} T^{(2)}_{pq,\alpha\beta} \mu_{q,\beta}(\omega) \right], \tag{3.90}$$

and then Eqs. 3.9 to 3.12 may be applied in order to get the frequency-dependent polarizability. If we instead want to use the nonlinear interaction model we can generalized the two-atom relay tensor in Eq. 3.66 to include frequency-dependence as

$$B_{pq,\alpha\beta}(-\omega; \omega) = \frac{\partial \mu_{p,\alpha}(\omega)}{\partial E^{\text{ext}}_{q,\beta}(\omega)}, \tag{3.91}$$

where the frequency-dependent atomic induced dipole moment is given in line with Eq. 3.2 as

$$\begin{aligned} \mu_{p,\alpha}(\omega) &= \alpha_{p,\alpha\beta}(-\omega; \omega)\, E^{\text{tot}}_{p,\beta}(\omega) \\ &+ \frac{1}{6} K(-\omega; \omega_1, \omega_2, \omega_3)\, \gamma_{p,\alpha\beta\gamma\delta}(-\omega; \omega_1, \omega_2, \omega_3)\, E^{\text{tot}}_{p,\delta}(\omega_3)\, E^{\text{tot}}_{p,\gamma}(\omega_2)\, E^{\text{tot}}_{p,\beta}(\omega_1), \end{aligned} \tag{3.92}$$

with $\omega = \omega_1 + \omega_2 + \omega_3$. Following the discussion in section 3.7.1, we have that the total field, $E^{\text{tot}}_{p,\alpha}(\omega)$ becomes zero when $E^{\text{ext}}(\omega) \to 0$ apart from a static term, $E^{\text{tot}}_{p,\alpha}(\omega = 0)$, when we

have included atomic charges. Since we only differentiate ones with respect to the frequency-dependent field we can in order to get a contribution from γ_p only have one frequency-dependent field in Eq. 3.92, and it reduces to

$$\mu_{p,\alpha}(\omega) = \alpha_{p,\alpha\beta}(-\omega;\omega)\, E^{\text{tot}}_{p,\beta}(\omega) + \frac{1}{2}\gamma_{p,\alpha\beta\gamma\delta}(-\omega;\omega,0,0)\, E^{\text{tot}}_{p,\delta}(0)\, E^{\text{tot}}_{p,\gamma}(0)\, E^{\text{tot}}_{p,\beta}(\omega). \tag{3.93}$$

We can therefore obtain the two-atom relay tensor as

$$B_{pr,\alpha\epsilon}(-\omega;\omega) = \left[\alpha_{p,\alpha\beta}(-\omega;\omega) + \frac{1}{2}\gamma_{p,\alpha\beta\gamma\delta}(-\omega;\omega,0,0)E^{\text{tot}}_{p,\delta}(0)E^{\text{tot}}_{p,\gamma}(0)\right]\tilde{B}_{pr,\beta\epsilon}(-\omega;\omega), \tag{3.94}$$

if we similar to Eq. 3.91 generalize Eq. D.5 to

$$\tilde{B}_{pr,\beta\epsilon}(-\omega;\omega) = \left[\frac{\partial E^{\text{tot}}_{p,\beta}(\omega)}{\partial E^{\text{ext}}_{r,\epsilon}(\omega)}\right]_{E^{\text{ext}}(\omega)=0} = \delta_{pr}\delta_{\beta\epsilon} + \sum_{q\neq p}^{N} T^{(2)}_{pq,\beta\gamma}B_{qr,\gamma\epsilon}(-\omega;\omega), \tag{3.95}$$

and Eqs. 3.74 to 3.76 can be applied in order to extrakt the molecular polarizabilty.

3.8.2 Second-Harmonic Generation

The frequency-dependent first hyperpolarizability can be derived in a similar way as was done for the frequency-dependent polarizability. The hyperpolarizability which corresponds to SHG is given by $\beta(-2\omega;\omega,\omega)$. Therefore, the relay tensor corresponding to SHG is defined as

$$C_{pqr,\alpha\beta\gamma}(-2\omega;\omega,\omega) = \frac{\partial^2\mu_{p,\alpha}(2\omega)}{\partial E^{\text{ext}}_{q,\beta}(\omega)\,\partial E^{\text{ext}}_{r,\gamma}(\omega)}. \tag{3.96}$$

Following the same line of argument as for the two-atom relay tensor we have that the only term contributing to Eq. 3.96 is

$$\begin{aligned}\mu_{p,\alpha}(2\omega) &= \alpha_{p,\alpha\beta}(-2\omega;2\omega)\, E^{\text{tot}}_{p,\beta}(2\omega) + \frac{1}{2}\gamma_{p,\alpha\beta\gamma\delta}(-2\omega;2\omega,0,0)\, E^{\text{tot}}_{p,\delta}E^{\text{tot}}_{p,\gamma}E^{\text{tot}}_{p,\beta}(2\omega)\\ &+ \frac{1}{2}\gamma_{p,\alpha\beta\gamma\delta}(-2\omega;\omega,\omega,0)\, E^{\text{tot}}_{p,\delta}E^{\text{tot}}_{p,\gamma}(\omega)\, E^{\text{tot}}_{p,\beta}(\omega).\end{aligned} \tag{3.97}$$

Using this equation for the induced dipole moment we can derive the frequency-dependent three-atom relay tensor following the same strategy as in the static case. This allows us to write the SHG three-atom relay tensor as

$$\begin{aligned}C_{pqr,\alpha\beta\gamma}(-2\omega;\omega,\omega) &= \gamma_{p,\alpha\epsilon\sigma\delta}(-2\omega;\omega,\omega,0)\, E^{\text{tot}}_{p,\delta}\tilde{B}_{pr,\sigma\gamma}(-\omega;\omega)\,\tilde{B}_{pq,\epsilon\beta}(-\omega;\omega)\\ &+ \left(\alpha_{p,\alpha\epsilon}(-2\omega;2\omega) + \frac{1}{2}\gamma_{p,\alpha\epsilon\gamma\delta}(-2\omega;2\omega,0,0)\, E^{\text{tot}}_{p,\delta}E^{\text{tot}}_{p,\gamma}\right)\times\\ &\quad \tilde{C}_{pqr,\epsilon\beta\gamma}(-2\omega;\omega,\omega),\end{aligned} \tag{3.98}$$

where we have generalized Eq. D.12 to be frequency-dependent. From this and the previous discussion of the polarizability we see that we are able to calculate the frequency-dependent (hyper)polarizabilities once we know the atomic frequency-dependent (hyper)polarizabilities. In the next section we will discuss how we can model the frequency-dependence of the atomic polarizability and thereby the frequency-dependence of the molecular properties.

3.8.3 Modelling the Frequency-dependence

Well below any electronic absorption bands the molecular (hyper)polarizabilities often has a smooth dependence on the frequency and can therefore be modelled with a simple dispersion formular [24,26]. If we asumme that the atomic (hyper)polarizabilities have the same frequency dependence we can use the dispersion formulars to describe the frequency dependence. Often a Taylor expansion of the (hyper)polarizability is used which in our case gives [71]

$$\begin{aligned}\xi^{(n)}\left(-\omega_\sigma;\omega_1,\ldots,\omega_l,\ldots,\omega_n\right) &= \lim_{\text{all }\omega\to 0}\xi^{(n)}\left(-\omega_\sigma;\omega_1,\ldots,\omega_l,\ldots,\omega_n\right)\\ &+ \sum_l \omega_l \lim_{all\ \omega\to 0}\frac{\partial}{\partial\omega_l}\left[\xi^{(n)}\left(-\omega_\sigma;\omega_1,\ldots,\omega_l,\ldots,\omega_n\right)\right]\\ &+ \cdots. \end{aligned} \tag{3.99}$$

However, optical properties are invariant to a sign change in ω_l [24] and thus the odd terms in ω_l vanish. If we use the Taylor expansion we can for the atomic polarizability write

$$\alpha_p(-\omega;\omega) = \alpha_p(0;0)\times[1 + A_p\omega^2 + B_p\omega^4\cdots], \tag{3.100}$$

where the expansion coefficience A_p and B_p are regarded as atom-type parameters. Instead of the Taylor expansion in Eq. 3.99, we can use the Unsöld approximation to model the isotropic atomic polarizability as

$$\alpha_p\left(-\omega;\omega\right) = \alpha_p\left(0;0\right)\times\left[\frac{\overline{\omega}_p^2}{\overline{\omega}_p^2-\omega^2}\right], \tag{3.101}$$

where two atom-type parameters are used, the static atomic polarizability, α_p, introduced in Eq. 3.62 and $\overline{\omega}_p$ that describes the frequency-dependence. Generally, for an atomic hyperpolarizability, $\xi_p^{(n)}$, the frequency-dependence may be modelled as

$$\xi_p^{(n)}\left(-\omega_\sigma;\omega_1,\omega_2,\ldots,\omega_n\right) = \xi_p^{(n)}\left(0;0,0,\ldots,0\right)\prod_{i=1}^{n}\left[\frac{\overline{\omega}_p^2}{\overline{\omega}_p^2-\omega_i^2}\right]. \tag{3.102}$$

We have now described how to model the frequency-dependent (hyper)polarizability and in the following chapters we will describe how to obtain the parameters used in the different models described in this chapter.

Chapter 4

Parametization of the Frequency-dependent Polarizability

We will in this chapter investigate the three interaction models describe in section 3.4 and 3.5 in order to parameterize the molecular polarizability. Furthermore, we investigate the two dispersion models described in section 3.8.3. In all of the models the atomic parameters are fitted to molecular polarizabilities of a trail set of molecules. If experimental molecular polarizabilities are used, it should be noted that they also include zero-point vibrational and pure vibrational contributions that most propably are not negligible [42,80,81]. In the interaction model it is only the electronic polarization that is considered and therefore, it may not be suitable to parameterize experimental molecular polarizabilities. Instead it is preferable to use quantum chemical calculations of molecular electronic polarizabilities for the parameterization and then treat the vibrational effects separately.
The models and parameters used for parameterization of the static molecular polarizability are

- The Applequist model. Parameter: α_p.
- The Thole model. Parameter: α_p and $c_d = 1.662$.
- The Thole model. Parameters: α_p and c_d optimized.
- The modified Thole model. Parameters: α_p and Φ_p

For the parameterization of the frequency-dependent molecular polarizability we use the optimized parameters from the modified Thole model and the following models and parameters

- Unsöld model. Parameter: $\overline{\omega}_p$.
- Quadratic model. Parameter: A_p.
- Quartic model. Parameter: A_p and B_p.

We have used a trail set of molecules containg the elements hydrogen, carbon, nitrogen, oxygen, fluorid and chlorid.

4.1 Quantum Chemical Calculation

The quantum chemical computations of frequency-dependent polarizabilities were invoked at the SCF level, see appendices B and C. We used the Dalton program package [82] as described in Refs. [83–85]. The basis set by Sadlej [86] was used since it has been shown previously

that it gives good results for polarizabilities considering its limitted size [55]. The following frequencies have been used: ω=0.0, 0.02389, 0.04282 and 0.0774 au (1 au = 27.21 eV), and we carried out calculations for 115 molecules (the frequency-dependence has been calculated for 112 molecules)[1] adopting standard bond lengths and bond angles taken from Refs [87,88]. The molecules considered were restricted to aliphatic and aromatic molecules. Olephines have not been included since in this case intramolecular charge-transfer effects are important, and these effects cannot be modelled on the basis of atomic polarizabilities only [67,68]. We tried to add a set of 13 small alkenes, but did not obtain any reasonable results. It should, however, be noted that we have included for example *p*-nitroaniline which indeed has large charge-transfer effects.

4.2 Fitting of Atomic Parameters

The parameters describing the static polarizabilities have been optimized by minimizing the difference between the quantum chemical molecular polarizability tensors, $\alpha^{QC}_{\alpha\beta,i}$, and the model molecular polarizability tensors, $\alpha^{model}_{\alpha\beta,i}$,as

$$rms = \sqrt{\frac{\sum_{i=1}^{N}\sum_{\alpha,\beta=1}^{3}\left(\alpha^{model}_{\alpha\beta,i} - \alpha^{QC}_{\alpha\beta,i}\right)^2}{N-1}}, \tag{4.1}$$

where N is the number of molecules.
The parameters describing the frequency-dependence of the molecular polarizability have been optimized by minimizing

$$rms = \sqrt{\frac{\sum_{i=1}^{N}\sum_{\alpha,\beta=1}^{3}\left[\left(\alpha^{model}_{\alpha\beta,i}(\omega) - \alpha^{model}_{\alpha\beta,i}(0)\right) - \left(\alpha^{QC}_{\alpha\beta,i}(\omega) - \alpha^{QC}_{\alpha\beta,i}(0)\right)\right]^2}{N-1}}, \tag{4.2}$$

i.e. we parameterize the frequency-dependence only and do not attempt to correct for errors obtained in the parameterization of the static polarizability. For the frequency-dependence, we have adopted both the Unsöld model and the Taylor expansion as described previously.

4.3 Results

The optimized parameters are given in Table 4.1 and are compared to the parameters given in previous work on the Applequist model [62] and the Thole model [66,89], respectively. The results are displayed in Figure 4.1, where the quantum chemically derived polarizabilities have been plotted against the model molecular polarizabilities, including all diagonal components of the polarizability tensors for the 115 molecules using the parameters obtained in this work.

A detailed comparison with the Applequist model is not possible since we have used only one atom-type polarizability for each element whereas normally two or three types have been used for H, C, N and O, respectively [62]. Such results are included, however, for comparison with the other models. Nonetheless, in comparison with previous work [62], we find a reasonable agreement for the atomic polarizabilities of most of the elements. Especially, F and Cl are in good agreement and our C polarizability is close to the carbonyl C parameter of 4.16 [62]. Our H polarizability is considerably higher, but especially N and O give different results. The large spread in Figure 4.1 a is probably due to that we included both aliphatic and aromatic molecules since previously, it has been demonstrated that polarizabilites obtained by the Applequist model cannot be adopted for both kinds of molecules [68].

[1] For a list of the molecules studied see appendix F.

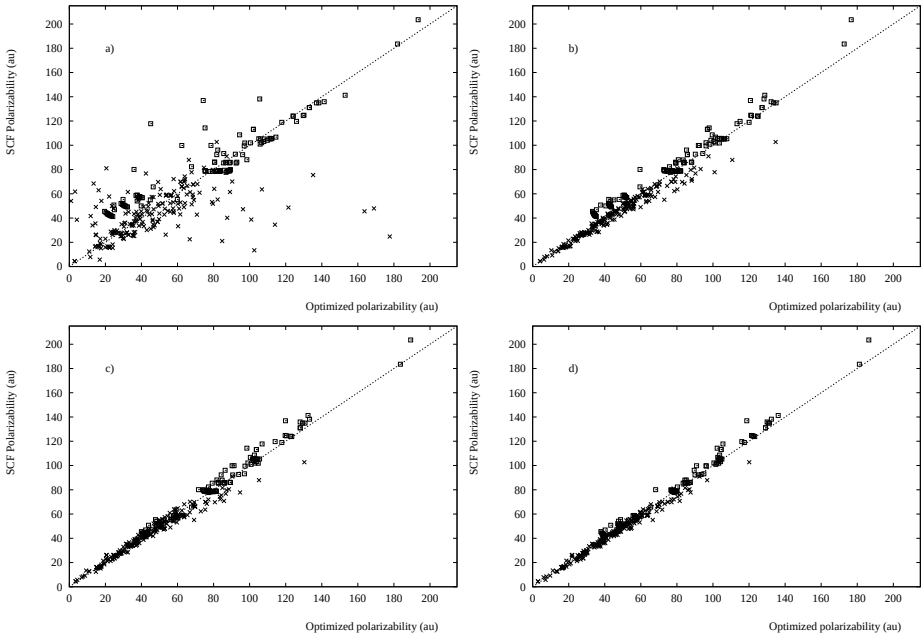

Figure 4.1: Parameterization of quantum chemically derived polarizabilities with interacting atom models. a) The Applequist model. b) The Thole model. c) The c_d parameter in the Thole model being optimized. d) Individual damping parameters for each element. ($\times$) indicates aliphatic molecules and ($\boxdot$) aromatic molecules, respectively.

For the Thole model, we find a good agreement between our results and previous work [66,89]. In line with previous investigations, we find that the Thole model gives a much better description of the molecular polarizability tensor than the Applequist model even though the number of fitting parameters is the same. Further, the *rms*-value is reduced with more than an order of magnitude. Recently, van Duijnen and Swart compared Thole polarizabilities fitted to quantum chemical calculations for various basis sets [89]. However, their results show large differences if they are fitted to experimental data or to *ab initio* calculations. Our parameters compare well to their parameters fitted to experimental data, but not to their *ab initio* parameters. By comparing the SCF molecular polarizabilities, it is clear that the more flexible Sadlej basis set employed here gives a better description of the molecular polarizabilities than for the series of basis sets adopted by van Duijnen and Swart. Therefore, we restrict the comparison to the parameters they obtained by parameterizing experimental data. Especially for F and C, we find good agreement. The largest relative difference is found for H, where our polarizability is about 20% smaller than the previous values fitted to experimental data [66, 89]. This difference for α^H is in line with the results by van Duijnen and Swart, who also found substantially smaller polarizabilities for hydrogen when they fitted to quantum chemical calculations, compared to experimental data. This may imply that α^H obtained from experimental data contains large contributions from vibrational effects. Our N parameters are slightly larger and the O and Cl parameters slightly lower than the parameters presented previously [66, 89]. Since we find the expected relative magnitudes of the parameters (for example $\alpha^C > \alpha^N > \alpha^O > \alpha^F$), and in general a good agreement with previous work, we may conclude that the Thole polarizabilities have a physical significance and are not only fitting parameters.

It should be noted that the parameterizations employed here and elsewhere are quite different, especially with respect to the choice of molecules. If we optimize also c_d, we obtain a value of 1.991, a relatively large deviation from the original value of Thole of 1.662 [66], compared to the

Table 4.1: Atomic parameters fitted to model the static polarizability (in au, 1 au=0.1482 Å^3).

	Applequist		Thole model				Modified Thole model		
Atom	α	α^a	α	α	α^b	α^c	α	Φ	$c_{d,pp}$
H	1.61	0.91–1.13	2.84	1.83	3.47	3.50	1.84	2.75	0.965
C	4.20	4.16, 5.92	10.20	12.19	9.46	10.18	11.52	20.99	2.029
N	8.44	3.58	9.03	7.88	7.46	7.60	10.55	26.55	2.349
O	8.78	2.93–3.14	5.18	5.78	5.82	6.39	5.64	12.16	1.959
F	2.44	2.16	2.91	2.54		2.94	2.25	4.78	1.668
Cl	12.65	12.89	14.93	16.21		16.11	16.08	17.64	0.600
c_d	–		1.662	1.991^d	1.662	1.7278			
rms	139.44		11.30	8.26			6.67		

[a] See Ref. [62]
[b] See Ref. [66]
[c] See Ref. [89]. Fitted to experimental polarizabilities.
[d] Optimized

recent optimized value of 1.7278 [89]. The improvement of the fit is about 25% which is good considering that only one extra fitting parameter has been added. The atomic polarizabilities change quite substantially, even though the trends are the same. Since c_d is increasing compared to the original value of 1.662 [66], it is expected either that α_p decreases to maintain the same damping in Eq. 3.20, or that α_p is increasing to compensate for the increased damping in Eq. 3.19. Actually, we find that the polarizabilities of H, N, and F decrease whereas the polarizabilities of C, O, and Cl increase. The largest effect is found for H which decrease from 2.84 to 1.83 au. The damping of the electric field is a consequence of the charge distributions being smeared out and that they are overlapping. It is then expected that the damping is more due to the extension of the charge distribution rather than the polarization, even though the electronic second moment and the polarizability are related to each other. Nonetheless, a fit with an additional atomic parameter describing the damping only gives a minor improvement (around 20%) considering that two parameters are used for each element (see Table 4.1). It is also of interest to rewrite Φ_p in terms of α_p and an atomic damping factor, $c_{d,pp}$ to compare with the parameters of the other models. From Eqs. 3.20 and 3.21, we get

$$c_{d,pp} = \frac{\Phi_p^{\frac{1}{2}}}{\alpha_p^{\frac{1}{3}}} \tag{4.3}$$

which also are presented in Table 4.1. The $c_{d,pp}$ parameters thus describe the relation between an atomic second order moment and an atomic polarizability. For the second-row elements (C, N, O, and F), $c_{d,pp}$ are in the range 1.6–2.4 which is about the same size as the general c_d values. It is difficult to deduce a trend and the differences may not be significant. The $c_{d,pp}$ parameter of H is, however, a factor of two smaller than for the second-row elements which probably is due to its small second order moment. This result is in line with the distributed multipole moments and polarizabilities calculated in order to obtain intermolecular potentials [90, 91]. For the Cl atom, the $c_{d,pp}$ parameter is also much smaller which could be due to its large polarizability. However, further investigations of third-row elements should be carried out before any definitive conclusions can be drawn. Perhaps, a suitable partition scheme for the damping factors, c_d, is one parameter for each row of elements in the periodic table. Thus, the various values obtained for c_d in the Thole model are probably due to that different sets of molecules have been used with different weight for each element.

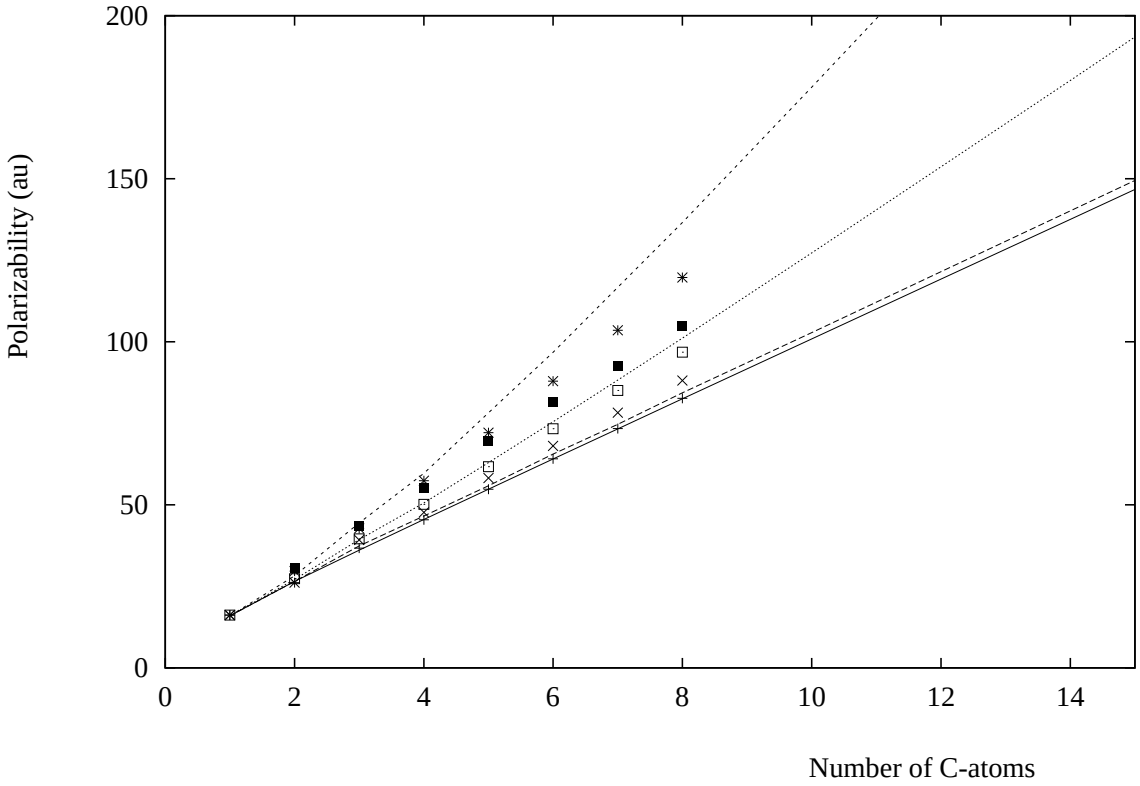

Figure 4.2: The static polarizability tensors for the n-alkanes as a function of the chain length. Quantum chemically calculated and experimental data are presented as dots; the results from the parameterized electrostatic models as lines. (— , +) and (– – , ×) denote components perpendicular to the chain. (- - , ∗) denotes the component along the chain. ($\cdots$, ⊡) denotes the isotropic part of the polarizability. (■) denotes the experimental data taken from Ref. [92].

In Figure 4.2, the static polarizability tensor as function of the length of the molecule is presented for the n-alkanes. Here, it should be noted that alkanes longer than hexane have not been included in the parameterization and thus they may be regarded as a test of the parameters. In all calculations on n-alkanes, we have used completely staggered conformations. SCF calculations are compared to the modified Thole model. For the components perpendicular to the chain, we find a linear dependence with the length of the chain which means that these components can be described with an additive model. For these two components, we also find an excellent agreement between the parameterized model and the SCF calculations. For the component along the chain, we find a super linear dependence with increasing length of the chain. For the parameterized model, this component increases even faster than for the SCF data, but for the largest molecule, C_8H_{18}, the difference is still less than 15%. We also find a good agreement between the model and the quantum chemical calculations for the isotropic part of the polarizability. In this case, we can compare to experiment [92] and as displayed in Figure 4.2 the agreement is excellent. Results for the frequency-dependent polarizabilities of the n-alkanes show a behaviour almost identical to the static polarizability.

For the frequency-dependence, we have studied three different models: the Unsöld approximation in Eq. 3.101, a truncation of Eq. 3.100 after the quadratic term (denoted the quadratic model) and a truncation of Eq. 3.100 after the quartic term (denoted the quartic model). If all the molecules are included in the parameterization, an rms of 0.809 au is obtained for all three models (see Table 4.2). In the Unsöld and the quadratic models only one parameter is used per element, whereas two parameters per element have been used in the quartic model.

Table 4.2: Parameters describing the frequency-dependence of molecular polarizabilities (in au).

	all molecules				aliphatic				aromatic			
Atom	Unsöld	Quadratic	Quartic		Unsöld	Quadratic	Quartic		Unsöld	Quadratic	Quartic	
	$\overline{\omega_p}$	A_p	A_p	B_p	$\overline{\omega_p}$	A_p	A_p	B_p	$\overline{\omega_p}$	A_p	A_p	B_p
H	0.6052	3.0366	2.4521	98.9024	0.4140	6.0475	5.3256	122.6902	0.3509	6.4859	5.8306	126.6553
C	0.4446	5.1418	4.5048	107.9280	0.7141	1.9712	1.3768	100.7323	0.3959	7.1876	6.4144	126.5659
N	0.3423	8.7909	8.0585	124.7032	0.4322	5.5416	4.8219	121.8716	0.2232	17.1930	16.0513	202.0394
O	0.5608	3.8037	3.1573	109.3189	0.4299	5.6044	4.8682	124.5673	1.3390	8.7929	8.0042	139.1782
F	0.4039	6.6054	5.9458	112.1713	0.9725	1.6196	0.9918	103.0175	1.0849	-2.3109	-2.6209	69.1134
Cl	0.4413	5.3456	4.6413	119.3990	0.5299	3.6324	2.9841	109.8527	0.4319	5.2235	4.5482	117.7529
rms	0.809	0.809	0.809		0.424	0.424	0.424		0.712	0.689	0.689	

Even if the magnitude of the B_p parameters is significant and the A_p parameters are different in the quadratic and quartic models, the actual contribution from a quartic term of the atomic frequency-dependence is negligible for the molecules studied here since the fitting has not improved. Hence, the Unsöld and quadratic models can be regarded as identical since we can carry out a Taylor expansion of Eq. 3.101 and keep only the quadratic term since, as just argued, the higher order terms would be negligible.

If the molecules are divided into aliphatic and aromatic molecules, we find a significant improvement of the description within each family (see Table 4.2 and Figure 4.3). The *rms* value is reduced with a factor of two if only the aliphatic molecules are included and with about 10% for a parameterization of the aromatic molecules alone. However, the frequency-dependence is much larger for the aromatic molecules (see Figure 4.3) and thus they will still dominate the parameterization when aliphatic molecules are included. Nonetheless, it has been demonstrated that the frequency-dependence of molecular polarizabilities can be described with atom-type parameters.

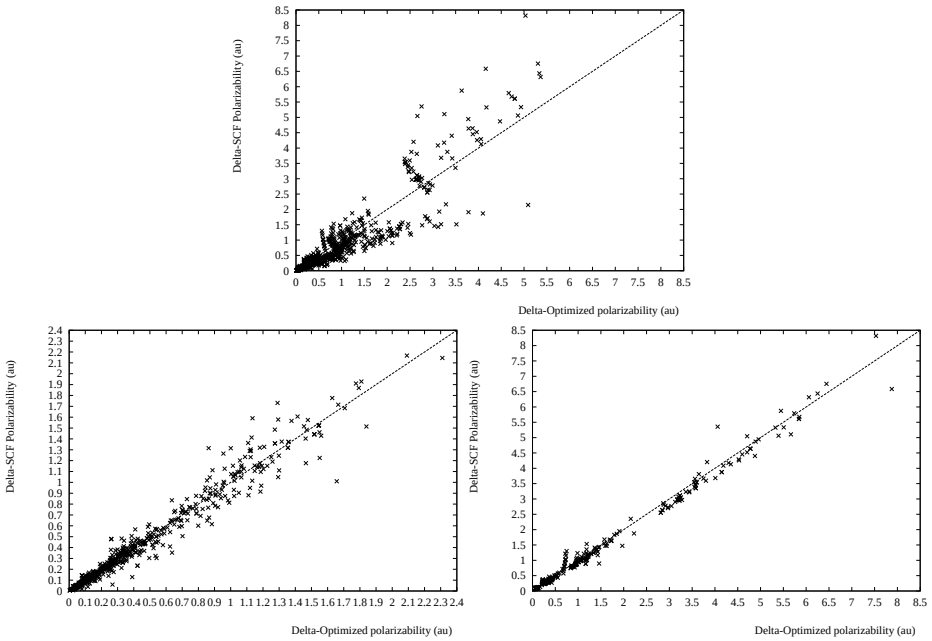

Figure 4.3: Parameterization of the frequency-dependence adopting the Unsöld model. a) all molecules. b) aliphatic molecules. c) aromatic molecules

4.4 Conclusions

In this work, we have investigated the parameterization of frequency-dependent molecular polarizabilities based on a model for interacting atoms. The study has been carried out for 115 molecules, which is a considerably larger set of molecules than used previously. By adopting one set of parameters for each element, we find that the Thole model is successful in reproducing the static molecular polarizability tensor. The modifications discussed here give significant improvements. Especially the behaviour of the damping at the hydrogen atoms are different from the other elements and should be treated differently. It is also found that aliphatic and aromatic molecules can be described with the same set of parameters. Furthermore, it is the first investigation where an interacting atom model has been extended also to include the frequency-dependence of the molecular polarizability. It has been shown that the frequency-dependence of molecular polarizabilities can be described with one parameter for each element.

Chapter 5

Carbon Nanotubes

Conjugated organic molecules with delocalized electron systems are interesting because of their potentially large optical properties. The new class of carbon materials, fullerenes and carbon nanotubes, has an extended π-system and are therefore promising candidates for new photonic materials. The linear and nonlinear optical properties of C_{60} and C_{70} have been studied extensively, both theoretically [93–99] and experimentally [100–106] since their discovery. The polarizabiltities of the larger fullerenes and the carbon nanotubes have been studied less extensively and only in the static limit. The static polarizabilities of the larger fullerens have been calculated within the atom monopole-dipole interaction (AMDI) theory [68] by Shanker and Applequist [97]. In the case of the carbon nanotubes Benedict *et. al* used a tight-binding model [107] to study the static polarizability of infinitely long tubes.

The basic research on fullerenes and carbon fibers has provided ways to synthesize, to characterize and to understand carbon nanotubes [108–111]. The work by Kroto *et. al* on laser vaporization of graphite giving C_{60} clusters has lead to the large family of fullerenes [112]. The synthesis procedure by Kratschmer *et. al* giving macroscopic amounts of fullerenes was a giant step forward [100]. Iijima utilized this procedure for making multiple-shell carbon nanotubes [113]. These nanotubes were much smaller than the ones normally obtained when making graphite fibers [114].

We investigate the frequency-dependent polarizability of single-walled carbon nanotubes by a modified version of Thole's interaction model [66] extended to the frequency-dependent regime see chapter 4. Both zigzag, (9,0), and armchair, (5,5), nanotubes and the effect of closing one or two ends are investigated. This is done in order to investigate purely geometric factors involved in the determination of the polarizability. Here we regard fullerenes as end capped nanotubes.

5.1 Computational Methods

The quantum chemical computations of the polarizability tensors were restricted to the static regime at the SCF level using the Gaussian 94 program package [115]. A minimal basis set, STO-3G, was used in order to get the results of the larger carbon nanotubes. The geometry of the nanotubes were first optimized with a molecular mechanics (MM2) method and afterwards with a semi-empirical method (PM3). The optimized bond length is between 1.35-1.45Å for the (9,0) nanotube and between 1.38-1.45 Å (1.23 Å in the ends) for the (5,5) nanotube. The bond length in C_{60} is 1.46 Å. The interaction model (IM) parameters used for carbon is (in au) : $\alpha_C = 11.52, \Phi_C = 20.99$ and $\overline{\omega_C} = 0.39$. The parameters were taking from table 4.1 and 4.2 assuming a benzene-like dispersion.

Table 5.1: Static isotropic polarizability of C_{60}, C_{70} and C_6H_6 (in Å^3).

Technique	$\overline{\alpha}$			Reference
	C_{60}	C_{70}	C_6H_6	
Experimental				
Refractive index of thin film[a]	86.5	-	-	[100, 102]
Refractive index of liquid[b].	-	-	10.4	[117]
Dielectric constant of thin film[c]	91.9	107.2	-	[101]
Dielectric constant of thin film[c]	80.5	96.8	-	[103]
Dielectric constant of thin film[c]	87.6	-	-	[104, 105]
Molecular beam deflection	76.5	-	-	[106]
Theoretical				
SCF 6-31++G	75.1	89.8	9.4	[99]
SCF 6-31G + sd	78.8	-	-	[96]
SCF STO-3G	51.1	57.6	4.8	This work
MNDO/PM3	63.9	79.0	6.8	[94]
LDF	79.9	-	10.12	[95]
INDO-TDCPHF	81.69	-	6.1	[93]
AMDI	60.8	73.8	10.0[d]	[97]
IM	66.2	77.2	9.5	This work

[a]Calculated using the Lorentz-Lorentz equation and a density of 1.65 g/cm^3. [100]
[b]Calculated using the Lorentz-Lorentz equation and a density of 0.8765 g/cm^3
[c]Calculated using the Clausius-Mossotti equation and the same density as in[a].
[d]This value is taking from Ref. [68]

5.2 Results

The results for the static mean polarizability of C_{60}, C_{70} and C_6H_6 are presented in table 5.1 and they are compared to a collection of experimental and other theoretical studies. The mean polarizability is defined as $\overline{\alpha} = \frac{1}{3}(\alpha_{xx} + \alpha_{yy} + \alpha_{zz})$. Most of the experiments have been done on films and they include the determination of the refractive index [100, 102] or the dielectric constant [101,103–105]. The dielectric constant, ϵ, has been converted to molecular polarizability using the Clausius-Mossotti equation [38]

$$\overline{\alpha} = \frac{3M}{4\pi N_a \rho} \frac{\epsilon - 1}{\epsilon + 2} \tag{5.1}$$

where M is the molecular weight, N_a is Avogadro's number and ρ is the density. In the case of the refractive index, the Lorentz-Lorentz equation (Eq.5.1 with $n^2 = \epsilon$) [38] is used. The experimental data from films yield polarizabilities between 80.5-91.9 Å for C_{60}, 96.8-107.2 Å for C_{70} and a ratio $\frac{C_{70}}{C_{60}}$ of 1.17-1.20. Recently, a measurement of the polarizability of molecular C_{60} using a molecular beam deflection technique [106] was reported yielding a polarizability of 76.5 ±8 Å. This value indicates that the molecular polarizability is only slightly lower than the results measured for films. The theoretical polarizabilities are in good agreement with experiments, yielding polarizabilities of 51.1-81.7 Å for C_{60}, 57.6-89.8 Å for C_{70} and a ratio $\frac{C_{70}}{C_{60}}$ of 1.13-1.24.

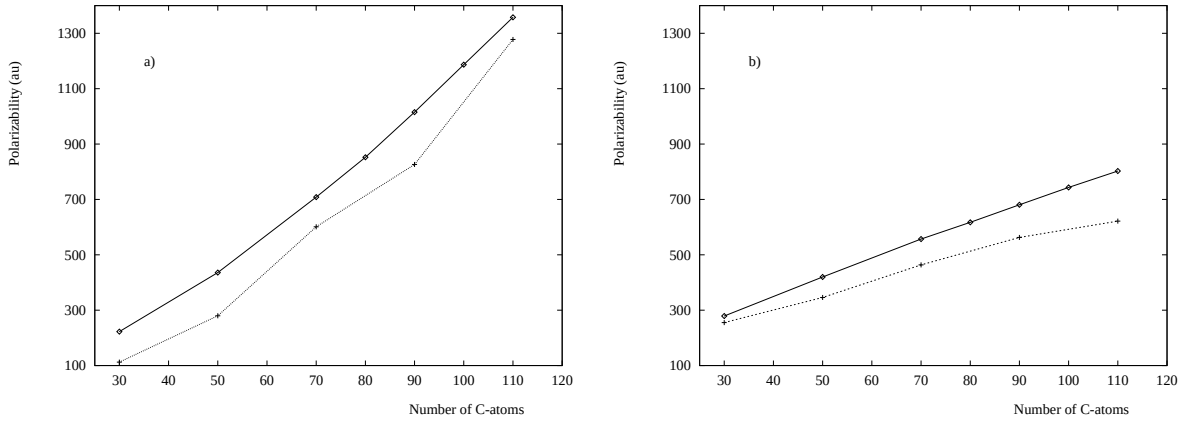

Figure 5.1: Static polarizability of the (5,5) nanotube as a function of the number of atoms. (— , ⋄) IM and (- - , +) SCF STO-3G. a) Polarizability along the tube and b) polarizability perpendicular to the tube.

Our SCF calculation using a STO-3G basis set gives values that are low compared to the previous results, indicating the need of having polarization functions in the basis set. The IM value of 66.2 for C_{60} is about 16% lower than the best SCF calculation [96, 99] and 8% higher that the value of the similar AMDI model [68]. For benzene, which has been included in the original fitting-set, we find a better agreement with the SCF result but a smaller value compared to the AMDI value.

In Figure 5.1, we present a comparison of the static polarizability of (5,5) tubes calculated with SCF and the interaction model (IM) as a function of the number of carbon atoms. We find an excellent agreement between the two methods. The value of polarizability calculated with IM is higher than the corresponding SCF value in good agreement with the results of Table 5.1. If we extend the number of carbon atoms beyond the SCF regime, see Figure 5.2, we observe that the polarizability along the tube increases rapidly compared to the polarizability perpendicular to the tube. Both $\alpha_{\parallel}$ and $\alpha_{\perp}$ increase in a non-linear way and can therefore not be described using an additivity model [54, 55]. The increase of $\alpha_{\perp}$ slows down whereas for $\alpha_{\parallel}$ it continues. The large difference between the polarizability along the tube and perpendicular to the tube is also found in the case of infinitely long tubes [107].

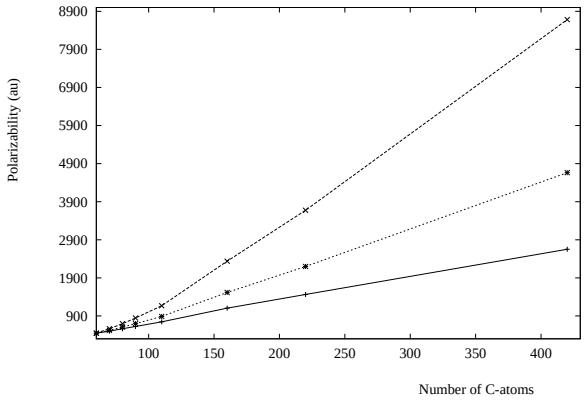

Figure 5.2: IM static polarizability tensors of the (5,5) carbon nanotube. (− − , ×) polarizability along the tube, (- - , ∗) mean polarizability and (— , +) polarizability perpendicular to the tube.

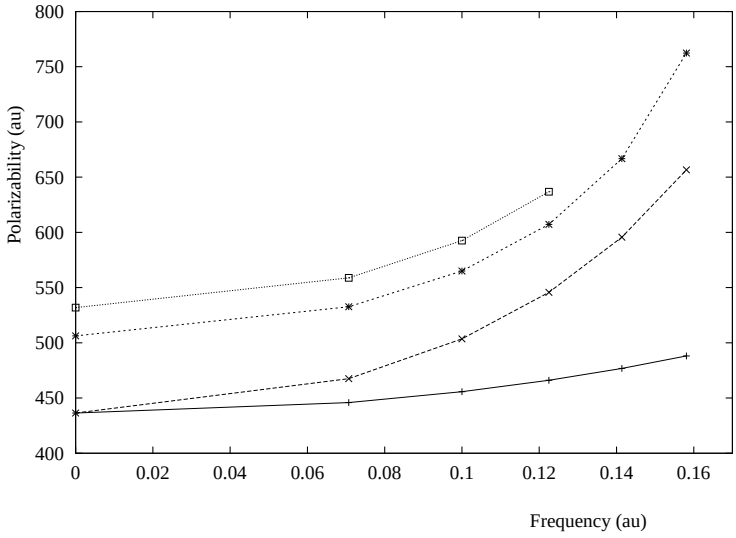

Figure 5.3: Polarizability of C_{60} as a function of frequency (au). ($\cdots$, $\Box$) SCF 6-31G + sd [96], ($-\ -$, $*$) SCF 6-31G + s [96], (- - , $\times$) IM with $\overline{\omega_C} = 0.22$ au and (— , +) IM with $\overline{\omega_C} = 0.39$ au.

The frequency-dependent polarizability of C_{60} is displayed in Figure 5.3. We have also included the work by Weiss *et. al.* [96]. From this we see that if we use a dispersion similar to what we found for a series of substituted benzenes in Chapter 4 we underestimate the frequency-dependence. This can be corrected by choosing another value of the frequency parameter $\overline{\omega}_C$. This has been done by inspection of Figure 5.3, and a reasonable value was found to be $\overline{\omega}_C = 0.22$. If we interpret $\overline{\omega}_C$ as approximately the first electronic excitation energy we get a value of 5.99 eV compared to the value of 5.22 eV in the RPA case [96]. Adopting this value of $\overline{\omega}_C$, in the case of the carbon nanotubes, we present in Figure 5.4 the frequency-dependent polarizability of a (5,5) nanotube with 110 carbon atoms. We find that the frequency-dependence along the tube is larger than that perpendicular to the tube.

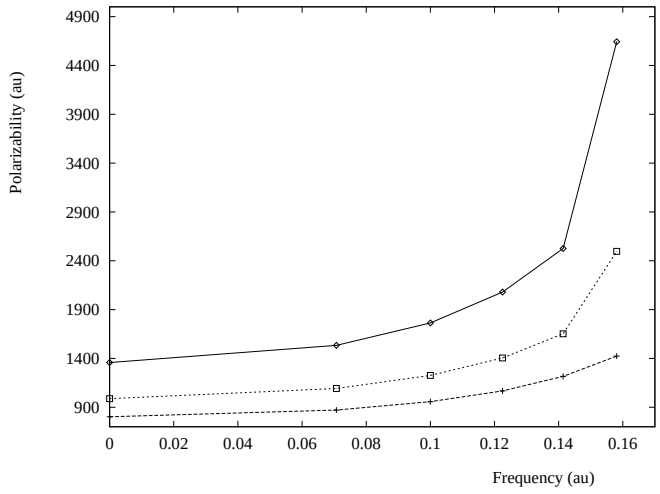

Figure 5.4: The frequency-dependent polarizability of the (5,5) carbon nanotube with 110 atoms, calculated using IM with $\overline{\omega_C} = 0.22$. (- - , $\Box$) Mean polarizability, (—, $\diamond$) polarizability along the tube and ($-\ -$, +) polarizabilty perpendicular to the tube.

Table 5.2: Static polarizabilities of selected nanotubes (in au).

Nanotube[a]	$\overline{\alpha}$	κ^b	$\alpha_{\parallel}$	$\alpha_{\perp}$
$(5,5)_0^{110}$	987.7	0.187	1357.8	802.6
$(5,5)_1^{110}$	936.5	0.173	1260.1	774.7
$(5,5)_2^{110}$	886.2	0.159	1168.2	745.2
$(5,5)_0^{90}$	792.3	0.141	1015.4	680.7
$(9,0)_0^{90}$	791.7	0.122	984.4	695.4

[a]Superscript indicates number of atoms and under-script indicates number of closed ends
[b]The anisotropy κ is defined as $\kappa^2 = [(\alpha_{xx} - \overline{\alpha})^2 + (\alpha_{yy} - \overline{\alpha})^2 + (\alpha_{zz} - \overline{\alpha})^2]/6\overline{\alpha}^2$ [116]

The geometric influence on the polarizability is illustrated in Table 5.2. Keeping the total number of carbon atoms constant we find that closing the ends lowers the polarizability, especially along the tube. This means that the polarizability of an fullerene is lower that the polarizability of an nano-tube with the same number of atoms. Also, going from an armchair configuration to a zig-zag configuration lowers the polarizability along the tube but the polarizability perpendicular to the tube increases, keeping the mean polarizability almost constant. This trend for the polarizability perpendicular to the tube is also found by Bendict *et. al.* [107] and is similar to that Jiang *et. al.* found for the static mean hyperpolarizability of C_{60}-derived tubes [119]. From this we see that the specific symmetry/intramolecular geometry of the tube has great influence on the molecular polarizability.

5.3 Conclusion

We have successfully used a frequency-dependent interaction model to calculate the frequency-dependent polarizability of C_{60}, C_{70}, (5,5)-nanotubes and (9,0)-nanotubes. The usefulness of the interaction model in dealing with systems out of the normal *Ab initio* regime has been illustrated. IM provides a straightforward way of dealing with large systems. The inclusion of new types of atom is also straightforward and opens for the possibility of dealing with other types of nano-systems. The calculated polarizabilities of C_{60} and C_{70} are around 15% lower that the best SCF calculations. We find excellent agreement between the SCF calculations and our model calculation of the increase in polarizability when the number of carbon atoms is increased. It is also found that the symmetry/intramolecular geometry of the tube and caps have great influence on the polarizability of the tubes.

Chapter 6

Parametization of the Charge-Transfer Model

As discussed in chapter 5 it is especially conjugated organic molecules with extended π-systems that are promising candidates for new materials having large optical properties. The trail set used in parameterizing the frequency-dependent polarizabililties in chapter 4 only included small aliphatic and aromatic molecules. A small set of olefines were included but we did not obtain any reasonable results in line with previous results [63]. The inclusion of atomic capacitances allows for intramolecular charge transfer and should thereby give better describtion of π-systems. The Applequist model extended in this way [68, 69] has been used to investigate the molecular polarizability of fullerenes [97], nitrogen heterocyclic molecules [120] and polyenes [121].

In this work we will use the modified Olson-Sundberg model for calculating the molecular polarizability. As described in section 3.6.1 the modification of the model by Olson and Sundberg [67] is a division of the atomic charge into nuclear charge and a charge due to the electron distibution. This lead to that also permanent dipole moments can be modelled and that an apparant atomic capacitance can be defined which is different from the parametrized atom-type capacitances. Here, we have extended the set of 115 aliphatic and aromatic molecules employed in chapter 4 with 46 olefines and parameterized a capacitance-polarizability model from *ab initio* molecular polarizabilities and dipole moments.

6.1 Computational Methods

Quantum chemical calculations of the molecular polarizability tensor and dipole moment of 46 olefines [1] have been carried out, and the molecules have been added to the set used in the previous investigation of aliphatic and aromatic molecules in chapter 4. The Dalton program package has been used [82] and response theory has been employed to obtain the molecular polarizability [83]. The calculations have been performed at the self-consistent field (SCF) level with the basis set by Sadlej [86]. Furthermore, standard bond lengths and bond angles have been employed [87, 88].

The model parameters have been optimized by minimizing the root mean square of the polarizability, Eq. 4.1, and a similar rms defined for the molecular dipole moments

$$rms = \sqrt{\frac{\sum_{i=1}^{N}\sum_{\alpha=1}^{3}\left(\mu_{\alpha,i}^{model} - \mu_{\alpha,i}^{QC}\right)^2}{N-1}}, \tag{6.1}$$

[1] A list of the molecules are given in appendix F.

where $\mu_{\alpha,i}^{QC}$ is a component of the quantum chemically derived dipole moment, $\mu_{\alpha,i}^{model}$ is the corresponding dipole moment derived from an interaction model, and N is the number of molecules with dipole moment that differs from zero. When both properties are optimized at the same time, we have simply added the two rms for the polarizability and the dipole moment, respectively.

6.2 Results

The optimized parameters are given in table 6.1 for the different model employed here. The Olson-Sundberg (**OS**) model has previously been investigated by Applequist [68]. However, a detailed comparison with this work is not possible because Applequist invokes anisotropic atomic polarizability for the carbon atoms. Also, it should be noted that we include damping of the electric field in this work. The results obtained by the modified Thole (**MT**) model, the **OS** model and the modified Olson-Sundberg (**MOS**) model are displayed in figure 6.1. Here, the quantum chemically derived polarizabilities have been plotted against the model polarizabilities, including all diagonal polarizability tensor components for the 161 molecules using the parameters obtained in this work.

If we compare this work with the results from chapter 4 we find that the Thole model and the **MT** model gives results similar to that previous obtained. The parameters are slightly different but the same expected relative magnetudes of the parameters are obtained, e.g. $\alpha^C > \alpha^N > \alpha^O > \alpha^F$. The parameters in the Applequist model is somewhat different, especially the parameter for carbon is very different from that previous obtained. Upon adopting the **OS** model we obtain the same relative magnetude of the polarizability parameters but it is noted that especially the damping parameter of N is different from that obtained by the (modified)Thole model.

Table 6.1: Atomic parameters fitted to model the static polarizability (in au, 1 au=0.1482 Å^3).

	Applequist	Thole	Modified Thole		Olson-Sundberg			Modified Olson-Sundberg		
Atom	α	α	α	Φ	α	Φ	a_p	α	Φ	a_p
H	3.34	1.24	1.86	3.18	2.55	4.79	0.1186	1.95	4.31	0.0073
C	13.86	14.06	12.05	20.99	14.21	20.32	-0.0491	12.96	20.99	0.0526
N	9.38	9.51	10.94	22.70	8.93	8.34	0.1712	7.33	7.79	0.0615
O	6.15	4.82	5.46	9.75	6.01	7.76	0.1696	4.73	6.59	0.0703
F	1.41	1.53	2.05	4.98	2.13	9.40	0.0827	2.07	3.95	0.0815
Cl	16.42	15.82	15.20	14.64	14.87	15.99	0.0746	15.68	13.17	0.1581
c_d	–	2.05	–		–			–		
rms	149.40	10.02	8.85		7.72			8.49 (0.85)[a]		

[a] number in parantese is rms of the dipole moment

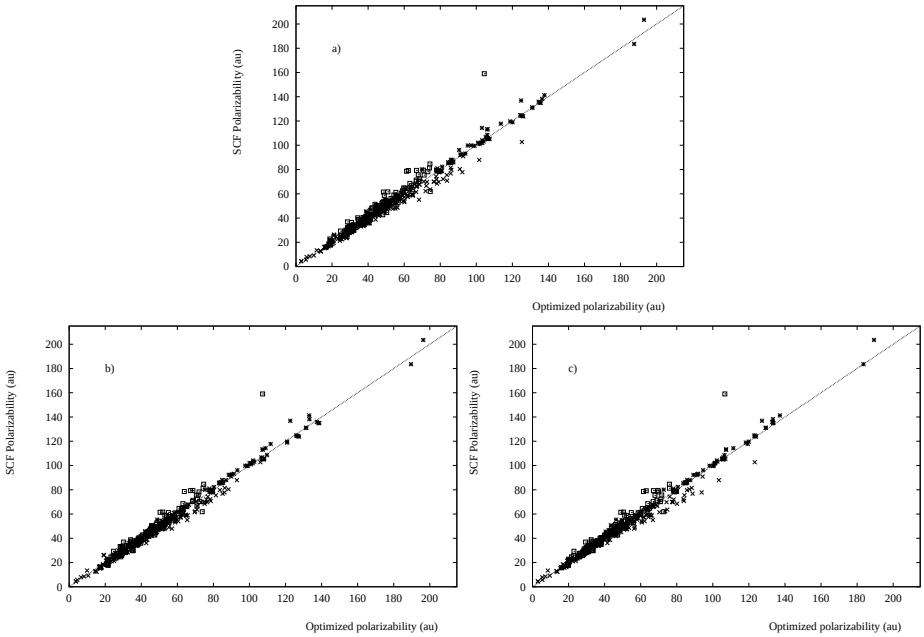

Figure 6.1: Parameterization of the molecular polarizability. a) The modified Thole model. b) The Olson-Sundberg model. c) The modified Olson-Sundberg model. ($*$) denotes aromatic molecules, ($\times$) denotes aliphatic molecules and ($\boxdot$) denotes olefinic molecules.

Also, the capacitance on C is negative which is not physical correct and the relative magnetudes of the capitance parameters are not the physical expected e.g. $a^H > a^{Cl}$. The **MOS** model gives identical results as the **OS** model when the dipole moments are not included in the optimization, which is expected since the polarizability arises from the external field. Therefore, we only refer to **MOS** when the dipole moments have been included in the optimization. The inclusion of the dipole moments yields a more physical correct set of capacitance parameters. We find that all parameters are positive and follow the number of electrons in the element. However, the inclusion of atomic capacitances only yield a very slim improvement of the polarizability which are illustrated in figure 6.1. For the dipole moments no good fit were obtained even when only the dipole moments were optimized. Therefore, we tested a model where the internal fields were calculated without damping but no improvement was found. The **MOS** model also predicted the atomic charges of the molecules studied. These were found to have reasonable magnetude but showing little differences between atoms of the same element although their chemical environment were different. This indicated that only little charge transfer occurs, even in molecules like p-nitroaniline.

In line with the work presented in chapter 4 we adopt the **OS** and **MOS** models for a series of all trans n-alkenes. The models with atomic capacitances should improve the description of these extended π-systems. The results obtained by the different models are displayed in figure 6.2. We clearly see that no improvement is obtained using either the **OS** model or the **MOS** model. In fact, we obtain an incorrect description of the polarizability component along the chain when the size of the chain increases. For the polarizability components perpendicular to the chain we find excellent agreement between the different models and quantum chemical results. Therfore, an optimization of the **MOS** parameters using only the n-alkenes were employed. These result are displayed in figure 6.3 and shows good agreement for all polarizabillity components. However, the results obtained with the original parameters indicates some fundamental problems with the charge transfer models and are discussed in more detail in the next section.

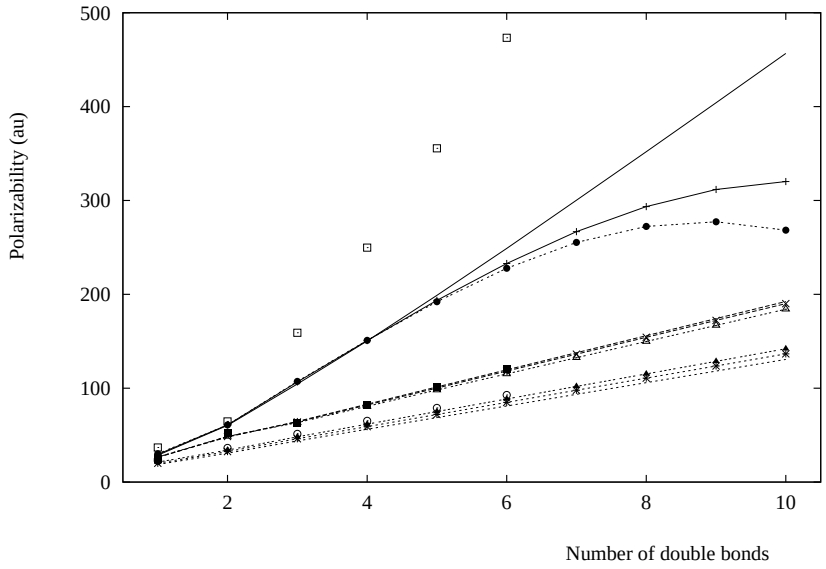

Figure 6.2: The static polarizazbility tensor for the trans-n-alkenes as a function of double bonds. The parameters were taken from table 6.1. ($\boxdot$) denotes QM component along($\|$) the chain. ($\circ, \blacksquare$) denotes QM components perpendicular ($\perp$) to the chain. For the modified Thole model (—), (- -) denotes $\|$ and $\perp$ components, respectively. Results from the Olson-Sundberg model is denoted by ($\bullet$) and ($\triangle, \blacktriangle$) for $\|$ and $\perp$ components, respectively. The modified Olson-Sundberg model is denoted by ($+$) and ($\times, *$) for $\|$ and $\perp$ components, respectively.

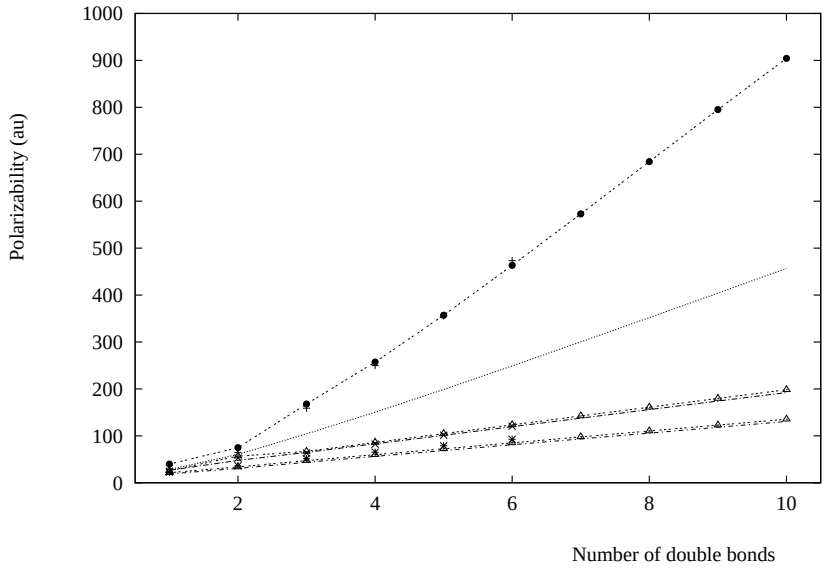

Figure 6.3: The static polarizazbility tensor for the trans-n-alkenes as a function of double bonds. The parameters used in the modified Olson-Sundberg model were optimized for the n-alkenes. ($+$) denotes QM component $\|$ to the chain. ($\times, *$) denotes QM components $\perp$ to the chain. For the modified Thole model ($\cdots$), ($\cdot - \cdot$) denotes $\|$ and $\perp$ components, respectively. The modified Olson-Sundberg model is denoted by ($\bullet$) and ($\triangle$) for $\|$ and $\perp$ components, respectively.

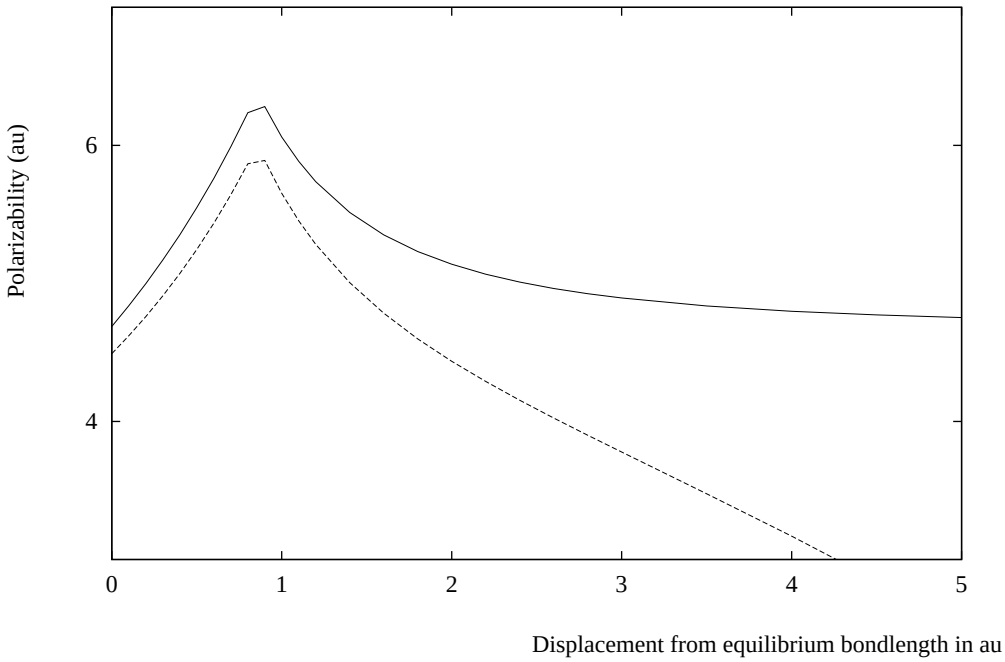

Figure 6.4: Polarizability along the bond-axis of HF as a function of the displacement from equilibrium bondlength. (—) denotes the modified Thole model and (- - -) denotes the Olson-Sundberg model.

6.3 Size Extensivity and the Interaction Model

Here we investigate the polarizability of the HF molecule as a function of the displacement from equilibrium. The results are plotted for the **MT** model and the **OS** model in figure 6.4. This is done in order to deduce whether the models are size-extensive or not. Size-extensivety means that in the limit of large separations the polarizability is given by the sum of the atomic contributions. From figure 6.4 it is clear that only the **MT** model is size-extensive. This explains the incorrect behaviour observed for the n-alkenes. This incorrect behaviour in the charge transfer models occur because there always is a contribution to the polarizability arising from the atomic capacitances, even at large separations. We also note that the damping function employed here is discontinuous, this will be discussed further in chapter 7. However, as indicated in figure 6.3 an optimization can hide the size-extensivity problem which could explain why this problem was not observed in the previous studies reported. Since the atomic capacitances gives the wrong long-range behaviour we will analyse the terms contributing to the induced atomic charge. This is done by written the energy of an atom p as

$$\mathrm{W} = \mathrm{W}_0 + q^{(0)}\phi + \frac{1}{2}a_p\phi^2 + \frac{1}{6}d_p\phi^3 - \frac{1}{2}\alpha_{p,\alpha\beta}E_\alpha E_\beta + \cdots, \tag{6.2}$$

which is an extention of Eq. 2 in Ref. [33]. Here, we have connected the atom to an external source such that charge may be transfered. ϕ is the potential difference between the source and the atom. Thus, the total charge are give by

$$q = \frac{\partial \mathrm{W}}{\partial \phi} = q^{(0)} + a_p\phi + \frac{1}{2}d_p\phi^2 + \cdots. \tag{6.3}$$

Therefore, the term that should be included instead of a_p is $\frac{1}{2}d_p\phi$. When considering interacting atoms the potential, ϕ, will depend on the atomic charges and the dipole moments and therefore an interative scheme must be adopted.

6.4 Conclusion

We have parameterized an atomic capacitance-polarizability model for 161 molecules. Also shown is that a small modification of the existing model a conceptualy new approach is obtained where the dipole moment, atomic charges and molecular polarizabilities can be calculated. However, it was shown that the atomic capacitances lead to an incorrect description for large separations of interacting atoms. This failure of size-extensivity of the charge transfer model gave incorrect behaviour in a series of n-alkens. Therefore, care must be taken when employing the model on large systems. General agreement with previous investigations were obtained but only minor improvements was observed. Finally, we discussed a possibly solution to the size-extensivity problem which hopefully also leads to an improvement in the model.

Chapter 7

Interaction Induced Polarizability in Dimers

In molecular crystals and polymers the macroscopic polarizability is a result of intermolecular interaction between individual molecules or single polymer chains. These intermolecular effect can have great influence on the macroscopic (hyper)polarizability of the material [122, 123]. Therefore, when discussing new materials for nonlinear optics it is important to have an understanding of the effects arising from the surrounding medium. As briefly discussed in section 2.5 the effective polarizability has to be calculated such that it takes account of the influence of the surrounding enviroment. In chapter 4, 5 and 6 we focused on describing the polarizability of single molecules. Here we investigate the interaction induced polarizability in three different homo-molecular dimers. The dimers chosen consist of hydrogenfluorid, methane and benzene molecules. These molecules have been chosen because they represents different kinds of interactions, i.e. hydrogen bonding, weak interactions and interactions between π-systems. The induced polarizability is studied both by quantum chemical methods and by the modified Thole model described in chapter 4.

7.1 Computational Methods

We will follow the same approach for the quantum chemical calculations as for the monomers, i.e using the Sadlej basis set [86] and the Dalton program package [82] at the SCF level. The geometry were taken as standard bond length and angles from Ref. [87, 88]. The alignment of the dimers are displayed in figure 7.1. The variable distance for the HF dimer is between F on molecule A and H on molcule B. For methane it is the distance between C on molecule A on H on molecules B, and in the benzene dimer it is the distance between the two planer molecules in the sandwich formation also indicated in figure 7.1.

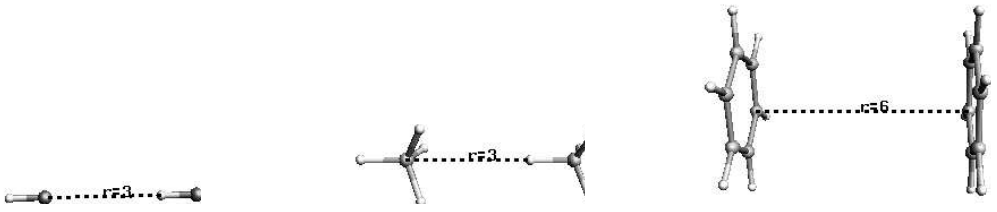

(a) HF dimer (b) Methane dimer (c) Benzene dimer

Figure 7.1: The alignment of the three dimers.

In all cases the variable distance will be refered to as the z-axis. The parameters used in the modified Thole model were taken from table 4.1. The interaction induced polarizability was calculated as the polarizability of the dimer substracted 2 times the polarizability of the monomer

$$\Delta\alpha^{ind} = \alpha^{dimer} - 2\alpha^{monomer}. \tag{7.1}$$

This implies that the model used has to be size extensive with respect to the polarizability. As discussed in section 6.3 the modified Thole model is size-extensive, in contrast to the modified Olson-Sundberg model which gives an incorrect description at large separations. Also the SCF method is size extensive [136]. However, in the case of the SCF calculations we have corrected for Basis Sets Superposition Errors (BSSE). This was done with the counterpoise method advogated by Boys and Bernardi [124]. BSSE occurs when basis functions at site A compensate for the basis set incompleteness at site B. Therefore in the counterpoise method the property of molecule A is calculated with the basis function from molecule B included as ghost atoms (no charge).

7.2 Results

The induced polarizability for the three dimers is displayed in figures 7.2, 7.3 and 7.4 for HF, methane and benzene respectively. The calculation were performed in the range from 10 au (20 au for the benzene dimer) to just below their equilibrium distance. For the HF dimer the equilibrium distance was taken to be around 3.5 au [125], in methane as 5.9 au [126] and for the benzene dimer as 7.2 au [127]. We find that the BSSE gives minor corrections to the induced polarizability, i.e the largest corrections was for the HF dimer about 6 %, for methane 5% and for benzene the largest correction, 14%, was for the polarizability perpendicular to the z-axis.

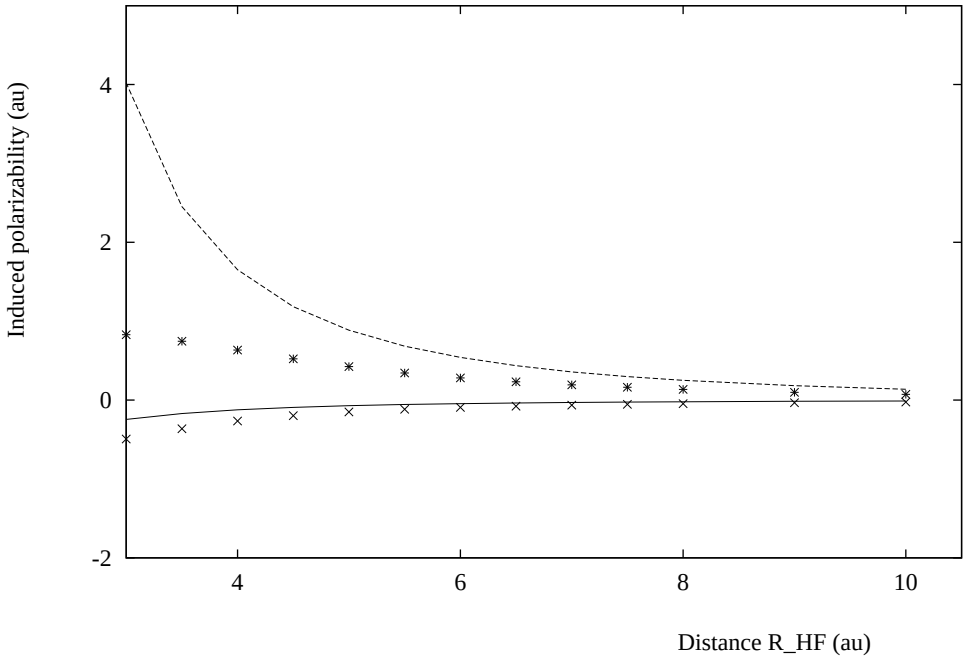

Figure 7.2: Induced polarizability in the HF dimer as a function of the distance between the HF units. Results from the modified Thole model is represented with lines and SCF results corrected for BSSE by dots. (- -,$*$) denote component along the z-axis and (—,$\times$) denotes the component perpendicular to he z-axis.

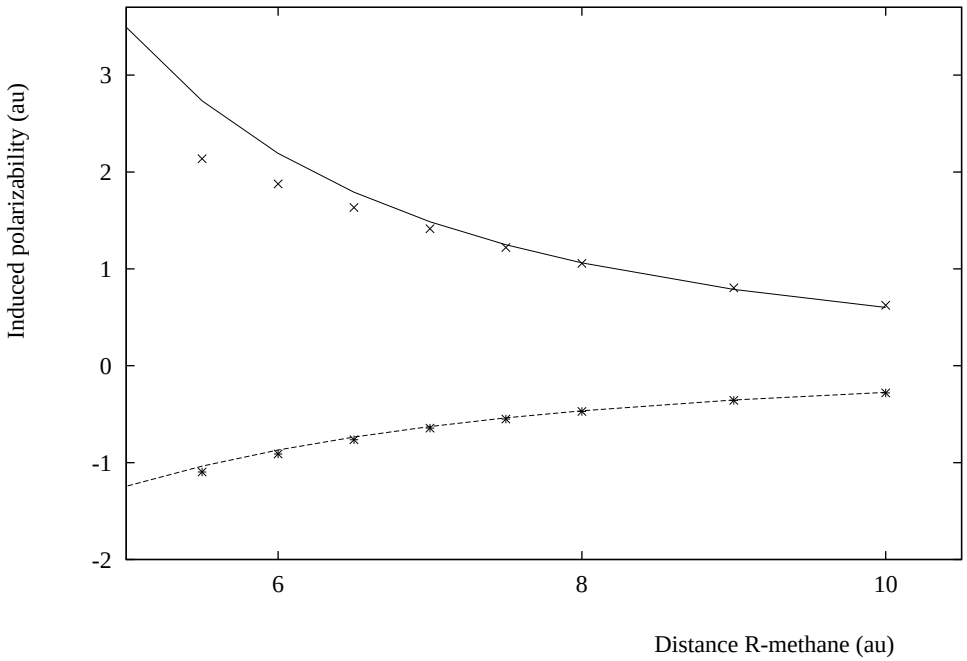

Figure 7.3: Induced polarizability in the methan dimer as a function of the distance between the methan units. Results from the modified Thole model is represented with lines and SCF results corrected for BSSE by dots. (—, $\times$) denote component along the z-axis and (- -, $*$) denotes the component perpendicular to the z-axis.

For the three dimers studied we find a very similar picture in spite of there different chemical composition. The induced polarizability along the z-axis is increased whereas the components perpendicular to the z-axis is decreased when the distance between the dimers is decreased. The increasement along the z-axis is caused by the cooperative interaction (head to tail) between two induced dipoles in the direction of the z-axis. This is also the same behavior that gave the infinite polarizabilities in the Applequist model described in section 3.5 which was corrected for in the modified Thole model. However, we still find that the modified Thole model predicts an induced polarizability along the z-axis which increases exponentialy for short distances. This indicates that the damping, that we introduced by modifing the interaction tensor, only occurs at intramolecular distances where as the SCF calculations predict a damping at short intermolecular distances. This is clearly illustrated in the figures 7.2 and 7.4 of the HF and benzene dimers at short intermolecular distances. The damping function that we have adopted from Thole [66] is discontinuos which is seen from figure 6.4, therefore it might be better to use a continous damping function which Burnham *et al* [129] also advocates in there aplication of Thole's model in molecular dynamics simulations.

We find for all three dimers good agreement between the modified Thole model and the SCF results when the distance between the dimers is larger than 6-7 au. Especially, the induced polarizability perpendicular to the z-axis is in very good agreement in the range investigated. This indicates that the long-range induced polarizability at the SCF level is well described in terms of dipole-induced dipole (DID) interactions and in good agreement with the results of Bishop and Dupuis for the He dimer [128]. At the shortest seperation the increasement in the SCF polarizability parallel to the z-axis is around 7% for all the dimers and perpendicular to the z-axis the decrease is between 8-16%, largest for the benzene dimer. Hättig et al [130] have shown that the static interaction induced properties of He dimer is only moderatly sensitive

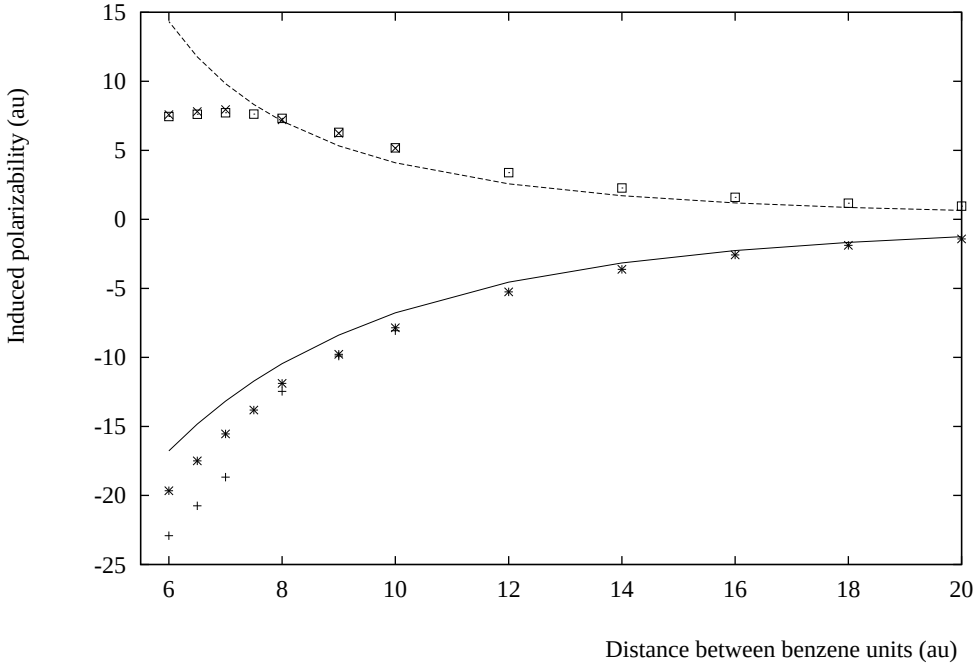

Figure 7.4: Induced polarizability in the benzene sandwich dimer as a function of the distance between the benzene units. Results from the modified Thole model is represented with lines and SCF results by dots. (- -, ⊡, ×) denote component along the z-axis and (—, ∗, +) denotes the component perpendicular to the z-axis. (×, +) denotes SCF results corrected for BSSE.

to the level of correlation and there findings are in good agreement with that of Bishop and Dupois [128]. This indicates that the results from this SCF investigation describes to a good extent the induced polarizability in the dimes. However, further investigation of the correlations effects on these larger dimers are needed before any definitive conclusions can be drawn.

7.3 Conclusion

In this work we have investigated the interaction induced static polarizability in three dimers using SCF calculations and a modified dipole interaction model. We have shown that for separations larger than 6 au the SCF results are reproduced by the modified Thole model. The difference between the SCF results and the modified Thole model at short separation is due to the lack of damping at intermolecular distances. We have shown that the induced polarizability in the dimer is not negliable at distances normal found in polymers and molecular crystals. Therefore it is very important to account for the pertubation arising from the surrounding medium when considering new photonic materials.

Chapter 8

Summary and Outlook

In this thesis we have presented an investigation of a classical atomic interaction model for the parameterization of the frequency-dependent molecular polarizabilities. We have shown that by adopting one set of parameters for each elements the (modified) Thole model successfully reproduces the static molecular SCF polarizability tensors of aliphatic and aromatic molecules. The extension of the interaction model to also include the frequency-dependence of the molecular polarizability is the first of its kind. It has been shown that the frequency-dependence of the polarizability well below any electronic absorbtions bands can be described with one parameter for each element. The model used to describe the frequency-dependence has previously been use at the molecular level but is here applied at the atomic level. However, the frequency-dependence of aromatic and aliphatic molecules are somewhat different and are best described with two sets of parameters.

The usefulness of the frequency-dependent interaction model has clearly been demonstrated in predicting frequency-dependent polarizabilities of carbon nanotubes. Becourse of the size of the nanotubes the aplication ofgh level *ab initio* methods are not feasible due to the massive computational resources needed. We have in good agreement with other reported studies demonstated the influence of symmetry/intramolecular geometry, length and caps on the polarizability of the tubes. The results are also in good agreement with our SCF calculations. The interaction model presented here provides a straightforward way of dealing with large systems out of the normal *ab initio* regime.

In order to improve the description of molecules containing extended π-systems we employed the concept of atomic capacitances modelling intramolecular charge transfer. By dividing the atomic charges into a nuclear charge and a charge arising from the electron distribution we modified the existing capacitance-polarizability model. This is a conceptually new approach which enables that also permanent molecular dipole moments and atomic charges can be modelled by an interaction model. However, this approach only gave minor improvement with respet to the modified Thole model. This could be due to the fact that the capacitance model was shown not to be size-extensive. The lack of size-extensivity lead to an incorrect description of the interaction at large seperations, and thereby limiting the model to small systems. A physical correct solution is to adopt a capacitance which is propertional to the total potential this ensures that for large distances the capacitance goes towards zero. The total potential needed arises from the charges and dipole moments and therefore an interative scheme is needed.

All of the above investigation were for isolated molecules and therefore the next step was the investigation of the interaction induced polarizability in dimers. The interaction between the dimers was shown to be rather similar in spite of their different chemical composition. For longer

seperation we found good agreement between the modified Thole model and SCF calculations. At shortere separations SCF calculations showed that the induced polarizability along the z-axis was damped. The modified Thole model did not predict this damping of the induced polarizability at short interaction. This is probably due to that the damping function employed here is intramolecular and therefore an investigation of a damping function showing the right intermolecular damping is in it place.

All of the investigation presented in this thesis revolves around the molecular polarizability. However, as mentioned in the introduction the purpose of this project was the development of a model capable of calculating both polarizabilities and hyperpolarizabilities. Also, the theory presented in chapter 3 describes both polarizabilities and hyperpolarizabilities. In fact we also implemented the procedure for calculating the static polarizabililty and first hyperpolarizaility using interacting atomic hyperpolarizabilities as described in section 3.7.1 and 3.7.2. The atomic charges needed in this procedure was calculated using Cioslowski's [131] Generalized Atomic Polar Tensor (GAPT) charges at the SCF level. The calculation of the GAPT charges is a computational expensive method due to that GABT charges are defined as derivatives of the dipole moment. We were unable to find any reasonabel fit to the first hyperpolarizability of a small set of aliphatic molecules and no improvement in the polarizability was obtained. This could indicate that the GAPT charges are not transferable in the sense needed in the interaction model or that the interaction of atomic hyperpolarizabilities is not the dominate contributions to the first hyperpolarizability.

Using the concept of interacting atoms, a nonvanishing term arises from the dipole-quadrupole polarizability, σ [33, 79]. Interacing dipole-quadrupole polarizability enables a description of the molecular first hyperpolarizability in a manner similar to that derived in section 3.7.2 using atomic hyperpolarizabilities. In this procedure there is no need for the atomic charges and is therefore a more atractive approach.

This project has clearly shown the usefulness of the interaction model. Also, illustrated was that there are some short-comings with the interaction model and therefore it should be used as a suplement to *ab initio* methods. However, further investigation using this model is still encouraged. Here we list some further directions and suggestions for further work employing the interaction model.

- Correction of the size-extensivity problem with the capacitance model. Hopefully this could lead to a better discription of molecules with extended π-systems which are very promising candidates for nonlinear optics. An improvement of the capacity model could also lead to the prediction of atomic charges and molecular dipole moment which may be used as representation of the electrostatics in Molecular Dynamics simulation.

- Frequency-dependent atomic capacitances. Using a frequency-dependent capacitance model the description of the frequency-dependent polarizability of aromatic, olefinic and aliphatic molecules with the same set of parameters could be possible.

- Implementing the dipole-quadrupole model. This could give a model capable of calculating the first hyperpolarizability without reference to the atomic charges. This opens for the possibly prediction of the very important SHG hyperpolarizability.

- Atomic capacitances and dipole-quadrupole model. Combining the capacitance and dipole-quadrupole model could improve the description of the hyperpolarizability where charge transfer is very important.

- Calculations on Boron-Nitride (BN) nanotubes [132–134]. The BN-nanotubes are predicted to have nonlinear optical properties that are larger that the corresponding carbon nanotubes. Also, such effects as doping the carbon nanontubes with small amounts of BN leads to an increase in their response properties.

Hopefully, the above-mentioned suggetions will lead to further investigations and improvement of the interaction model employed in this thesis.

Appendix A

Quantum Mechanics

A.1 The Schrödinger Equation

The world of molecules is governed by the laws of quantum mechanics. Therefore, in non-relativistic theory, we can obtain all information of a molecule by solving the time-dependent Schrödinger equation

$$\hat{H} \mid \Psi(t)\rangle = \mathrm{i}\frac{\partial}{\partial t} \mid \Psi(t)\rangle \,. \tag{A.1}$$

The Scrödinger equation can unfortunately only be solved for very simple systems. Therefore, when dealing with molecules, we have to use approximate methods. One standard approximation is the Born-Oppenheimer approximation which will be derived in the following section. This approximation leads to a separation of the Schrödinger equation into a part dealing with the electronic wave function and another part describing the nuclear wave function. It is the solution to the electronic Schrödinger equation which is the topic of appendix B and C.

A.2 Born-Oppenheimer Approximation

The following derivation of the Born-Oppenheimer approximation is based on Ref. [141]. The molecular Hamiltonian, $\hat{H}^{\mathrm{mol}}$, can be written as

$$\hat{H}^{\mathrm{mol}} = \sum_K \frac{1}{2M_K}\hat{P}_K^2 + \hat{H}^{\mathrm{el}}(R) + \hat{H}^{\mathrm{coupl}}, \tag{A.2}$$

where we have introduced the electronic Hamiltonian

$$\hat{H}^{\mathrm{el}}(\vec{R}) = \frac{1}{2m}\sum_i \hat{p}_i^2 - \sum_K \sum_i \frac{Z_K}{r_{iK}} + \sum_{j>i}\frac{1}{r_{ij}} + \sum_{L>K}\frac{Z_K Z_L}{R_{KL}} \tag{A.3}$$

and the molecular coupling operator

$$\hat{H}^{\mathrm{coupl}} = \frac{1}{2M_Q}\sum_{ji}\hat{p}_i\hat{p}_j - \frac{1}{M_Q}\sum_K\sum_i \hat{P}_K\hat{p}_i. \tag{A.4}$$

M_K, $\hat{P}_K$ and Z_K are the mass, momentum operator and charge of the K'th nucleus, respectively. For the i'th electron the mass is m, the momentum operator $\hat{p}_i$. $M_Q = \sum_K M_K$ is the total nuclear mass. We are interested in solving the time-independent Schrödinger equation given as

$$\hat{H}^{\mathrm{mol}}\Phi^{\mathrm{mol}}(\vec{r},\vec{R}) = E\Phi^{\mathrm{mol}}(\vec{r},\vec{R}). \tag{A.5}$$

Assuming that we have solved the electronic Schrödinger equation corresponding to the Hamiltonian in Eq. A.3 for all nuclear position ($\vec{R}$), we can expand our molecular wave function in terms of these solutions

$$\Phi^{\mathrm{mol}}(\vec{r},\vec{R}) = \sum_q \left|\Psi_q^{\mathrm{el}}(r;R)\right\rangle \left|\Theta_q^{\mathrm{nucl}}(R)\right\rangle, \tag{A.6}$$

where $\left|\Psi_q^{\mathrm{el}}(\vec{r};\vec{R})\right\rangle$ is a parametric function of the nuclear positions. Projection of the p'th electronic wave function and inserting the molecular Hamiltonian gives

$$\begin{aligned} & \left\langle \Psi_p^{\mathrm{el}}(\vec{r};\vec{R})\right| \textstyle\sum_K \frac{\hat{P}_K^2}{2M_K} \left|\Psi_p^{\mathrm{el}}(\vec{r};\vec{R})\Theta_p^{\mathrm{nucl}}(\vec{R})\right\rangle \\ + & \left\langle \Psi_p^{\mathrm{el}}(\vec{r};\vec{R})\right| \hat{H}^{coupl} \left|\Psi_p^{\mathrm{el}}(\vec{r};\vec{R})\Theta_p^{\mathrm{nucl}}(\vec{R})\right\rangle + (E_p^{\mathrm{el}} - E)\left|\Theta_p^{\mathrm{nucl}}(\vec{R})\right\rangle = \\ - & \textstyle\sum_{q\neq p}\left[\left\langle \Psi_p^{\mathrm{el}}(\vec{r};\vec{R})\right| \sum_K \frac{\hat{P}_K^2}{2M_K} \left|\Psi_q^{\mathrm{el}}(\vec{r};\vec{R})\Theta_q^{\mathrm{nucl}}(\vec{R})\right\rangle + \left\langle \Psi_p^{\mathrm{el}}(\vec{r};\vec{R})\right| \hat{H}^{\mathrm{coupl}} \left|\Psi_q^{\mathrm{el}}(\vec{r};\vec{R})\Theta_q^{\mathrm{nucl}}(\vec{R})\right\rangle\right]. \end{aligned} \tag{A.7}$$

Neglection of the terms on the right hand side, i.e. neglecting the coupling between differerently electronic wave function, and assuming the p'th electronic state nondegenerated yields the adiabatic approximation

$$\begin{aligned} \Bigg\{ \sum_K \frac{\hat{P}_K^2}{2M_K} + \sum_K \frac{1}{2M_K} \left\langle \Psi_p^{\mathrm{el}}(\vec{r};\vec{R})\right| \hat{P}_K^2 \left|\Psi_p^{\mathrm{el}}(\vec{r};\vec{R})\right\rangle + \frac{1}{2M_Q} \left\langle \Psi_p^{\mathrm{el}}(\vec{r};\vec{R})\right| \sum_{i,j} \hat{p}_i\hat{p}_j \left|\Psi_p^{\mathrm{el}}(\vec{r};\vec{R})\right\rangle \\ - \frac{1}{M_Q} \left\langle \Psi_p^{\mathrm{el}}(\vec{r};\vec{R})\right| \sum_{i,K} \hat{P}_K\hat{p}_i \left|\Psi_p^{\mathrm{el}}(\vec{r};\vec{R})\right\rangle + E_p^{\mathrm{el}} \Bigg\} \left|\Theta_p^{\mathrm{ad}}(\vec{R})\right\rangle = E_p^{\mathrm{ad}} \left|\Theta_p^{ad}(\vec{R})\right\rangle. \end{aligned} \tag{A.8}$$

Finally, by neglecting the terms that scale by the inverse of the nuclear masses, we obtain the Born-Oppenheimer approximation

$$\left\{ \sum_K \frac{1}{2M_K} \hat{P}_K^2 + E_p^{\mathrm{el}} \right\} \left|\Theta_p^{\mathrm{BO}}(\vec{R})\right\rangle = E_p^{\mathrm{BO}} \left|\Theta_p^{\mathrm{BO}}(\vec{R})\right\rangle. \tag{A.9}$$

The essence of the B.O. approximation is that the Schrödinger equation can be separated into an electronic and a nuclear equation. The approximations made is base on the neglection of the coupling between different electronic states and the great difference in masses between the electrons and the nuclei. Therefore the B.O. approximation is expected to break down for close-lying electronic states.

A.3 Second Quantization

In the following appendices we will shift to the second quantization representation. In second quantization we have a unified description of operators and states in terms of a single set of elementary creation, $a_p^\dagger$, and annihilation, a_q, operator. The elementary fermion operators fulfils the following set of anticommutator relations.

$$[a_p^\dagger, a_q]_+ = \delta_{pq}, \tag{A.10}$$

$$[a_p^\dagger, a_q^\dagger]_+ = 0, \tag{A.11}$$

$$[a_p, a_q]_+ = 0. \tag{A.12}$$

The wave function is written as a string of creation operators acting on a vacuum state

$$\Psi = a_1^\dagger a_2^\dagger \cdots a_N^\dagger \left|\text{vac}\right\rangle. \tag{A.13}$$

The antisymmetry of the electronic wave function is build into the operators, which is seen from the anticommutator relations. The spin-free non-relativistic electronic Hamilton operator is in second quantization given by

$$H^{\text{el}} = \sum_{pq} h_{pq} a_p^\dagger a_q + \frac{1}{2} \sum_{pqrs} g_{pqrs} a_p^\dagger a_r^\dagger a_s a_q + h^{\text{nuc}}, \tag{A.14}$$

where

$$h_{pq} = \int \phi_p(x)^* \left(-\frac{1}{2}\nabla^2 - \sum_i \frac{Z_i}{r_i} \right) \phi_q(x) dx \tag{A.15}$$

$$g_{pqrs} = \int\int \frac{\phi_p^*(x_1)\phi_r^*(x_2)\phi_q(x_1)\phi_s(x_2)}{r_{12}} dx_1 dx_2 \tag{A.16}$$

$$h^{\text{nuc}} = \frac{1}{2} \sum_{K \neq L} \frac{Z_K Z_L}{R_{KL}} \tag{A.17}$$

This means that the second quantization Hamiltonian, H^{el}, is the projection of the first quantizations operators onto a one-electron basis, $\{|\phi_p\rangle\}_{p=0,\ldots}$. The advantage of second quantization is that the antisymmetrizing operator in first quantization is replaced by algebraic rules for the creation and annihilation operators. Also, the fact that information of the number of electrons in the system is put in the wave function and therefore the Hamiltonian is independent of the size of the system [135].

Appendix B

Hartree-Fock Theory

When considering the electronic Schrödinger equation in the B.O. approximation, it can only be solved exactly for a one-electron system. In general we are interested in systems having many electrons and therefore we have to introduce some approximations. In accordance with the Pauli principle the total electronic wave function must be antisymmetric with respect to interchange of any two electron coordinates. This can be achieved by constructing the wavefuntion from Slater determinants. If we choose a single determinant or more general a single space- and spin-adapted Configuration State Function $|\text{CSF}\rangle$ we can derive the Hartree-Fock (HF) equations. The HF approximation is very important in electronic-structure theory. It is a starting point for either more approximative or more accurate models. The use of further approximations lead to semi-empirical methods, whereas the addition of extra determinants improve the solution upon correction for electron correlation and generates better models, which can be made converge towards the exact solution of the electronic Schrödinger equation [135]. In this chapter the Roothaan-Hall equations are derived based on Ref. [136].

B.1 Parametrization of the Wave Function

In Restricted Hartree-Fock (RHF) theory the electronic wave function is approximated by a single configuration function $|\text{CSF}\rangle$. Restricted refers to the fact that the wave function is conditioned to be an eigenfunction of the total and projected spin. This is done by requiring that the spin orbitals have the samme spatial parts for alpha and beta spins. The wave function is also required to transform as an irreducible representation of the molecular point group. For a closed shell configuration, which only consists of occupied (inactive) and empty (vitual) orbitals, the $|\text{CSF}\rangle$ can be written as:

$$|\text{CSF}\rangle = \prod_i a^\dagger_{i\alpha} a^\dagger_{i\beta} |\text{vac}\rangle \,. \tag{B.1}$$

$a^\dagger_{i\alpha}$ and $a_{i\alpha}$ fulfil the fermion algebra and $a^\dagger_{i\alpha}$ creates an electron in the i'th orbital with α-spin wheras $a_{i\alpha}$ annihiletes it. If we consider a real transformation (rotation of the molecular orbitals, MO's) of the original $|\text{CSF}\rangle$

$$|\,|\text{CSF}(\boldsymbol{\kappa})\rangle = \exp(-\kappa)\,|\text{CSF}\rangle \tag{B.2}$$

where the orbital rotation operator κ is an antiHermitian one-electron operator given by

$$\kappa = \sum_{p>q} \kappa_{pq}(E_{pq} - E_{qp}) = \sum_{p>q} \kappa_{pq} E^-_{pq}, \tag{B.3}$$

then the transformation preserves the orthonormality of the MO's and the spin of the $|\text{CSF}\rangle$. In order to preserve the spatial symmetry we only include the rotations among the orbitals that transform as the totally symmetric representation of the molecular point group. The one-electron operator E_{pq} is also called the excitation operator and is defined as:

$$E_{pq} = a^{\dagger}_{p\alpha}a_{q\alpha} + a^{\dagger}_{p\beta}a_{q\beta} \tag{B.4}$$

Not all of the rotations (κ_{pq}) in the orbital rotation operator B.3 are needed in the transformation of the wave function . The rotations that are not needed are refered to as redundent and are identified from the condition

$$E^{-}_{pq}\,|\text{CSF}\rangle = 0. \tag{B.5}$$

If we consider a closed shell configuration only rotations among occupied-virtuel orbitals are non-redundant.

B.2 The Energy Expansion

The energy of the transformed $|\text{CSF}\rangle$ is given by the expectation value of the hamiltonian

$$E(\boldsymbol{\kappa}) = \langle \text{CSF}(\boldsymbol{\kappa})|\, H\, |\text{CSF}(\boldsymbol{\kappa})\rangle \tag{B.6}$$

and this can be expanded using the Baker-Campbell-Hausdorff (BCH) series E.1 as

$$\begin{aligned} E(\boldsymbol{\kappa}) &= \langle \text{CSF}(\boldsymbol{\kappa}) \mid H \mid \text{CSF}(\boldsymbol{\kappa})\rangle \\ &= \langle \text{CSF} \mid \exp(\boldsymbol{\kappa}) H exp(-\boldsymbol{\kappa}) \mid \text{CSF}\rangle \\ &= \langle \text{CSF} \mid H \mid \text{CSF}\rangle + \langle \text{CSF} \mid [\boldsymbol{\kappa}, H] \mid \text{CSF}\rangle \\ &\quad + \frac{1}{2}\langle \text{CSF} \mid [\boldsymbol{\kappa}, [\boldsymbol{\kappa}, H]] \mid \text{CSF}\rangle + \cdots . \end{aligned} \tag{B.7}$$

If we instead use a Taylor expansion of the energy around $\boldsymbol{\kappa} = \mathbf{0}$ we can identify the terms in Eq. B.7

$$E(\boldsymbol{\kappa}) = E^{(0)} + \boldsymbol{\kappa}^T \boldsymbol{E}^{(1)} + \frac{1}{2}\boldsymbol{\kappa}^T \boldsymbol{E}^{(2)} \boldsymbol{\kappa} + \cdots \tag{B.8}$$

where $E^{(0)}$ is the total energy, $\boldsymbol{E}^{(1)}$ the gradient vector and $\boldsymbol{E}^{(2)}$ the electronic hessian at the expansion point. If we compare Eq. B.8 with Eq. B.7 we optain explicit expressions for the gradiant and hessian.

B.3 The Hartree-Fock Wave Function

The HF wave function corresponds to the $|\text{CSF}(\boldsymbol{\kappa})\rangle$ obtained by minimizing the expectation value of the Hamiltonian, $E(\boldsymbol{\kappa})$, with respect to the first order variation in the orbital-rotation parameters $\boldsymbol{\kappa}$

$$\delta E(\boldsymbol{\kappa}) = \delta \langle \text{CSF}(\boldsymbol{\kappa}) \mid H \mid \text{CSF}(\boldsymbol{\kappa})\rangle = 0. \tag{B.9}$$

The set of parameters κ^{HF}_{pq} that satisfies Eq.B.9 dfine the HF state. When the electronic gradient is zero the expectation value of the Hamiltonian is stationary and we can therefore write the variational condition, Eq. B.9 as

$$\left.\frac{\partial E(\boldsymbol{\kappa})}{\partial \kappa_{pq}}\right|_{\boldsymbol{\kappa}=\mathbf{0}} = \left\langle \mathrm{HF} \mid [E^-_{pq}, H] \mid \mathrm{HF} \right\rangle = 2 \left\langle \mathrm{HF} \mid [E_{pq}, H] \mid \mathrm{HF} \right\rangle = 0, \tag{B.10}$$

where the last equality holds for real wave functions only.

B.3.1 The Brillouin Theorem

The HF variational condition, Eq. B.10, can be written in the form

$$\langle \mathrm{HF} \mid H E_{pq} \mid \mathrm{HF} \rangle = \langle \mathrm{HF} \mid H E_{qp} \mid \mathrm{HF} \rangle \tag{B.11}$$

or written in terms of the excitations

$$\langle \mathrm{HF} \mid H \mid q \to p \rangle = \langle \mathrm{HF} \mid H \mid p \to q \rangle \,. \tag{B.12}$$

Eq. B.12 is called the generalized Brillouin theorem and states that the HF-state is in perfect balance between excitations and deexcitations. For a closed shell $|\mathrm{cs}\rangle$ which consist only of double occupied orbitals, all but single excited states are zero and Eq. B.12 reduces to

$$\langle \mathrm{cs} \mid [E_{ai}, H] \mid \mathrm{cs} \rangle = \langle cs \mid H \mid i \to a \rangle = 0, \tag{B.13}$$

which is refered to as the Brillouin theorem (BT).

B.4 The Fock-matrix

For a closed shell system the necessary condition for being in a optimized state is

$$2 \left\langle \mathrm{cs} \mid [E_{ai}, H] \mid \mathrm{cs} \right\rangle = 0, \tag{B.14}$$

which includes only the non-redundent parameters. If we want to include the redundent parameters we have to rearrange the operator in Eq. B.14 in such a way that it can be generalized to all elements p,q :

$$\begin{aligned}
\langle \mathrm{cs} \mid [E_{ai}, H] \mid \mathrm{cs} \rangle &= \sum_\sigma \Big\langle \mathrm{cs} \mid [a^\dagger_{a\sigma} a_{i\sigma}, H] \mid \mathrm{cs} \Big\rangle \\
&= \sum_\sigma \Big\langle \mathrm{cs} \mid [a^\dagger_{a\sigma}, H] a_{i\sigma} \mid \mathrm{cs} \Big\rangle \\
&= \sum_\sigma \Big\langle \mathrm{cs} \mid [a^\dagger_{a\sigma}, H] a_{i\sigma} + a_{i\sigma} [a^\dagger_{a\sigma}, H] \mid \mathrm{cs} \Big\rangle \\
&= \sum_\sigma \Big\langle \mathrm{cs} \mid [[a^\dagger_{a\sigma}, H], a_{i\sigma}]_+ \mid \mathrm{cs} \Big\rangle \\
&= -\sum_\sigma \Big\langle \mathrm{cs} \mid [a^\dagger_{a\sigma}, [a_{i\sigma}, H]]_+ \mid \mathrm{cs} \Big\rangle
\end{aligned} \tag{B.15}$$

which holds for closed shell states with real wave functions. If we now insert the expression for the total hamiltonial H, Eq. A.14, we can derive a more explicit expression of Eq. B.15. The constant nuclear part h^{nuc} makes no contribution and the contribution from the one-electron operator is

$$\begin{aligned}\sum_\sigma \left\langle \text{cs} \mid [a^\dagger_{n\sigma}, [a_{m\sigma}, h]]_+ \mid \text{cs} \right\rangle &= \sum_{pq}\sum_\sigma h_{pq} \left\langle \text{cs} \mid [a^\dagger_{n\sigma}, [a_{m\sigma}, E_{pq}]]_+ \mid \text{cs} \right\rangle \\ &= \sum_{pq}\sum_\sigma h_{pq} \left\langle \text{cs} \mid [a^\dagger_{n\sigma}, \delta_{pm} a_{q\sigma}]_+ \mid \text{cs} \right\rangle \\ &= \sum_{pq}\sum_\sigma h_{pq}\delta_{pm}\delta_{nq} \\ &= 2h_{mn}, \end{aligned} \tag{B.16}$$

where we have uses Eq. E.5. In the case of the two-electron operator

$$\sum_\sigma \left\langle \text{cs} \mid [a^\dagger_{n\sigma}, [a_{m\sigma}, \hat{g}]]_+ \mid \text{cs} \right\rangle = \frac{1}{2}\sum_\sigma \sum_{\substack{pqrs \\ \tau\upsilon}} g_{pqrs} \left\langle \text{cs} \mid [a^\dagger_{n\sigma}, [a_{m\sigma}, a^\dagger_{p\upsilon} a^\dagger_{r\tau} a_{s\tau} a_{q\upsilon}]]_+ \mid \text{cs} \right\rangle, \tag{B.17}$$

we first evaluate the inner commutator

$$\begin{aligned}\frac{1}{2}\sum_{\substack{pqrs \\ \tau\upsilon}} g_{pqrs}[a_{m\sigma}, a^\dagger_{p\upsilon} a^\dagger_{r\tau} a_{s\tau} a_{q\upsilon}] &= \frac{1}{2}\sum_{\substack{pqrs \\ \tau\upsilon}} g_{pqrs}\left([a_{m\sigma}, a^\dagger_{p\upsilon}]_+ a^\dagger_{r\tau} a_{s\tau} a_{q\upsilon} - a^\dagger_{p\upsilon}[a_{m\sigma}, a^\dagger_{r\tau}]_+ a_{s\tau} a_{q\upsilon}\right) \\ &= \frac{1}{2}\sum_{\substack{pqrs \\ \tau\upsilon}} g_{pqrs}\left(\delta_{mp}\delta_{\sigma\upsilon} a^\dagger_{r\tau} - \delta_{mr}\delta_{\sigma\tau} a^\dagger_{p\upsilon}\right) a_{s\tau} a_{q\upsilon} \\ &= \sum_{\substack{qrs \\ \tau}} g_{mqrs} a^\dagger_{r\tau} a_{s\tau} a_{q\sigma}, \end{aligned} \tag{B.18}$$

where we have used the permutational symmetry $g_{pqrs} = g_{rspq}$ and Eq. E.4. Inserting this into Eq. B.17 we can derive the final expression for the two-electron contribution

$$\begin{aligned}\sum_\sigma \left\langle \text{cs} \mid [a^\dagger_{n\sigma}, [a_{m\sigma}, g]]_+ \mid \text{cs} \right\rangle &= \sum_\sigma \sum_{\substack{qrs \\ \tau}} g_{mqrs} \left\langle \text{cs} \mid [a^\dagger_{n\sigma}, a^\dagger_{r\tau} a_{s\tau} a_{q\sigma}]_+ \mid \text{cs} \right\rangle \\ &= \sum_\sigma \sum_{\substack{qrs \\ \tau}} g_{mqrs} \left\langle \text{cs} \mid a^\dagger_{r\tau} a_{s\tau}[a^\dagger_{n\sigma}, a_{q\sigma}]_+ - a^\dagger_{r\tau}[a^\dagger_{n\sigma}, a_{s\tau}]_+ a_{q\sigma} \mid \text{cs} \right\rangle \\ &= \sum_\sigma \sum_{\substack{qrs \\ \tau}} g_{mqrs} \left\langle \text{cs} \mid \delta_{nq} a^\dagger_{r\tau} a_{s\tau} - \delta_{ns}\delta_{\sigma\tau} a^\dagger_{r\tau} a_{q\sigma} \mid \text{cs} \right\rangle \\ &= \left\langle \text{cs} \mid 2\sum_{rs} g_{mnrs} \sum_\tau a^\dagger_{r\tau} a_{s\tau} - \sum_{qr} g_{mqrn} \sum_\tau a^\dagger_{r\tau} a_{q\tau} \mid \text{cs} \right\rangle \\ &= \sum_{rs} (2g_{mnrs} - g_{msrn}) \left\langle \text{cs} \mid E_{rs} \mid \text{cs} \right\rangle, \end{aligned} \tag{B.19}$$

where Eq. E.6 has be utilized. From this we see that we have reduced our original operator in Eq. B.15 to an one-electron operator. The expectation value of the excitation operator, the one-electron density matrix, is zero unless p equals q and belongs to the set of occupied orbitals. When p equals q, the excitation operator becomme equal to the occupation number operator. This means that we can write our final equations as

$$-\frac{1}{2}\sum_\sigma \left\langle \text{cs} \mid [a^\dagger_{q\sigma}, [a_{p\sigma}, H]]_+ \mid \text{cs} \right\rangle = h_{pq} + \sum_i (2g_{pqii} - g_{piiq}). \tag{B.20}$$

The elements in Eq. B.20 are part of a matrix refered to as the Fock-matrix. The Fock-matrix is by contruction an effective one-electron Hamiltonian, which upon diagonalization yields a set of orbitals, called the canonical orbitals, from which the optimized HF wave function can be constructed. We can diagonalize the Fock-matrix with a similarity transformation and by rearraging we can write it as a pseudo-eigenvalue problem

$$\begin{aligned} \boldsymbol{U}^{-1}\boldsymbol{f}\boldsymbol{U} &= \boldsymbol{\epsilon} \\ \boldsymbol{f}\boldsymbol{U} &= \boldsymbol{U}\boldsymbol{\epsilon}. \end{aligned} \tag{B.21}$$

Eq. B.21 is an pseudo eigenvalue problem since the Fock-matrix contains contributions from the occupied canonical orbitals. Therefore, we need an interative scheme in order to solve the HF problem. From an initial set of orbitals we calculate the Fock-matrix using Eq. B.20, then the matrix is diagonalized and a new set of orbitals constructed using the transformation matrix $\boldsymbol{U}$. The Fock-matrix is now recalculated and the iterative scheme have been established. The iterations continue until the orbitals from which the Fock-matrix is contructed are the samme as the ones generated by diagonalization. We now have a solution that is self-consitent and this approach is referred to as the Self-Consistent Field (SCF) method.

B.5 The Roothaan-Hall Equations

The SCF procedure consist of calculations of the Fock-matrix in the MO basis, an approach that is computational expensive. Therefore, the MO's are expanded in terms of a set of known basis functions. The basis function are choosen as simple analytical functions centered at the nucleus of the atoms and are referred to as atomic orbitals AO's. For a description of basis sets see e.g. Ref. [135, 136]. The expansion of the MO's can be written in the following way, where we have arranged the AO's and MO's as row vectors $\boldsymbol{\chi}$ and $\boldsymbol{\phi}$, respectively

$$\boldsymbol{\phi} = \boldsymbol{\chi}\boldsymbol{C}. \tag{B.22}$$

Considering the elements of the Fock-matrix as matrix elements of an one-electron operator f and inserting the expansion of the MO's we get

$$\begin{aligned} f_{pg} &= \int d\tau \phi_p^* f \phi_q \\ &= \int d\tau \sum_\mu C_{p\mu}^* \chi_\mu^* f \sum_\upsilon C_{\upsilon q}\chi_\upsilon \\ &= \sum_{\mu\upsilon} C_{p\mu}^* \left[\int d\tau \chi_\mu^* f \chi_\upsilon\right] C_{\upsilon q} \\ &= \sum_{\mu\upsilon} C_{p\mu}^* f_{\mu\upsilon}^{AO} C_{\upsilon q}, \end{aligned}$$

or written as a matrix equation where we have the transformation of the Fock-matrix from the MO basis to the AO basis

$$\boldsymbol{f} = \boldsymbol{C}^T \boldsymbol{f}^{AO} \boldsymbol{C}. \tag{B.23}$$

Inserting this transformation into Eq. B.20 we obtain

$$\boldsymbol{C}^T \boldsymbol{f}^{AO} \boldsymbol{C}\boldsymbol{U} = \boldsymbol{U}\boldsymbol{\epsilon}, \tag{B.24}$$

where we have used that the coefficient matrix $\boldsymbol{C}$ are real. Using the fact that the MO's are orthonormal

$$\mathbf{1} = \boldsymbol{\phi}^\dagger \boldsymbol{\phi} = \boldsymbol{C}^T \boldsymbol{\chi}^\dagger \boldsymbol{\chi} \boldsymbol{C} = \boldsymbol{C}^T \boldsymbol{S} \boldsymbol{C}, \tag{B.25}$$

where $\boldsymbol{S}$ is the AO overlap matrix, we can write Eq. B.24 as

$$\boldsymbol{f}^{AO} \boldsymbol{C} \boldsymbol{U} = \boldsymbol{S} \boldsymbol{C} \boldsymbol{U} \boldsymbol{\epsilon} = \boldsymbol{S} \boldsymbol{C}' \boldsymbol{\epsilon} = \boldsymbol{f}^{AO} \boldsymbol{C}'. \tag{B.26}$$

This equation is referred to as the Roothaan-Hall equation, and the elements of the Fock-matrix in the AO basis can now be evaluated as

$$f_{\mu\upsilon}^{AO} = h_{\mu\upsilon} + \sum_i (2g_{\mu\upsilon ii} - g_{\mu ii\upsilon}), \tag{B.27}$$

where the transformation of the integral $g_{\mu\upsilon ii}$ is

$$\begin{aligned} g_{\mu\upsilon ii} &= \int \chi_\mu^* \phi_i^* \hat{g} \chi_\upsilon \phi_i d\tau \\ &= \sum_{\rho\sigma} C_{\rho i} C_{\sigma i} \int \chi_\mu^* \chi_\rho^* \hat{g} \chi_\upsilon \chi_\sigma d\tau \\ &= \sum_{\rho\sigma} C_{\rho i} C_{\sigma i} g_{\mu\upsilon\rho\sigma}. \end{aligned}$$

Inserting this expansion into Eq. B.27 we get

$$\begin{aligned} f_{\mu\upsilon}^{AO} &= h_{\mu\upsilon} + \sum_{\rho\sigma} \sum_i C_{\rho i} C_{\sigma i} (2g_{\mu\upsilon\rho\sigma} - g_{\mu\rho\sigma\upsilon}) \\ &= h_{\mu\upsilon} + \sum_{\rho\sigma} P_{\rho\sigma} (g_{\mu\upsilon\rho\sigma} - \frac{1}{2} g_{\mu\rho\sigma\upsilon}) \end{aligned} \tag{B.28}$$

where $P_{\rho\sigma}$ is the one-electron density matrix in the AO basis. We can now establish a very simple iterative scheme as

1. Calculation of density matrix P^n from $P_{\rho\sigma} = 2\sum_i C_{\rho i} C_{\sigma i}$
2. Calculate $\boldsymbol{f}^{AO}$ from Eq. B.28
3. Transform $\boldsymbol{f}^{AO}$ to $\boldsymbol{f}$ using Eq. B.23
4. Generate the n'th errorvector e_n from the occupied-virtual block of $\boldsymbol{f}$. See Eq. B.14
   (a) if $|e_n| < \epsilon$ then convergence.
   (b) otherwise generate a new set of orbitals C^{n+1} by diagonalization of the Fock-matrix using Eq. B.24 and return to step 1.

This is only a very simple scheme and in real calculation other methods are used in order to speed up the optimization procedure. [136]

Appendix C

Response Theory

In order to calculate properties of molecules subjected to a time-dependent external pertubation we adopt quantum-chemical response theory. We restrict the treatment to situations where the interaction between the external field and the molecular system is considered in the perturbation limit. In this chapter the response function of an exact and an SCF state is derived, following the derivations in Ref. [137, 138]. The explicit derivation is limited to the linear response functions.

C.1 Response Theory for an Exact State

The time-dependent schrödinger equation A.1 describes the time-development of an exact wave function $\left|\overline{0}(t)\right\rangle$. The total Hamiltonian of the molecular system interacting with an external field is:

$$H = H_0 + V^t, \tag{C.1}$$

where H_0 is the time independent Hamiltonian of the unperturbed system and where V^t is the time dependent perturbation. The perturbation is assumed switched on adiabatically (slowly) at $t \to -\infty$ and can therefore be represented by its Fourier composition

$$V^t = \int_{-\infty}^{\infty} d\omega V^\omega e^{(-\mathrm{i}\omega+\epsilon)t}, \tag{C.2}$$

where ϵ is a positive infinitisimal number ensuring that the perturbation is zero at $t \to -\infty$. The frequency domain function here is continuous, but in many cases only a few discrete frequencies are involved. It is required that the perturbation is hermitian and therefore $(V^\omega)^\dagger = V^{-\omega}$. It is assumed that $\left|\overline{0}(t)\right\rangle$ is an eigenfunction $|0\rangle$ of H_0 at $t \to -\infty$. Let us consider the time-development of the density operator $\rho(t)$ of the state $\left|\overline{0}(t)\right\rangle$: according to the Quantum-Liouville equation

$$\mathrm{i}\frac{\partial \rho(t)}{\partial t} = [H, \rho(t)], \tag{C.3}$$

where the density operator is given by $\rho(t) = \left|\overline{0}(t)\right\rangle \left\langle\overline{0}(t)\right|$. Changing to the interaction representation the density operator become

$$\rho^I(t) \equiv e^{\mathrm{i}H_0 t}\rho(t)e^{-\mathrm{i}H_0 t} \tag{C.4}$$

and the Quantum-Liouville equation can be written as [31]

$$\mathrm{i}\frac{\partial \rho^I(t)}{\partial t} = \mathrm{i}\left\{\mathrm{i}[H_0, \rho^I(t)] + e^{\mathrm{i}H_0 t}\frac{\partial \rho(t)}{\partial t}e^{-\mathrm{i}H_0 t}\right\}$$

$$
\begin{aligned}
&= \mathrm{i}\left\{\mathrm{i}[H_0, \rho^I(t)] - \mathrm{i}e^{\mathrm{i}H_0 t}[H_0 + V^{t'}, \rho(t)]e^{-\mathrm{i}H_0 t}\right\} \\
&= [V_{t'}(t), \rho^I(t)] = \mathcal{L}_{t'}(t)\rho^I(t), \qquad \text{(C.5)}
\end{aligned}
$$

where we have introduced the so-called Liouvillian operator, $\mathcal{L}_{t'}(t)$, and

$$V_{t'}(t) = e^{\mathrm{i}H_0 t} V^{t'} e^{-\mathrm{i}H_0 t}. \qquad \text{(C.6)}$$

Integration of C.5 yields

$$\rho^I(t) = \rho_0 - \mathrm{i}\int_{-\infty}^{t} dt' \mathcal{L}_{t'}(t')\rho^I(t'), \qquad \text{(C.7)}$$

A solution of Eq. C.7 can be obtained iteratively by using ρ_0 as the zeroth order approximation for ρ^I [138]. Thus, to first order we get

$$\rho^I(t) = \rho_0 - \mathrm{i}\int_{-\infty}^{t} dt' \mathcal{L}_{t'}(t')\rho_0, \qquad \text{(C.8)}$$

which can be rewritten using Eq. C.4 and Eq. C.6 as

$$\rho(t) = \rho_0 - \mathrm{i}\int_{-\infty}^{t} dt' \mathcal{L}_{t'}(t'-t)\rho_0. \qquad \text{(C.9)}$$

As in time-independent pertubation theory it is the expectation value of an operator more than the specific wave function that is of interest. Using that the expectation value can be written as the trace of the corresponding density operator times the operator, we may write to first order

$$
\begin{aligned}
\left\langle \overline{0}(t) \mid A \mid \overline{0}(t) \right\rangle &= \mathrm{Tr}(\rho(t)A) \\
&= \langle 0 \mid A \mid 0 \rangle - \mathrm{i}\int_{-\infty}^{t} dt' \mathrm{Tr}(\mathcal{L}_{t'}(t'-t)\rho_0 A) \\
&= \langle 0 \mid A \mid 0 \rangle - \mathrm{i}\int_{-\infty}^{t} dt' \mathrm{Tr}[V_{t'}(t'-t)\rho_0 A - \rho_0 V_{t'}(t'-t)A] \\
&= \langle 0 \mid A \mid 0 \rangle - \mathrm{i}\int_{-\infty}^{t} dt' \mathrm{Tr}(\rho_0 [A, V_{t'}(t'-t)]) \\
&= \langle 0 \mid A \mid 0 \rangle - \mathrm{i}\int_{-\infty}^{t} dt' \left\langle 0 \mid [A, V_{t'}(t'-t)] \mid 0 \right\rangle, \qquad \text{(C.10)}
\end{aligned}
$$

where we have used Eq. C.9 and the cyclic invariance of the trace. We now introduce the two-time retarded Green's function or propagator [138, 139] defined as

$$\left\langle\left\langle A; V_{t'}(t'-t) \right\rangle\right\rangle = -\mathrm{i}\Theta(t-t') \left\langle 0 \mid [A, V_{t'}(t'-t)] \mid 0 \right\rangle, \qquad \text{(C.11)}$$

where $\Theta(t-t')$ is the Heaviside step function which is equal to one when $t' < t$ and otherwise zero. Inserting this into Eq. C.10 and using Eq. C.2 we get

$$
\begin{aligned}
\left\langle \overline{0}(t) \mid A \mid \overline{0}(t) \right\rangle &= \langle 0 \mid A \mid 0 \rangle + \int_{-\infty}^{\infty} d\omega \int_{-\infty}^{\infty} dt' \left\langle\left\langle A; V^{\omega}(t'-t) \right\rangle\right\rangle e^{(-\mathrm{i}\omega+\epsilon)t'} \qquad \text{(C.12)} \\
&= \int_{-\infty}^{\infty} d\omega \left\langle\left\langle A; V^{\omega} \right\rangle\right\rangle_{\omega} e^{(-\mathrm{i}\omega+\epsilon)t}. \qquad \text{(C.13)}
\end{aligned}
$$

Continuing the iterative procedure of Eq. C.7 to higher order we can write the expectation value as

$$\left\langle \overline{0}(t) \mid A \mid \overline{0}(t) \right\rangle = \langle 0 \mid A \mid 0 \rangle + \int_{-\infty}^{\infty} d\omega_1 e^{(-\mathrm{i}\omega_1+\epsilon)t} \left\langle\left\langle A; V^{\omega_1} \right\rangle\right\rangle_{\omega_1}$$
$$+\frac{1}{2}\int_{-\infty}^{\infty} d\omega_1 \int_{-\infty}^{\infty} d\omega_2 e^{(-\mathrm{i}(\omega_1+\omega_2)+2\epsilon)t} \left\langle\left\langle A; V^{\omega_1}, V^{\omega_2} \right\rangle\right\rangle_{\omega_1,\omega_2} + \cdots . \tag{C.14}$$

The functions $\left\langle\left\langle A; V^{\omega_1} \right\rangle\right\rangle_{\omega_1}$ and $\left\langle\left\langle A; V^{\omega_1}, V^{\omega_2} \right\rangle\right\rangle_{\omega_1,\omega_2}$ are the linear and quadratic response functions, respectively.

C.1.1 The Spectral Representation

Using the definition of the linear response function we can rewrite it in order to extract physical information. The response function is in the frequency representation given by

$$\left\langle\left\langle A; V^{\omega} \right\rangle\right\rangle_{\omega} = \lim_{\epsilon\to 0} \int_{-\infty}^{\infty} dt \left\langle\left\langle A; V^{\omega}(t) \right\rangle\right\rangle e^{(-\mathrm{i}\omega+\epsilon)t}. \tag{C.15}$$

Inserting Eq. C.11 and the resolution of the identity $1 = \sum_n |n\rangle \langle n|$ gives

$$\begin{aligned}
\left\langle\left\langle A; V^{\omega} \right\rangle\right\rangle_{\omega} &= -\mathrm{i}\lim_{\epsilon\to 0} \int_{-\infty}^{\infty} dt \Theta(-t) \langle 0 \mid [A, V^{\omega}(t)] \mid 0 \rangle e^{(-\mathrm{i}\omega+\epsilon)t} \\
&= -\mathrm{i}\lim_{\epsilon\to 0} \int_{-\infty}^{0} dt \sum_n e^{(-\mathrm{i}\omega+\epsilon)t} \left\{ \langle 0 \mid A \mid n \rangle \left\langle n \mid e^{\mathrm{i}H_0 t} V^{\omega} e^{-\mathrm{i}H_0 t} \mid 0 \right\rangle \right. \\
&\quad \left. - \left\langle 0 \mid e^{\mathrm{i}H_0 t} V^{\omega} e^{-\mathrm{i}H_0 t} \mid n \right\rangle \langle n \mid A \mid 0 \rangle \right\} \\
&= -\mathrm{i}\lim_{\epsilon\to 0} \int_{-\infty}^{0} dt \sum_n e^{(-\mathrm{i}\omega+\epsilon)t} \left\{ \langle 0 \mid A \mid n \rangle \langle n \mid V^{\omega} \mid 0 \rangle e^{\mathrm{i}\omega_n t} \right. \\
&\quad \left. - \langle 0 \mid V^{\omega} \mid n \rangle \langle n \mid A \mid 0 \rangle e^{-\mathrm{i}\omega_n t} \right\} \\
&= \lim_{\epsilon\to 0} \sum_{n\neq 0} \frac{\langle 0 \mid A \mid n \rangle \langle n \mid V^{\omega} \mid 0 \rangle}{\omega - \omega_n + \mathrm{i}\epsilon} - \frac{\langle 0 \mid V^{\omega} \mid n \rangle \langle n \mid A \mid 0 \rangle}{\omega + \omega_n + \mathrm{i}\epsilon},
\end{aligned} \tag{C.16}$$

where $\omega_n = E_n - E_0$. Eq. C.16 is refered to as the spectral representation of the linear response function [137,138]. The linear response function has poles at frequency $\pm\omega_n$, which corresponds to the excitation energies of the unperturbed system. We also see that the residues at the poles corresponds to transitions matrix elements.

C.1.2 Time-development of an Exact State

In order to determine the time-development of an exact state we rewrite the time-dependent Schrödinger equation. We can write the wave function in the phase isolated form as

$$\mid \overline{0} \rangle = e^{-\mathrm{i}\mathrm{F}(t)} \mid \tilde{0} \Big\rangle, \tag{C.17}$$

and introducing this into the Schrödinger equation we can write it as

$$\left(H - \mathrm{i}\frac{\partial}{\partial t} - \dot{\mathrm{F}}(t) \right) \mid \tilde{0} \rangle = 0. \tag{C.18}$$

$\dot{\mathrm{F}}(t)$ is denoted the time-dependent quasienergy and can be used to derive the response function from time-average variational pertubation theory. [140] Projection of Eq. C.18 onto a first-order variation gives

$$\langle \delta\overline{0} \mid \left(H - \mathrm{i}\frac{\partial}{\partial t} - \dot{\mathrm{F}}(t) \right) \mid \tilde{0} \rangle = 0. \tag{C.19}$$

A variation of the complete wave function, $\left|\overline{0}\right\rangle$, can be seperated into

$$\left|\delta\overline{0}\right\rangle = e^{-\mathrm{iF}}\left|\delta\tilde{0}\right\rangle - \mathrm{i}\delta\mathrm{F}e^{-\mathrm{iF}}\left|\tilde{0}\right\rangle. \tag{C.20}$$

This allows us to rewrite Eq. C.19 as

$$\left\langle\delta\tilde{0}\mid\left(H-\mathrm{i}\frac{\partial}{\partial t}-\dot{\mathrm{F}}(t)\right)\mid\tilde{0}\right\rangle = 0. \tag{C.21}$$

An allowed variation of $\left|\tilde{0}\right\rangle$ can be written as a variation along $\left|\tilde{0}\right\rangle$ and along its orthogonal complement

$$\left|\delta\tilde{0}\right\rangle = \left|\delta\tilde{0}^{\perp}\right\rangle + \mathrm{i}\alpha\left|\tilde{0}\right\rangle, \tag{C.22}$$

where $\left|\delta\tilde{0}^{\perp}\right\rangle$ is orthogonal to $\left|\tilde{0}\right\rangle$ and α is real. The fact that the variation along $\left|\tilde{0}\right\rangle$ is imaginary can be seen from the normalization condition on $\left|\overline{0}\right\rangle$ and the allowed variations of $\left|\delta\tilde{0}\right\rangle$

$$\left\langle\overline{0}\mid\overline{0}\right\rangle = \left\langle\tilde{0}\mid\tilde{0}\right\rangle = 1 \tag{C.23}$$

$$\left\langle\delta\tilde{0}\mid\tilde{0}\right\rangle + \left\langle\tilde{0}\mid\delta\tilde{0}\right\rangle = 0. \tag{C.24}$$

Using this expansion of the variations we see that the variations along $\left|\delta\tilde{0}\right\rangle$ vanish and Eq. C.21 can be written as

$$\left\langle\delta\tilde{0}^{\perp}\mid\left(H-\mathrm{i}\frac{\partial}{\partial t}\right)\mid\tilde{0}\right\rangle = 0. \tag{C.25}$$

If we use the fact that $\mathrm{i}\alpha\left\langle\tilde{0}\mid H-\mathrm{i}(\partial/\partial t)\mid\tilde{0}\right\rangle$ is purely imaginary we can reintroduce $\left|\delta\tilde{0}\right\rangle$ and write Eq. C.25 as

$$\mathrm{Re}\left\langle\delta\tilde{0}\mid\left(H-\mathrm{i}\frac{\partial}{\partial t}\right)\mid\tilde{0}\right\rangle = 0. \tag{C.26}$$

For an exact state we have that $i\left|\delta\tilde{0}^{\perp}\right\rangle$ is an allowed variation if $\left|\delta\tilde{0}^{\perp}\right\rangle$ is allowed. This gives us the following equation

$$\mathrm{Im}\left\langle\delta\tilde{0}\mid\left(H-\mathrm{i}\frac{\partial}{\partial t}\right)\mid\tilde{0}\right\rangle = 0. \tag{C.27}$$

Equation C.26 and Eq. C.27 will be used to determine the time-development of the SCF state.

C.2 Response Functions for an SCF Wave Function

The Hartree-Fock wave function is an approximate wave function and therefore the linear response function is not equal to Eq. C.16. To obtain the response functions we have to make some restrictions on how the SCF state evolves in time. The time development of an SCF state is given by [137]

$$\left|\tilde{0}\right\rangle = \exp[\mathrm{i}\kappa(t)]\left|0_{\mathrm{HF}}\right\rangle, \tag{C.28}$$

where the reference wave function $\left|0_{\mathrm{HF}}\right\rangle$ is a single CSF which fulfills the Brillouin theorem Eq.B.13. The orbital rotation operator is given by

$$\kappa = \sum_{k}[\kappa_k(t)q_k^{\dagger} + \kappa_k^{*}(t)q_k], \tag{C.29}$$

where we have introduced the notation $q_k^\dagger = E_{pq}$ for $p > q$ and $q_k = E_{pq}$ for $p < q$. The index k runs over the nonredundant orbital operators. The restiction that we will make is that the allowed variation of the state can be written as

$$\left|\delta\tilde{0}\right\rangle = \mathrm{i}\sum_k (\eta_k \tilde{q}_k^\dagger + \eta_k^* \tilde{q}_k)\left|\tilde{0}\right\rangle, \tag{C.30}$$

where η_k are the varational parameters and $\tilde{q}_k$ the transformed operators

$$\tilde{q}_k = \exp[\mathrm{i}\kappa(t)] q_k \exp[-\mathrm{i}\kappa(t)]. \tag{C.31}$$

This variation ensures that if $\left|\delta\tilde{0}^\perp\right\rangle$ is an allowed variation then also $\mathrm{i}\left|\delta\tilde{0}^\perp\right\rangle$ is also allowed. The approach using an SCF reference state and the restictions on the variations, i.e. Eq. C.30, is referred to as the Random Phase Approximation (RPA). Introducing this approximation into Eq. C.26 and Eq. C.27 we have

$$\mathrm{Re}\left\langle\tilde{0}\right| (\tilde{q}_k^\dagger - \tilde{q}_k)\left(H - \mathrm{i}\frac{\partial}{\partial t}\right)\left|\tilde{0}\right\rangle = 0, \tag{C.32}$$

$$\mathrm{Im}\left\langle\tilde{0}\right| (\tilde{q}_k^\dagger + \tilde{q}_k)\left(H - \mathrm{i}\frac{\partial}{\partial t}\right)\left|\tilde{0}\right\rangle = 0. \tag{C.33}$$

Using that $\mathrm{Re}A = \frac{1}{2}(A + A^*)$ and $\mathrm{Im}A = \frac{1}{2}(A - A^*)$ we expand Eqs. C.32, C.33 and get the Ehrenfest equations of motion (EOM) for $\tilde{q}_k$ and $\tilde{q}_k^\dagger$, respectively

$$\mathrm{i}\frac{d}{dt}\left\langle\tilde{0} \mid \tilde{q}_k \mid \tilde{0}\right\rangle = \mathrm{i}\left\langle\tilde{0}\right| \frac{\partial\tilde{q}_k}{\partial t}\left|\tilde{0}\right\rangle + \left\langle\tilde{0} \mid [\tilde{q}_k, H] \mid \tilde{0}\right\rangle, \tag{C.34}$$

$$\mathrm{i}\frac{d}{dt}\left\langle\tilde{0} \mid \tilde{q}_k^\dagger \mid \tilde{0}\right\rangle = \mathrm{i}\left\langle\tilde{0}\right| \frac{\partial\tilde{q}_k^\dagger}{\partial t}\left|\tilde{0}\right\rangle + \left\langle\tilde{0} \mid [\tilde{q}_k^\dagger, H] \mid \tilde{0}\right\rangle. \tag{C.35}$$

Using a more general operator basis we can write the orbital rotation operator, eq. C.29, as

$$\kappa = \boldsymbol{O}\boldsymbol{\alpha}, \tag{C.36}$$

$$\boldsymbol{O} = (\boldsymbol{q}^\dagger, \boldsymbol{q})\boldsymbol{X}, \tag{C.37}$$

$$\boldsymbol{\alpha} = \boldsymbol{X}^{-1}\begin{pmatrix} \boldsymbol{\kappa} \\ \boldsymbol{\kappa}^* \end{pmatrix}, \tag{C.38}$$

where the transformation matrix, $\boldsymbol{X}$, has the structure

$$\boldsymbol{X} = \begin{bmatrix} {}^1\boldsymbol{X} & {}^2\boldsymbol{X}^* \\ {}^2\boldsymbol{X} & {}^1\boldsymbol{X}^* \end{bmatrix} \tag{C.39}$$

This allows us to rewrite the EOM as a single matrix equation

$$\frac{d}{dt}\left\langle\tilde{0}\right| \tilde{\boldsymbol{O}}^\dagger \left|\tilde{0}\right\rangle - \left\langle\tilde{0}\right| \frac{\partial\tilde{\boldsymbol{O}}^\dagger}{\partial t}\left|\tilde{0}\right\rangle = -\mathrm{i}\left\langle\tilde{0}\right| [\tilde{\boldsymbol{O}}^\dagger, H]\left|\tilde{0}\right\rangle, \tag{C.40}$$

with the j'th component of $\tilde{\boldsymbol{O}}$ given as

$$\tilde{O}_j = \exp[\mathrm{i}\kappa(t)] O_j \exp[-\mathrm{i}\kappa(t)] \tag{C.41}$$

subjectet to the boundary condition $\kappa(t) \to 0$ for $t \to -\infty$, ensuring that $\left|\tilde{0}\right\rangle \to |0\rangle$ for $t \to -\infty$. Using Eq. E.3 we can rewrite the left side of Eq. C.40 as

$$\sum_{n=0}^{\infty} \frac{(-1)^n (\mathrm{i})^{n+1}}{(n+1)!} \langle 0| \left[O_j^\dagger, (\hat{\kappa}^n \dot{\kappa})\right] |0\rangle \tag{C.42}$$

$$= \sum_{n=0}^{\infty} \frac{(-1)^n (\mathrm{i})^{n+1}}{(n+1)!} \langle 0| \left[O_j^\dagger, \left(\prod_{\mu=2}^{n+1} \hat{O}_{l_\mu} O_{l_1}\right)\right] |0\rangle \, \dot{\alpha}_{l_1} \prod_{\mu=2}^{n+1} \alpha_{l_\mu} \tag{C.43}$$

$$= \sum_{n=0}^{\infty} \mathrm{i}^n S^{[n+1]}_{j l_1 l_2 \cdots l_n} \dot{\alpha}_{l_1} \prod_{\mu=2}^{n} \alpha_{l_\mu}, \tag{C.44}$$

where we have shifted the summation and introduced the superoperator defined in Eq. E.2. The right-hand side of Eq. C.40 can be devided into two terms, one from H_0 and another from V^t. Each of these terms can be expanded using the BCH expansion E.1 as

$$-\mathrm{i} \langle 0| \left[\tilde{O}_j^\dagger, H_0\right] |0\rangle = \sum_{n=0}^{\infty} \frac{(-\mathrm{i})^{n+1}}{n!} \langle 0| \left[O_j^\dagger, (\hat{\kappa}^n H_0)\right] |0\rangle \tag{C.45}$$

$$= -\sum_{n=0}^{\infty} \mathrm{i}^{n+1} E^{[n+1]}_{j l_1 l_2 \cdots l_n} \prod_{\mu=1}^{n} \alpha_{l_\mu} \tag{C.46}$$

and

$$-\mathrm{i} \langle 0| \left[\tilde{O}_j^\dagger, V^t\right] |0\rangle = \sum_{n=0}^{\infty} \frac{(-\mathrm{i})^{n+1}}{n!} \langle 0| \left[O_j^\dagger, (\hat{\kappa}^n V^t\right] |0\rangle \tag{C.47}$$

$$= -\sum_{n=0}^{\infty} \mathrm{i}^{n+1} V^{t[n+1]}_{j l_1 l_2 \cdots l_n} \prod_{\mu=1}^{n} \alpha_{l_\mu}. \tag{C.48}$$

Using these expansions the EOM can be written as

$$\sum_{n=0}^{\infty} \mathrm{i}^n S^{[n+1]}_{j l_1 l_2 \cdots l_n} \dot{\alpha}_{l_1} \prod_{\mu=2}^{n} \alpha_{l_\mu} = -\sum_{n=0}^{\infty} \mathrm{i}^{n+1} (E^{[n+1]}_{j l_1 l_2 \cdots l_n} + V^{t[n+1]}_{j l_1 l_2 \cdots l_n}) \prod_{\mu=1}^{n} \alpha_{l_\mu}. \tag{C.49}$$

The parameters α determines the response of the SCF state to the pertubation and can be expanded in powers of the pertubation. Solving the EOM for each order in the perturbations yields the response functions. Collecting the terms in each order of the pertubations yields a set of coupled linear inhomogeneous differential equations, which to first order reads

$$\mathrm{i} S^{[2]}_{jl} \dot{\alpha}^{(1)}_l(t) - E^{[2]}_{jl} \alpha^{(1)}_l(t) = -\mathrm{i} V^{t[1]}_j, \tag{C.50}$$

where the matrices $S^{[2]}$, $E^{[2]}$ and $V^{t[1]}$ are given by

$$S^{[2]}_{jl} = \langle 0| \left[O_j^\dagger, O_l\right] |0\rangle, \tag{C.51}$$

$$E^{[2]}_{jl} = -\langle 0| \left[O_j^\dagger, [O_l, H_0]\right] |0\rangle, \tag{C.52}$$

$$V^{t[1]}_j = \langle 0| \left[O_j^\dagger, V^t\right] |0\rangle. \tag{C.53}$$

The differential equations separate in a representation where both $E^{[2]}$ and $S^{[2]}$ are diagonal. A simultaneous diagonalization of $S^{[2]}$ and $E^{[2]}$ is the same as solving the general eigenvalue equation

$$E_e^{[2]} X_j = \lambda_j S_e^{[2]} X_j. \tag{C.54}$$

The subscript e referes to the fact that the matrix is in the original basis. This means that the matrices $S_e^{[2]}$ and $E_e^{[2]}$ have the structure

$$E_e^{[2]} = \begin{pmatrix} A & B \\ B^* & A^* \end{pmatrix}, \; S_e^{[2]} = \begin{pmatrix} \Sigma & \Delta \\ -\Delta^* & -\Sigma^* \end{pmatrix} \tag{C.55}$$

with submatrix elements defined as

$$A_{ij} = \langle 0| \left[q_i, [H, q_j^\dagger]\right] |0\rangle \quad , \quad B_{ij} = \langle 0| \left[q_i, [H, q_j]\right] |0\rangle , \tag{C.56}$$

$$\Sigma_{ij} = \langle 0| \left[q_i, q_j^\dagger\right] |0\rangle \quad , \quad \Delta_{ij} = \langle 0| \left[q_i, q_j\right] |0\rangle . \tag{C.57}$$

In this representation we have $E_{ij}^{[2]} = \omega_j \delta_{ij}$, $S_{ij}^{[2]} = \mathrm{sgn}(j)\delta_{ij}$ and $\omega_j = \omega_{-j}$. We have used a notation where $(O_j, O_{-j}) = (q_j^\dagger, q_j)$ and $j > 0$. $\mathrm{sgn}(j)$ referes to the sign of j. This representation gives a separated first order equation as

$$\mathrm{i} \times \mathrm{sgn}(j) \dot{\alpha}_j^{(1)}(t) - \omega_j \alpha_j^{(1)}(t) = -\mathrm{i} V_j^{t[1]}. \tag{C.58}$$

Inserting the Fourier transform of $\alpha_j^{(1)}$

$$\alpha_j^{(1)} = \int d\omega_1 \exp[(-\mathrm{i}\omega_1 + \epsilon)t] \alpha_j^{(1)}(\omega_1), \tag{C.59}$$

in eq. C.58 we get

$$\alpha_j^{(1)}(\omega_1) = \frac{-\mathrm{i} \times \mathrm{sgn}(j) V_j^{\omega_1 [1]}}{\omega_1 - \mathrm{sgn}(j)\omega_j + \mathrm{i}\epsilon}. \tag{C.60}$$

Using the BCH expansion, Eq. E.1, we can expand the time dependent expectation value of a time-independent operator in the following way

$$\begin{aligned}
\left\langle \tilde{0} \right| A \left| \tilde{0} \right\rangle &= \langle 0| \exp(-\mathrm{i}\kappa(t)) A \exp(\mathrm{i}\kappa(t)) |0\rangle && \text{(C.61)} \\
&= \sum_{n=0}^{\infty} \frac{(-\mathrm{i})^n}{n!} \langle 0| \hat{\kappa}^n A |0\rangle && \text{(C.62)} \\
&= \sum_{n=0}^{\infty} \frac{(-\mathrm{i})^n}{n!} \langle 0| \left(\prod_{\mu=1}^{n} \hat{O}_{l_\mu} A \right) |0\rangle \prod_{\mu=1}^{n} \alpha_{l_{mu}} && \text{(C.63)} \\
&= \sum_{n=0}^{\infty} (\mathrm{i})^n A_{l_1 l_2 \cdots l_n}^{[n]} \prod_{\mu=1}^{n} \alpha_{l_\mu}. && \text{(C.64)}
\end{aligned}$$

Using the expansion of α in powers of the perturbation one obtains to first order

$$\left\langle \tilde{0} \right| A \left| \tilde{0} \right\rangle = \langle 0| A |0\rangle + \sum_j \mathrm{i} A_j^{[1]} \alpha_j^{(1)} + \cdots, \tag{C.65}$$

where

$$A_j^{[1]} = -\langle 0|\,[O_j, A]\,|0\rangle\,. \tag{C.66}$$

On inserting the Fourier transform of $\alpha_j^{(1)}(t)$ in Eq.C.65 one is able to obtain the linear response function for the SCF state as

$$\langle\langle A; V^{\omega_1}\rangle\rangle_{\omega_1} = \lim_{\epsilon\to 0}\sum_j \mathrm{i}A_j^{[1]}\alpha_j^{(1)}(\omega_1) \tag{C.67}$$

$$= \sum_j \frac{\mathrm{sgn}(j)A_j^{[1]}V_j^{[1]}}{\omega_1 - \mathrm{sgn}(j)\omega_j}. \tag{C.68}$$

Eq. C.68 contains a sum over all states in the eigenvalue basis and therefore a complete diagonalization of $S^{[2]}$ and $E^{[2]}$ is needed. This is only feasible for small dimensions and it is therefore necessary to remove the explicit summation. This is done by rewriting the equation in terms of the orginal basis, denoted by subscript e. Using the Einstein summation convention, i.e. summation over repeated indices, we can rewrite Eq. C.68 as

$$\langle\langle A; V^{\omega_1}\rangle\rangle_{\omega_1} = \frac{-A_j^{[1]}V_j^{[1]}}{\omega_j - \mathrm{sgn}(j)\omega_1}. \tag{C.69}$$

We note, that Eq. C.54 can be written as

$$\omega - \omega_1\sigma = X^\dagger(E_e^{[2]} - \omega_1 S_e^{[2]})X. \tag{C.70}$$

Inverting this equation and using that $A^{[1]} = A_e^{[1]}X$ and $V^{[1]} = X^\dagger V_e^{[1]}$ we can write the linear response function as

$$\langle\langle A; V^{\omega_1}\rangle\rangle_{\omega_1} = -A_e^{[1]}(E_e^{[2]} - \omega_1 S_e^{[2]})^{-1}V_e^{[1]} \tag{C.71}$$

Thus, in order to evaluate molecular properties we have to solve the set of linear equations

$$({}^eE^{[2]} - \omega_1\,{}^eS^{[2]})Z = {}^eV^{[1]}, \tag{C.72}$$

and (or) the generalized eigenvalues problem Eq. C.54. For large systems or large basis set we have to use an iterative method to solve the equations. This can be done by linear transformation of $S_e^{[2]}$ and $E_e^{[2]}$ on a set of trial vectors, thereby reducing the dimension of the problem. [84,137, 142,143]

Appendix D

Relay Tensors

D.1 Two-atom Relay Tensor

The defination of the two-atom relay tensor is given by Eq. 3.66 as

$$B_{pq,\alpha\beta} = \left[\frac{\partial \mu^{\text{ind}}_{p,\alpha}}{\partial E^{\text{ext}}_{q,\beta}}\right]_{E^{\text{ext}}_{q,\beta}=0}, \tag{D.1}$$

using the chain rule this can be rewritten as

$$B_{pr,\alpha\epsilon} = \frac{\partial \mu^{\text{ind}}_{p,\alpha}}{\partial E^{\text{tot}}_{p,\beta}} \left[\frac{\partial E^{\text{tot}}_{p,beta}}{\partial E^{\text{ext}}_{r,\epsilon}}\right]_{E^{\text{ext}}=0}. \tag{D.2}$$

The total field at atom p is given by Eq. 3.4

$$E^{\text{tot}}_{p,\beta} = E^{\text{ext}}_{\beta} + \sum_{q\neq p} T^{(2)}_{pq,\alpha\beta}\mu_{q,\beta}. \tag{D.3}$$

Thus, the derivative of the total field with respect to the external field is

$$\left[\frac{\partial E^{\text{tot}}_{p,\beta}}{\partial E^{\text{ext}}_{r,\epsilon}}\right]_{E^{\text{ext}}=0} = \delta_{pr}\delta_{\beta\epsilon} + \sum_{q\neq p}^{N} T^{(2)}_{pq,\beta\gamma}\left[\frac{\partial \mu^{\text{ind}}_{q,\gamma}}{\partial E^{\text{ext}}_{r,\epsilon}}\right]_{E^{\text{ext}}=0}. \tag{D.4}$$

Inserting the definition of the two-atom relay tensor, Eq. D.1, in Eq. D.4 we can recast it as

$$\left[\frac{\partial E^{\text{tot}}_{p,\beta}}{\partial E^{\text{ext}}_{r,\epsilon}}\right]_{E^{\text{ext}}=0} = \delta_{pr}\delta_{\beta\epsilon} + \sum_{q\neq p}^{N} T^{(2)}_{pq,\beta\gamma}B_{qr,\gamma\epsilon} \equiv \tilde{B}_{pr,\beta\epsilon}. \tag{D.5}$$

From Eq. 3.62 the induced dipolmoment is given by

$$\mu^{\text{ind}}_{p,\alpha} = \alpha_{p,\alpha\beta}E^{\text{tot}}_{p,\beta} + \frac{1}{6}\gamma_{p,\alpha\beta\gamma\delta}E^{\text{tot}}_{p,\beta}E^{\text{tot}}_{p,\gamma}E^{\text{tot}}_{p,\delta}. \tag{D.6}$$

If we take the derivative of Eq. D.6 with respect to the total field we get

$$\frac{\partial \mu^{\text{ind}}_{p,\alpha}}{\partial E^{\text{tot}}_{s,\sigma}} = \delta_{ps}\delta_{\beta\sigma}\alpha_{p,\alpha\beta} + \frac{1}{6}\delta_{ps}\delta_{\delta\sigma}\gamma_{\alpha\beta\gamma\delta}E^{\text{tot}}_{p,\beta}E^{\text{tot}}_{p,\gamma} + \frac{1}{6}\delta_{ps}\delta_{\gamma\sigma}\gamma_{\alpha\beta\gamma\delta}E^{\text{tot}}_{p,\beta}E^{\text{tot}}_{p,\delta} + \frac{1}{6}\delta_{ps}\delta_{\beta\sigma}\gamma_{\alpha\beta\gamma\delta}E^{\text{tot}}_{p,\gamma}E^{\text{tot}}_{p,\delta}, \tag{D.7}$$

which can be rearranged into

$$\frac{\partial \mu^{\mathrm{ind}}_{p,\alpha}}{\partial E^{\mathrm{tot}}_{s,\sigma}} = \delta_{ps}\delta_{\beta\sigma}\left(\alpha_{p,\alpha\beta} + \frac{1}{2}\gamma_{p,\alpha\beta\gamma\delta}E^{\mathrm{tot}}_{p,\delta}E^{\mathrm{tot}}_{p,\gamma}\right) \tag{D.8}$$

i.e. only $\frac{\partial \mu^{\mathrm{ind}}_{p,\alpha}}{\partial E^{\mathrm{tot}}_{p,\beta}}$ contributes since we regard all properties in Eq. D.6 as local. We can now substitute Eq. D.8 and Eq. D.5 into Eq. D.2 an get the final result Eq. 3.73

$$B_{pr,\alpha\epsilon} = \left(\alpha_{p,\alpha\beta} + \frac{1}{2}\gamma_{p,\alpha\beta\gamma\delta}E^{\mathrm{tot}}_{p,\delta}E^{\mathrm{tot}}_{p,\gamma}\right)\left(\delta_{pr}\delta_{\beta\epsilon} + \sum_{q\neq p}^{N} T^{(2)}_{pq,\beta\gamma}B_{qr,\gamma\epsilon}\right) \tag{D.9}$$

D.2 Three-atom Relay Tensor

The three-atom relay tensor is obtained by combining Eqs. 3.67, D.6 and D.3. We also need Eqs. D.5 and D.8 and their second derivatives given by

$$\frac{\partial^2 \mu_{p,\alpha}}{\partial E^{\mathrm{tot}}_{t,\tau}\partial E^{\mathrm{tot}}_{s,\sigma}} = \delta_{ps}\delta_{\beta\sigma}\delta_{pt}\delta_{\gamma\tau}\gamma_{p,\alpha\beta\gamma\delta}E^{\mathrm{tot}}_{p,\delta}, \tag{D.10}$$

and

$$\tilde{C}_{prs,\beta\epsilon\sigma} = \frac{\partial^2 E^{\mathrm{tot}}_{p,\beta}}{\partial E^{\mathrm{ext}}_{r,\epsilon}\partial E^{\mathrm{ext}}_{s,\sigma}} = \sum_{q\neq p}^{N} T^{(2)}_{pq,\beta\gamma}\frac{\partial^2 \mu_{q,\gamma}}{\partial E^{\mathrm{ext}}_{r,\epsilon}\partial E^{\mathrm{ext}}_{s,\sigma}} = \sum_{q\neq p}^{N} T^{(2)}_{pq,\beta\gamma}C_{qrs,\gamma\epsilon\sigma}. \tag{D.11}$$

Using the chain rule we obtain the three-atom relay tensor as

$$\begin{aligned}
C_{pqr,\alpha\beta\gamma} &= \frac{\partial^2 \mu_{p,\alpha}}{\partial E^{\mathrm{ext}}_{q,\beta}\partial E^{\mathrm{ext}}_{r,\gamma}} = \frac{\partial}{\partial E^{\mathrm{ext}}_{r,\gamma}}\left(\frac{\partial \mu_{p,\alpha}}{\partial E^{\mathrm{tot}}_{p,\epsilon}}\frac{\partial E^{\mathrm{tot}}_{p,\epsilon}}{\partial E^{\mathrm{ext}}_{q,\beta}}\right) \\
&= \left[\frac{\partial}{\partial E^{\mathrm{tot}}_{p,\epsilon}}\left(\frac{\partial \mu_{p,\alpha}}{\partial E^{\mathrm{ext}}_{r,\gamma}}\right)\right]\left(\frac{\partial E^{\mathrm{tot}}_{p,\epsilon}}{\partial E^{\mathrm{ext}}_{q,\beta}}\right) + \left(\frac{\partial \mu_{p,\alpha}}{\partial E^{\mathrm{tot}}_{p,\epsilon}}\right)\left(\frac{\partial^2 E^{\mathrm{tot}}_{p,\epsilon}}{\partial E^{\mathrm{ext}}_{q,\beta}\partial E^{\mathrm{ext}}_{r,\gamma}}\right) \\
&= \left[\frac{\partial}{\partial E^{\mathrm{tot}}_{p,\epsilon}}\left(\frac{\partial \mu_{p,\alpha}}{\partial E^{\mathrm{tot}}_{p,\sigma}}\frac{\partial E^{\mathrm{tot}}_{p,\sigma}}{\partial E^{\mathrm{ext}}_{r,\gamma}}\right)\right]\left(\frac{\partial E^{\mathrm{tot}}_{p,\epsilon}}{\partial E^{\mathrm{ext}}_{q,\beta}}\right) + \left(\frac{\partial \mu_{p,\alpha}}{\partial E^{\mathrm{tot}}_{p,\epsilon}}\right)\left(\frac{\partial^2 E^{\mathrm{tot}}_{p,\epsilon}}{\partial E^{\mathrm{ext}}_{q,\beta}\partial E^{\mathrm{ext}}_{r,\gamma}}\right) \\
&= \left(\frac{\partial^2 \mu_{p,\alpha}}{\partial E^{\mathrm{tot}}_{p,\epsilon}\partial E^{\mathrm{tot}}_{p,\sigma}}\right)\left(\frac{\partial E^{\mathrm{tot}}_{p,\sigma}}{\partial E^{\mathrm{ext}}_{r,\gamma}}\right)\left(\frac{\partial E^{\mathrm{tot}}_{p,\epsilon}}{\partial E^{\mathrm{ext}}_{q,\beta}}\right) + \left(\frac{\partial \mu_{p,\alpha}}{\partial E^{\mathrm{tot}}_{p,\epsilon}}\right)\left(\frac{\partial^2 E^{\mathrm{tot}}_{p,\epsilon}}{\partial E^{\mathrm{ext}}_{q,\beta}\partial E^{\mathrm{ext}}_{r,\gamma}}\right) \\
&= \gamma_{p,\alpha\epsilon\sigma\delta}E^{\mathrm{tot}}_{p,\delta}\tilde{B}_{pr,\sigma\gamma}\tilde{B}_{pq,\epsilon\beta} + \left(\alpha_{p,\alpha\epsilon} + \frac{1}{2}\gamma_{p,\alpha\epsilon\gamma\delta}E^{\mathrm{tot}}_{p,\delta}E^{\mathrm{tot}}_{p,\gamma}\right)\tilde{C}_{pqr,\epsilon\beta\gamma}.
\end{aligned} \tag{D.12}$$

Rearrange Eq. D.12 as

$$C_{pqr,\alpha\beta\gamma} - \left(\alpha_{p,\alpha\epsilon} + \frac{1}{2}\gamma_{p,\alpha\epsilon\gamma\delta}E^{\mathrm{tot}}_{p,\delta}E^{\mathrm{tot}}_{p,\gamma}\right)\sum_{t\neq p}^{N} T^{(2)}_{pt,\epsilon\sigma}C_{tqr,\sigma\beta\gamma} = \gamma_{p,\alpha\epsilon\sigma\delta}E^{\mathrm{tot}}_{p,\delta}\tilde{B}_{pr,\sigma\gamma}\tilde{B}_{pq,\epsilon\beta}. \tag{D.13}$$

Using that we can write the unit matrix as, $C_{pqr} = \sum_t \delta_{pt}C_{tqr}$, we can rewrite Eq. D.13 as

$$\sum_t \left(\delta_{pt} - \left(\alpha_{p,\alpha\epsilon} + \frac{1}{2}\gamma_{p,\alpha\epsilon\gamma\delta}E^{\mathrm{tot}}_{p,\delta}E^{\mathrm{tot}}_{p,\gamma}\right)T^{(2)}_{pt,\epsilon\sigma}\right)C_{tqr,\sigma\beta\gamma} = \gamma_{p,\alpha\epsilon\sigma\delta}E^{\mathrm{tot}}_{p,\delta}\tilde{B}_{pr,\sigma\gamma}\tilde{B}_{pq,\epsilon\beta}. \tag{D.14}$$

The left hand side of Eq. D.14 can be rewritten using

$$1 - \alpha_{\text{eff}} T^{(2)} = \alpha_{\text{eff}} \left(\alpha_{\text{eff}}^{-1} - T^{(2)} \right) = \alpha_{\text{eff}} B^{-1} = \left(1 + T^{(2)} B \right)^{-1} = \tilde{B}^{-1}. \tag{D.15}$$

Introducing this into Eq. D.14 we arrive at

$$\sum_t \tilde{B}_{pt}^{-1} C_{tqr} = \gamma_{p,\alpha\epsilon\sigma\delta} E_{p,\delta}^{\text{tot}} \tilde{B}_{pr,\sigma\gamma} \tilde{B}_{pq,\epsilon\beta}. \tag{D.16}$$

Finally we use the relations for matrix multiplication, in particular that $\sum_l A_{kl} B_{lm} = C_{km}$ is equivalent to $A_{kl} = \sum_m C_{km} B_{ml}^{-1}$, and the desired result is obtained as

$$C_{mqr,\sigma\tau\nu} = \sum_p^N \gamma_{p,\alpha\beta\gamma\delta} E_{p,\delta}^{\text{tot}} \tilde{B}_{pr,\gamma\nu} \tilde{B}_{pq,\beta\tau} \tilde{B}_{pm,\alpha\sigma}. \tag{D.17}$$

Appendix E

Mathematical Formulars

The Baker-Campbell-Hausdorf (BCH) expansion

$$e^{-\mathrm{i}A}Be^{\mathrm{i}} = \sum_{n=0}^{\infty} \frac{(-\mathrm{i})^n}{n!}(\hat{A}^n B). \tag{E.1}$$

If A and B are operators then $\hat{A}$ is a super-operator defined as

$$\hat{A}B = [A, B]. \tag{E.2}$$

Time derivative of a transformed operator B

$$\frac{d}{dt}(e^{\mathrm{i}A}Be^{-\mathrm{i}A}) = \sum_{n=0}^{\infty} \frac{\mathrm{i}^n}{n!}(\hat{A}^n \dot{B}) + e^{\mathrm{i}A}\left[\sum_{n=0}^{\infty} \frac{(-1)^n(\mathrm{i})^{n+1}}{(n+1)!}[\hat{A}^n \dot{A}, B]\right] e^{-\mathrm{i}A}. \tag{E.3}$$

Commutator relations

$$[A, B_1 \cdots B_n] = \sum_{k=1}^{n}(-1)^{k-1} B_1 \cdots [A, B_k] \cdots B_n \ \ (n \text{ even}). \tag{E.4}$$

$$[E_{mn}, a_{p\sigma}] = -\delta_{mp} a_{n\sigma}. \tag{E.5}$$

$$[A, B_1 \cdots B_n]_+ = \sum_{k=1}^{n}(-1)^{k-1} B_1 \cdots [A, B_k]_+ \cdots B_n \ \ (n \text{ odd}). \tag{E.6}$$

Appendix F

Molecules used in the Parametizations

Set 1: 115 aromatic and aliphatic molecules used in chapter 4

1,1,1-trichloroethane
1,1,1-trifluoroethane
1,1,2,2-tetrachloroethane
1,1,2,2-tetrafluoroethane
1,2,3,4-tetrafluorobenzene
1,2,3,5-tetrafluorobenzene
1,2,3-trifluorozbenzene
1,2,4,5-tetrafluorobenzene
1,2-dichloroethane
1,2-difluoroethane
1,3,5-trichlorobenzene
1,3,5-trifluorobenzene
1,3-dichlorotetrafluorobenzene
1-aminobutane
1-aminopropane
1-propanol
1,3-dichlorotetrafluorobenzene
2,3,5,6-tetrafluoro-1,4-dichlorobenzene
2,3-dichlorobutane
2,3-difluorobutane
2,4,6-trifluorochlorobenzene
2,5-difluoro-1,3-dichlorobenzene
2,6-difluoro-1,4-dichlorobenzene
2,6-difluorochlorobenzene
2-aminopropane
2-methylpropane
2-nitropropane
2-propanol
3,4,5-trifluorochlorobenzene
3,5-difluorochlorobenzene
3-pentanone
4,5-difluoro-1,2-dichlorobenzene
4,6-difluoro-1,3-dichlorobenzene
4-heptanone
N,N-dimethylformamide
N-methylacetamide
N-methylformamide
acetaldehyde
acetic acid
acetone
aminoethane
aminomethane
ammonia
aniline
benzene
biphenyl
butanal
butane
butanoic acid
butanol
chlorobenzene
chloroethane
chlorofluoromethane
chloroformamide
chloromethane
cyanobutane
cyanoethane
cyanomethane
cyanopropane
cyclohexane
cyclohexanol
cyclopentane
cyclopentanol
dichloromethane
difluorochloromethane
difluoromethane
ethane
ethanol
ethylamide
fluorobenzene
fluoroethane
fluoroformamide
fluoromethane
formaldehyde
formic acid
hexafluorobenzene
hexane
hydrogenfluoride
m-dichlorobenzene
m-difluorobenzene
malonic acid
methane
methanol
nitrobenzene
nitrobutane
nitroethane
nitromethane
nitropropane
o-dichlorobenzene
o-difluorobenzene
p-aminoaniline
p-dichlorobenzene
p-difluorobenzene
p-dinitrobenzene
p-fluorochlorobenzene
p-nitroaniline
pentafluorobenzene
pentafluorochlorobenzene
pentanal
pentane
pentanol
phenol
planer biphenyl
propanal
propane
propanic acid
propionamide
tetrachloromethane
tetrafluoromethane
toluene
trichlorofluoromethane
trichloromethane
trifluorochloromethane
trifluoromethane
water

Set 2: 46 Olephines added to set 1 used in chapter 6

ethylene	propylene	trans-2-butene
1,3-butadiene	1,3,5-hexatriene	ethyne
difluoroethyne	trans-1,2-difluoroethylene	dichloroethyne
trans-1,2-dichloroethylene	fluoroethylene	chloroethylene
fluoroethyne	nitroethylene	nitroethyne
trans-1-fluoropropylene	3-fluoropropylene	trans-1-chloropropylene
3-chloropropylene	trans-1-nitropropylene	3-nitropropylene
1-hydroxyethylene	trans-1-hydroxypropylene	3-hydroxypropylene
cyanoethylene	trans-3-cyano-2-propene	3-cyano-1-propene
propyne	3-hydroxypropyne	3-nitropropyne
3-chloropropyne	3-fluorpropyne	3-cyanopropyne
butadiyne	fluorobutadiyne	aminoethylene
aminoethyne	trans-1-aminopropylene	3-aminopropylene
3-butenal	3-butenoic acid	trans-2-butenoic acid
trans-2-butenal	3-butenon	propenal
propenoic acid		

Appendix G

Publications

Frequency-dependent molecular polarizability calculated within an interaction model

Lasse Jensen
Chem. Lab. III, Department of Chemistry, H. C. Ørsted Institute, University of Copenhagen, DK-2100 Copenhagen Ø, Denmark

Per-Olof Åstrand
Condensed Matter Physics and Chemistry Department, Risø National Laboratory, DK-4000 Roskilde, Denmark

Kristian O. Sylvester-Hvid
Department of Electromagnetic Systems, Danish Technical University, DK-2800 Lyngby, Denmark

Kurt V. Mikkelsen
Chem. Lab. III, Department of Chemistry, H. C. Ørsted Institute, University of Copenhagen, DK-2100 Copenhagen Ø, Denmark

Abstract

We have investigated different models for parameterizing the frequency-dependent molecular polarizability. The parameterization is based on an electrostatic model for interacting atoms and includes atomic polarizabilities, atom-type parameters describing the damping of the electric fields and the frequency-dependence. One set of parameters has been used for each element. The investigation has been carried out for 115 molecules with the elements H, C, N, O, F, and Cl, for which the frequency-dependent polarizability tensor has been calculated with *ab initio* methods. We find that the static polarizability of aliphatic and aromatic compounds can be described with the same set of parameters. The conclusion is that a simple electrostatic model to a good degree can model the essential behaviour of the frequency-dependent molecular polarizability.

J. Phys. Chem., accepted.

Static and frequency-dependent polarizability tensors for carbon nanotubes

Lasse Jensen
Chem. Lab. III, Department of Chemistry, H. C. Ørsted Institute, University of Copenhagen, DK-2100 Copenhagen Ø, Denmark

Ole H. Schmidt
Chem. Lab. III, Department of Chemistry, H. C. Ørsted Institute, University of Copenhagen, DK-2100 Copenhagen Ø, Denmark

Per-Olof Åstrand
Condensed Matter Physics and Chemistry Department, Risø National Laboratory, DK-4000 Roskilde, Denmark

Kurt V. Mikkelsen
Chem. Lab. III, Department of Chemistry, H. C. Ørsted Institute, University of Copenhagen, DK-2100 Copenhagen Ø, Denmark

Abstract

We have calculated the static and frequency-dependent polarizability tensor of a series of (5,5)- and (9,0)-carbon nanotubes. The calculations have been performed by a dipole-dipole interaction model based on classical electrostatics and an Unsöld dispersion formula. The model has previously been shown to predict successfully the frequency-dependent polarizability tensors of both aliphatic and aromatic molecules. In comparison we have carried out *ab initio* calculations at the Hartree-Fock level of the static polarizability of C_{60}, C_{70} and the smaller carbon nanotubes using the STO-3G basis set. We find that the interaction model is in good agreement with the SCF calculations and can be used to predict the polarizability tensors of carbon nanotubes. In addition, we find that the symmetry/intramolecular geometry of the tube has great influence on the polarizability.

J. Phys. Chem., submitted.

An atomic capacitance-polarizability model for the calculation of molecular dipole moments and polarizabilities

Lasse Jensen
Chem. Lab. III, Department of Chemistry, H. C. Ørsted Institute, University of Copenhagen, DK-2100 Copenhagen Ø, Denmark

Per-Olof Åstrand
Condensed Matter Physics and Chemistry Department, Risø National Laboratory, DK-4000 Roskilde, Denmark

Kurt V. Mikkelsen
Chem. Lab. III, Department of Chemistry, H. C. Ørsted Institute, University of Copenhagen, DK-2100 Copenhagen Ø, Denmark

Abstract

A classical interaction model for the calculation of molecular polarizabilities has been investigated. The model is described by atomic capacitancies, polarizabilities and a parameter related to the size of the atom, where one set of parameters have been employed for each element. The model has been parameterized for the elements H, C, N, O, F, and Cl from quantum chemical calculations of the molecular polarizability and dipole moment for 161 molecules at the Hartree-Fock level. The atomic charge has been divided into a nuclear charge and an electronic contribution, which allows for modelling also the permanent molecular dipole moment. Results are presented for polyenes. The deficiency of using atomic capacitancies for large molecules is discussed.

in preperation.

Bibliography

[1] M. Schulz. *Nature*, **399**, 729–730, 1999.

[2] D. A. Muller, T. Sorsch, S. Moccio, F. H. Baumann, K. Evans-Lutterodt, and G. Timp. *Nature*, **399**, 758–761, 1999.

[3] R. P. Feynmann. In *Engineering and Science*, The Caltech Alumni Magazine, February 1960.

[4] J. Jortner and M. A. Ratner, editors. *Molecular Electronics*. Blackwell Science Ltd, 1997.

[5] V. Balzani and F. Scandola, editors. *Supramolecular Photochemistry*. Ellis Horwoord, Chishester, West Sussex, England, 1991.

[6] S. J. Tans, A. R. M. Verschueren, and C. Dekker. *Nature*, **393**, 49–52, 1998.

[7] J. M. Tour, M. Kozaki, and J. M. Seminario. *J. Am. Chem. Soc.*, **120**, 8486–8493, 1998.

[8] W. B. Davis, W. A. Svec, M. A. Ratner, and M. R. Wasielewski. *Nature*, **396**, 60–63, 1998.

[9] M. A. Reed, C. Zhou, C. J. Muller, T. P. Burgin, and J. M. Tour. *Science*, **278**, 252–254, 1997.

[10] D. T. Colbert and R. E. Smalley. *Trends Biothecnol.*, **17**, 46–50, 1999.

[11] E. Bach, A. Condon, E. Glaser, and C. Tanguay. *J. Comp. Sys. Sci.*, **57**, 172–186, 1998.

[12] P. Ball. *Made to Measure, New materials for the 21st century*. Princeton University Press, Princeton, New Jersey, 1997.

[13] N. Peyghambarian and B. Kippelen. *Nature*, **383**, 481, 1996.

[14] R. H. Berg, S. Hvilsted, and P. S. Ramanulam. *Nature*, **383**, 505–508, 1996.

[15] B. Schlicke, P. Belser, L. De Cola, E. Sabbioni, and V. Balzani. *J. Am. Chem. Soc.*, **121**, 4207–4214, 1999.

[16] S. I. Yang, J. Seth, T. Balasubramanian, D. Kim, J. S. Lindsey, D. Holten, and D. F. Bocian. *J. Am. Chem. Soc.*, **121**, 4008–4018, 1999.

[17] L. D. Timberlake and H. Morrison. *J. Am. Chem. Soc.*, **121**, 3618–3632, 1999.

[18] J. K. Agyin, L. D. Timberlake, and H. Morrison. *J. Am. Chem. Soc.*, **119**, 7945–7953, 1997.

[19] D. Majumdar, H. M. Lee, J. Kim, and K. S. Kim. *J. Chem. Phys.*, **111**, 5866–5872, 1999.

[20] R. W. Wagner, J. S. Lindsey, J. Seth, V. Palaniappan, and D. F. Bocian. *J. Am. Chem. Soc.*, **118**, 3996–3997, 1996.

[21] D. P. Shelton and J. E. Rice. *Chem. Rev.*, **94**, 3–29, 1994.

[22] D. R Kanis, M. A. Ratner, and T. J. Marks. *Chem. Rev.*, **94**, 195–242, 1994.

[23] J. L. Brédas, C. Adant, P. Tackx, A. Persoons, and B. M. Pierce. *Chem. Rev.*, **94**, 243–278, 1994.

[24] D. M. Bishop. *Adv. Quant. Chem.*, **25**, 1–45, 1994.

[25] A. D. Buckingham. *Annu. Rev. Phys. Chem.*, **49**, xiii–xxxv, 1998.

[26] D. M. Bishop and D. W. Dee Kee. *J. Chem. Phys.*, **104**, 9876–9887, 1996.

[27] I. D. L. Albert, T. J. Marks, and M. A. Ratner. *J. Phys. Chem.*, **100**, 9714–9725, 1996.

[28] P. N. Prasad and D. J. Williams. *Introduction to Nonlinear Optical Effects in Molecules and Polymers*. Wiley,New York, 1991.

[29] N. Bloembergen. *Nonlinear Optics*. World Scientific, Singapore, 4th edition, 1996.

[30] H. Goldstein. *Classical mechanics*. Addison-Wesley, 2nd edition, 1980.

[31] G. C. Schatz and M. A. Ratner. *Quatum Mechanics in chemistry*. Prentice Hall, Inc., 1993.

[32] E. Merzbacher. *Quatum Mechanics*. John Wiley & Sons, Inc., 3rd edition, 1993.

[33] A. D. Buckingham. *Adv. Chem. Phys.*, **12**, 107–142, 1967.

[34] H. D. Cohen and C. C. J. Roothaan. *J. Chem. Phys.*, **43**, S34–38, 1965.

[35] H. J. Werner and W. Meyer. *Mol. Phys.*, **31**, 855–, 1976.

[36] H. Sekino and R. J. Bartlett. *J. Chem. Phys.*, **98**, 3022–3037, 1993.

[37] G. D. Billing and K. V. Mikkelsen. *Advanced Molecular Dynamics and Chemical kinetics*. Wiley,New York, 1997.

[38] C. J. F. Böttcher. *Theory of electric polarization*, volume 1. Elsevier: Amsterdam, 2nd edition, 1973.

[39] R. Cammi, B. Mennucci, and J. Tomasi. *J. Phys. Chem. A*, **102**, 870–875, 1998.

[40] R. Wortmann and D. M. Bishop. *J. Chem. Phys.*, **108**, 1001–1007, 1998.

[41] K. O. Sylvester-Hvid, K. V. Mikkelsen, and M. A. Ratner. *J. Phys. Chem. A*, **103**, 8447–8457, 1999.

[42] D. M Bishop. *Rev. Mod. Phys.*, **62**, 343–374, 1990.

[43] K. D. Bonin and V. V. Kresin. *Electric-Dipole Polarizabilities of Atoms, Molecules and Clusters*. World Scientific, Singapore, 1997.

[44] J. L. Oudar and D. S. Chemla. *J. Chem. Phys.*, **66**, 2664–2668, 1977.

[45] J. L. Oudar. *J. Chem. Phys.*, **67**, 446–457, 1977.

[46] D. R. Kanis, M. A. Ratner, and T. J. Marks. *L. Am. Chem. Soc.*, **114**, 10338–10357, 1992.

[47] P. N. Prasad, E. Perrin, and M. Samoc. *J. Chem. Phys.*, **91**, 2360–2365, 1989.

[48] K. G. Denbigh. *Trans. Faraday Soc.*, **36**, 936–948, 1940.

[49] B. C. Vickery and K. G. Denbigh. *Trans. Faraday Soc.*, **45**, 61–81, 1949.

[50] K. J. Miller and J. A. Savchik. *J. Am. Chem. Soc.*, **101**, 7206–7213, 1979.

[51] K. J. Miller. *J. Am. Chem. Soc.*, **112**, 8533–8542, 1990.

[52] Y. K. Kang and M. S. Jhon. *Theo. Chim. Acta*, **61**, 41, 1982.

[53] J. M. Stout and C. E. Dykstra. *J. Am. Chem. Soc.*, **117**, 5127–5132, 1995.

[54] J.M. Stout and C. Dykstra. *J. Phys. Chem A*, **102**, 1576–1582, 1998.

[55] K. O. Sylvester-Hvid, P. O. Åstrand, M. A. Ratner, and K. V. Mikkelsen. *J. Phys. Chem. A*, **103**, 1818–1821, 1999.

[56] B. F. Levine and C. G. Bethea. *J. Chem. Phys.*, **63**, 2666–2682, 1975.

[57] A. D. Buckingham and B. J. Orr. *Quart. Rev.*, **21**, 195–212, 1967.

[58] T. Zhou and C. E. Dykstra. *J. Phys. Chem. A*, **Web Release**, A–G, 1999.

[59] L. Silberstein. *Phil. Mag.*, **33**, 92–128, 1917.

[60] L. Silberstein. *Phil. Mag.*, **33**, 215–222, 1917.

[61] L. Silberstein. *Phil. Mag.*, **33**, 521–533, 1917.

[62] J. Appleguist, J. R. Carl, and K. F. Fung. *J. Am. Chem. Soc.*, **94**, 2952–2960, 1972.

[63] J. Appleguist. *Acc. Chem. Res.*, **10**, 79–85, 1977.

[64] K. A. Bode and J. Applequist. *J. Phys. Chem.*, **100**, 17820–17824, 1996.

[65] R. R. Birge. *J. Chem. Phys.*, **72**, 5312–5319, 1980.

[66] B. T. Thole. *Chem. Phys.*, **59**, 341–350, 1981.

[67] M. L. Olson and K. R. Sundberg. *J. Chem. Phys.*, **69**, 5400–5404, 1978.

[68] J. Applequist. *J. Phys. Chem*, **97**, 6016, 1993.

[69] K. R. Sundberg. *J. Chem. Phys.*, **66**, 114–118, 1977.

[70] K. R. Sundberg. *J. Chem. Phys.*, **66**, 1475–1476, 1977.

[71] C. K. Miller, B. J. Orr, and J. F. Ward. *J. Chem. Phys.*, **67**, 2109–2118, 1977.

[72] C. K. Miller, B. J. Orr, and J. F. Ward. *J. Chem. Phys.*, **74**, 4858–4871, 1981.

[73] J. Applequist. *J. Chem. Phys.*, **58**, 4251–4259, 1973.

[74] J. Applequist. *J. Phys. Chem. A*, **102**, 7723–7724, 1998.

[75] P. L. Prasad and D. F. Burow. *J. Am. Chem. Soc.*, **101**, 800–805, 1979.

[76] C. Voisin and A. Cartier. *J. Mol. Struct. (Theochem)*, **286**, 35–45, 1993.

[77] A. H. de Vries, P. T. van Duijnen, R. W. J. Zijlstra, and M. Swart. *J. Elec. Spec. Rel. Phen.*, **86**, 49–55, 1997.

[78] B. J Orr and J. F. Ward. *Mol. Phys.*, **20**, 513–526, 1971.

[79] A. D. Buckingham, E. P. Concannon, and I. D. Hands. *J. Phys. Chem.*, **98**, 10455–10459, 1994.

[80] D. M. Bishop. *Adv. Chem. Phys.*, **104**, 1–40, 1998.

[81] B. Champagne. *Int. J. Quant. Chem.*, **65**, 689, 1997.

[82] T. Helgaker, H.J.Aa. Jensen, P. Jørgensen, H. Koch, H. Ågren, K.L. Bak, V. Bakken, O. Christiansen, P. Dahle, E.K. Dalskov, T. Enevoldsen, A. Halkier, H. Hettema, D. Hettema, D. Jonsson, S. Kirpekar, R. Kobayashi, A.S. de Meras, K.V. Mikkelsen, P. Norman, M.J. Parker, K. Ruud, P.R. Taylor, and O. Vahtras. Dalton, an *ab initio* eletronic structure program., 1997.

[83] J. Olsen and P. Jørgensen. *J. Chem. Phys.*, **82**, 3235–3264, 1985.

[84] H. J. A. Jensen, H. Koch, P. Jørgensen, and J. Olsen. *Chem. Phys.*, **119**, 297, 1988.

[85] H. J. A. Jensen, P. Jørgensen, and J. Olsen. *J. Chem. Phys.*, **89**, 3654, 1988.

[86] A. J. Sadlej. *Coll. Czech. Chem. Commun.*, **53**, 1995–2015, 1988.

[87] R. C. Weast, editor. *Handbook of Chemistry and Physics.* CRC Press: Boca Raton, 62nd edition, 1981.

[88] J. A. Pople and M. Cordon. *J. Am. Chem. Soc.*, **89**, 4253–4261, 1967.

[89] P. T. van Duijnen and M. Swart. *J. Phys. Chem.*, **102**, 2399–2407, 1998.

[90] A. Wallqvist and G. Karlström. *Chem. Scr.*, **29A**, 131–137, 1989.

[91] P. O. Åstrand, A. Wallqvist, G. Karlström, and P. Linse. *J. Chem. Phys.*, **95**, 6395–6396, 1991.

[92] J. E. H. Haverkort, F. Baas, and J. J. M. Beenakker. *Chem. Phys.*, **79**, 105, 1983.

[93] G. B. Talapatra, N. Manickam, M. Samoc, M. E. Orczyk, S. P. Karna, and P. N. Prasad. *J. Phys. Chem.*, **96**, 5206–5208, 1992.

[94] N. Matzuzawa and D. A. Dixon. *J. Phys. Chem.*, **96**, 6241–6247, 1992.

[95] N. Matzuzawa and D. A. Dixon. *J. Phys. Chem.*, **96**, 6872–6875, 1992.

[96] H. Weiss, R. Ahlrichs, and M. Häser. *J. Chem. Phys.*, **99**, 1262–1270, 1993.

[97] B. Shanker and J. Applequist. *J. Phys. Chem*, **98**(26), 6486–6489, 1994.

[98] S. J. A. van Gisbergen, J. G. Snijders, and E. J. Baerends. *Phys. Rev. Lett.*, **78**, 3097–3100, 1997.

[99] D. Jonsson, P. Norman, K. Ruud, H. Ågren, and T. Helgaker. *J. Chem. Phys.*, **109**, 572–577, 1998.

[100] W. Krätschmer, L. D. Lamb, K. Fostiropoulos, and D. R. Huffman. *Nature*, **347**, 354–358, 1990.

[101] A. F. Hebard, R. C. Haddon, R. M. Fleming, and A. R. Kortan. *Appl. Phys. Lett.*, **59**, 2109–2111, 1991.

[102] Z. H. Kafafi, J. R. Lindle, R. G. S. Pong, F. J. Bartoli, L. J. Lingg, and J. Milliken. *Chem. Phys. Lett.*, **188**, 492–496, 1992.

[103] S. L. Ren, K. A. Wang, P. Zhou, Y. Wang, A. M. Rao, M.S. Meier, J. P. Selegue, and P. C. Eklund. *Appl. Phys. Lett.*, **61**, 124–126, 1992.

[104] A. Ritcher and J. Sturm. *Appl.Phys.A*, **61**, 163–170, 1995.

[105] P. C. Eklund, A. M. Rao, Y. Wang, K. A. Zhou, P.and Wang, J. M. Holden, M.S. Dresselhaus, and G. Dresselhaus. *Thin Solid Films*, **257**, 211–232, 1995.

[106] R. Antoine, Ph. Dugourd, D. Rayane, E. Benichou, F. Chandezon M. Broyer, and C. Guet. *J. Phys. Chem*, **110**, 9771–9772, 1999.

[107] L. X. Benedict, S. G. Louie, and M. L. Cohen. *Phys. Rev. B*, **52**, 8541–9549, 1994.

[108] W. E. Billups and M. A. Ciufolini, editors. *Buckminsterfullerenes*. VCH, New York, 1993.

[109] T. W. Ebbesen, editor. *Carbon Nanotubes*. CRC Press, New York, 1997.

[110] M. S. Dresselhaus, G. Dresselhaus, and P. C. Eklund. *Science of Fullerenes and Carbon Nanotubes*. Academic Press, New York, 1996.

[111] P. M. Ajayan. *Chem. Rev.*, **99**, 1787, 1999.

[112] H. W. Kroto, J. R. Heath, S. C. O'Brien, R. F. Curl, and R. E. Smalley. *Nature*, **381**, 162, 1985.

[113] S. Iijima. *Nature*, **354**, 56, 1991.

[114] J. S. Speck, M. Endo, and M. S. Dresselhaus. *J. Cryst. Growth*, **94**, 834, 1989.

[115] M. J. Frisch, G. W. Trucks, H. B. Schlegel, P. M. W. Gill, B. G. Johnson, M. A. Robb, J. R. Cheeseman, T. Keith, G. A. Petersson, J. A. Montgomery, K. Raghavachari, M. A. Al-Laham, V. G. Zakrzewski, J. V. Ortiz, J. B. Foresman, C. Y. Peng, P. Y. Ayala, W. Chen, M. W. Wong, J. L. Andres, E. S. Replogle, R. Gomperts, R. L. Martin, D. J. Fox, J. S. Binkley, D. J. Defrees, J. Baker, J. P. Stewart, M. Head-Gordon, C. Gonzalez, and J. A. Pople. Gaussian 94, Revision B.3, Gaussian, INC., Pittsburgh, PA, 1995.

[116] C.J.F. Böttcher and P. Bordewijk. *Theory of electric polarization*, volume 2. Elsevier: Amsterdam, 2nd edition, 1973.

[117] David R. Lide. *Handbook of Chemistry and Physics*. CRC Press, Inc., London, (1973).

[118] Luo Y., H. Ågren, P. Jørgensen, and K. V. Mikkelsen. *Adv. Quantum. Chem.*, **26**, 165, 1995.

[119] J. Jiang, J. Dong, X. Wan, and D.Y. Xing. *J. Phys. B: At. Mol. Opt. Phys.*, **31**, 3079–3086, 1998.

[120] B. Shanker and J. Applequist. *J. Phys. Chem.*, **100**, 3879–3881, 1996.

[121] B. Shanker and J. Applequist. *J. Phys. Chem.*, **100**, 10834–10836, 1996.

[122] B. Kirtman, C. E. Dykstra, and B. Champagne. *Chem. Phys. Lett.*, **305**, 132–138, 1999.

[123] M. G. Papadopoulos and A. J. Sadlej. *Chem. Phys. Lett.*, **288**, 377–382, 1998.

[124] S. F. Boys and F. Bernardi. *Mol. Phys.*, **19**, 553, 1970.

[125] M. P. Hodges, A. J. Stone, and E. C. Lago. *J. Phys. Chem. A*, **102**, 2455–2465, 1998.

[126] R. L. Rowley and T. Pakkanen. *J. Chem. Phys.*, **110**, 3368–3377, 1999.

[127] R. L. Jaffe and G. D. Smith. *J. Chem. Phys.*, **105**, 2780–2788, 1996.

[128] D. M. Bishop and M. Dupuis. *Mol. Phys.*, **88**, 887–898, 1996.

[129] C. J. Burnham, J. Li, S. S. Xantheas, and M. Leslie. *J. Chem. Phys.*, **110**, 4566–4580, 1999.

[130] Hättig C., H. Larsen, J. Olsen, H. Jørgensen, Koch, B. Fernández, and A. Rizzo. *J. Chem. Phys.*, **111**, 10099–10107, 1999.

[131] J. Cioslowski. *J. Am. Chem. Soc.*, **111**, 8333, 1989.

[132] B.-C. Wang, M.-H. Tsai, and Y.-M. Chou. *Synthetic Metals*, **86**, 2379–2380, 1997.

[133] M. Menon and D. Srivastava. *Chem. Phys. Lett.*, **307**, 407–412, 1999.

[134] R. H. Xie. *Chem. Phys. lett.*, **310**, 379–384, 1999.

[135] F. Jensen. *Introduction to computational chemistry.* Wiley, 1999.

[136] T. Helgaker, P. Jørgensen, and J. Olsen. Notes from The Fifth Sostrup Summer School, 1998.

[137] J. Olsen and P. Jørgensen. In *Modern Electronic Structure Theory*, volume 1, chapter 13. World Scientific Publishing Co.,Singapore, 1995.

[138] J. Oddershede, P. Jørgensen, and D.L. Yeager. In *Computer Physics Reports 2.* North-Holland, Amsterdam, 1984.

[139] J. Linderberg and Y. Öhrn. *Propagators in Quantum Chemistry.* Academic Press, London and New York, 1973.

[140] O. Christiansen, P. Jørgensen, and C. Hättig. *Int. J. Quantum Chem.*, **68**, 1–52, 1998.

[141] Aage E. Hansen. Notes from the course k4kk, 1997.

[142] H. Koch, H. Ågren, P. Jørgensen, and T. Helgaker. *Chem. Phys.*, **172**, 13–20, 1993.

[143] J. Olsen, H.J.Aa. Jensen, and P. Jørgensen. *J. Comput. Phys.*, **74**, 265–282, 1988.